Universitat Autònoma de Barcelona

Evolution of fluvial drainage during mountain building in the Eastern Cordillera of the Colombian Andes

Lucía Struth Izquierdo

Universitat Autònoma
de Barcelona

Department de Geologia

Evolution of fluvial drainage during mountain building in the Eastern Cordillera of the Colombian Andes

Ph. D. Thesis

2016

Lucía Struth Izquierdo

DRAINAGE REORGANIZATION DURING MOUNTAIN BUILDING IN THE EASTERN CORDILLERA OF THE COLOMBIAN ANDES

by

LUCÍA STRUTH IZQUIERDO

A Thesis Submitted

in Fulfillment of the Requirements for the

Degree of

DOCTOR IN GEOLOGY

by the

UNIVERSITAT AUTÒNOMA DE BARCELONA

PhD thesis supervised by

Dr. Antonio Teixell Cácharo

Departament de Geologia

Universitat Autònoma de Barcelona

June 2016

A mi familia.

“Talk about a dream, try to make it real”

Bruce Springsteen

Table of contents

Abstract

The Eastern Cordillera of Colombia is characterized by two topographic domains: i) an axial plateau (Sabana de Bogotá) dominated by longitudinal rivers, with low local relief and slope, where the mean erosion rate is calculated in 11 ± 1 mm/ka, and ii) the Cordillera flanks with high local relief and slope dominated by steep transverse rivers with a mean value of 70 ± 10 mm/ka, arguing for an erosive contrast between the two domains. These domains are separated by two main drainage divides in the eastern and western sides of the Sabana de Bogotá plateau. Morphometric analysis (including Specific Stream Power, channel gradient and chi values distribution) and field observations evidence a reorganization of the drainage network by progressive divide migration toward the inner plateau by discrete events of capture. Comparison of the erosion rates here obtained with the geomorphic digital parameters result in positive correlations. High values of SSP and/or channel gradient are directly related to high values of erosion rate and define a varying pattern in function of the mean annual precipitation in the sampled basin. In addition, new exposure age data is provided for the eastern flank of the Cordillera, a terrace of the Guayuriba river with an age of 655 ka which provides a an average incision rate of 62 mm/ka.

The erosive contrast between the two topographic domains is in agreement to the interpretation of fluvial reorganization from longitudinal to transverse-dominated drainage in the Eastern Cordillera. I interpret that drainage rearrangement was primarily driven to the increase of the orogen regional slope by progressive accumulation of crustal shortening and thickening and conditioned to fluvial captures. At a local scale, climate, tectonics and lithology play a secondary role in controlling the erosion rates and the basin dynamics.

A new model of drainage evolution for the Eastern Cordillera of Colombia is proposed in this thesis according to knickpoint distribution, chi analysis, field evidences, erosion rates and published paleodrainage data. I proposed that the decrease of the base level by the reopening of the Magdalena basin was the main precursor of the beginning of fluvial captures in the Eastern Cordillera, related to an erosion wave propagating upwards. This thesis provides an important contribution for the Bucaramanga fan knowledge. The cosmogenic depth profile dating in an abandoned terrace adjacent to the Bucaramanga deposit, provide us an estimation of the end of sediment supply of 400 ka. This estimation is related to the first capture in the Eastern Cordillera of the Suárez basin by a Magdalena tributary.

Since this first capture, the erosion wave began to propagate in the Suárez basin resulting in the capture of the Chicamocha basin. At the same time, the erosion was moving upwards along the Magdalena river, providing more potential energy to the tributaries located in the western flank, with the consequently threatening of the Sabana. In this way, the main divides begun to retreat and move towards the center of the plateau. Endorheic condition in the Sabana was interrupted by a first capture by the Sumapaz river. Finally, the Sabana was captured by a second time, resulting in the current drainage configuration.

Resumen

La Cordillera Oriental de Colombia se caracteriza por dos dominios topográficos: i) una meseta axial (Sabana de Bogotá) dominada por ríos longitudinales de baja pendiente, con bajo relieve y pendientes locales, cuya tasa de erosión media ha sido estimada en este trabajo en 11 ± 1 mm/ka; y ii) los flancos de la Cordillera, con alto relieve local y pendiente dominada por los ríos transversales con alta pendiente y con un valor erosivo medio de 70 ± 10 mm/ka, evidenciando un contraste erosivo entre los dos dominios. Estos dominios están separados por las dos divisorias de aguas principales al este y oeste de la meseta de la Sabana de Bogotá. Los análisis morfométricos (incluyendo el *Specific Stream Power*, el gradiente del canal y los valores de chi), así como con las observaciones de campo demuestran una reorganización de la red de drenaje por una migración progresiva de las divisorias hacia la parte interna de la cadena a partir de discretos eventos de captura fluvial. La comparación de las tasas de erosión obtenidas con los parámetros digitales geomorfológicos resulta en correlaciones positivas. Valores altos en *Specific Stream Power* y/o en gradiente del canal están directamente relacionados con valores altos en velocidad de erosión, definiendo un patrón que varía en función de la precipitación media anual en la cuenca muestreada. Se proporcionan nuevos datos de edad de exposición en una terraza fluvial para el flanco oriental de la Cordillera (río Guayuriba), para la que he obtenido edad de 655 ka y una consiguiente tasa de incisión media de 62 mm/ka.

Se interpreta la reorganización fluvial en la Cordillera Oriental desde un estado dominado por ríos longitudinales a otro con ríos transversales. El contraste erosivo entre los dos dominios topográficos mencionados arriba fue primariamente impulsado por el incremento en la pendiente regional del orógeno por acumulación progresiva del acortamiento y engrosamiento cortical, y condicionado por capturas fluviales. A nivel local, el clima, tectónica y litología juegan un rol secundario en el control de las tasas de erosión y la dinámica de cuencas.

Se propone un modelo de reorganización del drenaje para la Cordillera Oriental de Colombia basado en la distribución de knickpoints, el análisis de chi, evidencias de campo, las tasas de erosión y los datos publicados de paleodrenaje. En esta tesis interpreto el descenso de nivel de base por la reapertura de la cuenca del Magdalena como el principal precursor del inicio de las capturas fluviales en la Cordillera Oriental de Colombia, asociado a una onda erosiva que remonta aguas arriba. Esta tesis contribuye al conocimiento de la terraza de Bucaramanga. El análisis de isótopos cosmogénicos en un perfil vertical en una terraza cercana, nos proporciona una edad estimada de abandono de 400 ka, relacionado con el fin del aporte sedimentario en esta zona. Esta estimación se relaciona con la primera captura en la Cordillera Oriental, en la cual la cuenca del Suárez es capturada por un tributario del Magdalena.

A partir de esta primera captura en la Cordillera Oriental, la onda erosiva empieza a remontar aguas arriba en la cuenca del Suárez, resultando en la captura de la cuenca del Chicamocha. Al mismo tiempo, la onda erosiva iba remontando a través del Magdalena proporcionando más energía potencial a sus afluentes situados en el flanco occidental de la Cordillera, con la consiguiente amenaza de captura de la Sabana por estos ríos transversales. De esta manera, se promueve la migración lateral de las divisorias de aguas en dirección hacia el centro de la meseta. Las condiciones endorreicas de la Sabana fueron interrumpidas por una primera captura por el río Sumapaz. Finalmente, la Sabana de Bogotá fue capturada una segunda vez, resultando en la configuración de drenaje actual.

Chapter 1

1. Introduction

Mountain belts result from the interaction between deep and surface processes. Deep phenomena referrer to tectonic processes which increases or decreases the topography, and surface processes are controlled by the transport-erosion related to the relief modelling, eroding the high areas and filling the depressed. The Eastern Cordillera of Colombia shows that, apart from this interaction, are different extern factors as the large-scale drainage reorganization which also modifies the relief. This study aims to understand the large scale drainage network evolution and to quantify the erosion dynamics in the Eastern Cordillera of Colombia. The thesis project is part of a study of the relationship between the tectonic inversion processes and the long-term dynamics of erosion/sedimentation in intracontinental orogens, as the High Atlas of Morocco and Pyrenees. The incorporation of the study of a low mature drainage network as the Eastern Cordillera, will allow the comparison with the mature fluvial configuration of the orogens named before.

1.1. Geologic framework

The northern Andes in Colombia are divided into three belts: the Western, the Central, and the Eastern Cordilleras (Fig. 1.1). While the Western and Central Cordilleras are mainly composed of crystalline rocks, including Precambrian to Paleozoic basement and Mesozoic intrusives and ophiolites, the Eastern Cordillera is an inverted continental rift composed of a Precambrian-Paleozoic basement and a thick succession of Mesozoic and early Cenozoic sedimentary rocks (Julivert, 1970; Colletta et al., 1990; Cooper et al., 1995).

1.1.1. General evolution of the Eastern Cordillera and the northern Andes

The tectonic evolution since Mesozoic times is summarized as follows: During the Late Paleozoic-Early Cretaceous, a continuous subduction of the Farallon plate beneath the northwestern margin of South America was associated with igneous intrusions in the current Central Cordillera, Magdalena Valley, and Eastern Cordillera (Restrepo-Pace, 1995). During the Late Jurassic to early Cretaceous was the main stage of rifting in the Eastern Cordillera. Amaime terrain was accreted during the early Aptian, inducing deformation in the area of the Central Cordillera (Álvarez, 1983). During the late Cretaceous was a thermal subsidence period in the Eastern Cordillera related to the continuous subduction of the Farallon plate in the western border of Colombia, linked to a thick sequence (6 km) of shallow marine sediments in the current Eastern Cordillera area (Cooper et al., 1995; Sarmiento, 2001; Cortés et al., 2006). As a consequence of the accretion of oceanic terranes of the Western Cordillera along the Romeral fault system (Fig. 1.1.), the Central Cordillera experienced uplifting and basement structures in the Magdalena Valley became reactivated (Montes, 2001; Gómez et al., 2003; Cortés, 2004).

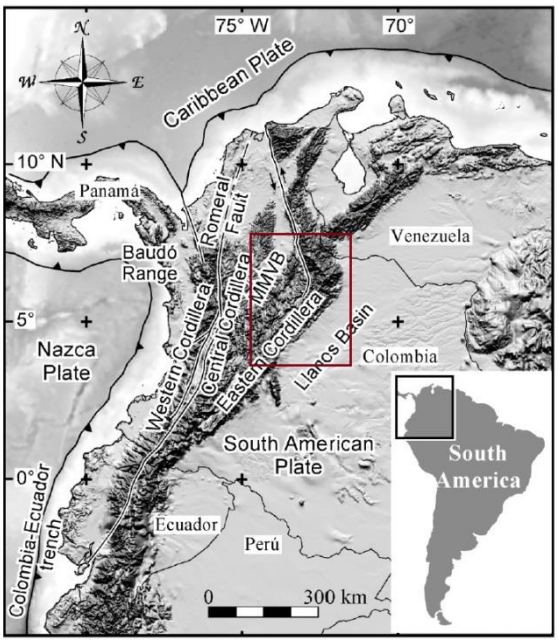

Fig. 1.1. *Shaded relief map of the northern Andes and nearby regions with general tectonic and physiographic configuration features (slightly modified from Gómez et al., 2003). Red polygon indicate the area of study in the Eastern Cordillera of Colombia.*

The Eastern Cordillera has a long convergence history since the latest Cretaceous or early Tertiary, with a main episode of shortening and thickening that began during the Miocene as a response to the accretion of the Panama arc to the western margin of Colombia (Colleta et al 1990, Dengo and Covey, 1993; Duque-Caro, 1990; Kellogg and Vega, 1995; Rolon, 2004; Taboada et al., 2000).

Before the late Eocene, the Eastern Cordillera s.s. was low emergent inside the Central Cordillera foreland basin (Cooper et al., 1995; Horton et al., 2010). Folds with angular and progressive discordances indicate a deformation stage in the Eastern Cordillera before the middle Eocene (Gómez, 2001). From this time to the middle Oligocene, were originated the folds in the Sabana de Bogotá (Julivert, 1970). Thermochronologic data from Sarmiento (2001) suggests surface uplift initiated during the Paleogene. Shortening and compartmentalization of the initial Central Cordillera foreland basin continued through the late Eocene-early Oligocene from observed growth-strata structures, for example, in the Guaduas syncline (Fig. 1.2; Julivert, 1963; Gómez et al, 2005; Horton et al., 2010).

Subsequent portioning of this initial foreland basin is result of the advance of fold-thrust deformation to the east, into the western and axial zones of the current Eastern Cordillera (Horton et al., 2010). Initial shortening and uplift in the inner part of the Eastern Cordillera was interpreted from detrital zircon ages, as occurred by Oligocene to early Miocene times (Horton et al., 2010). By middle Miocene time, uplift of the Eastern Cordillera by the inversion of ancient basement faults in both flanks must have created an effective topographic barrier that do not allow the communication between the drainage systems of the Central Cordillera with the fluvial network in the axial to foothills areas of the Eastern Cordillera and, the Llanos basin (Colletta et al., 1990; Cooper et al., 1995; Horton et al., 2010).

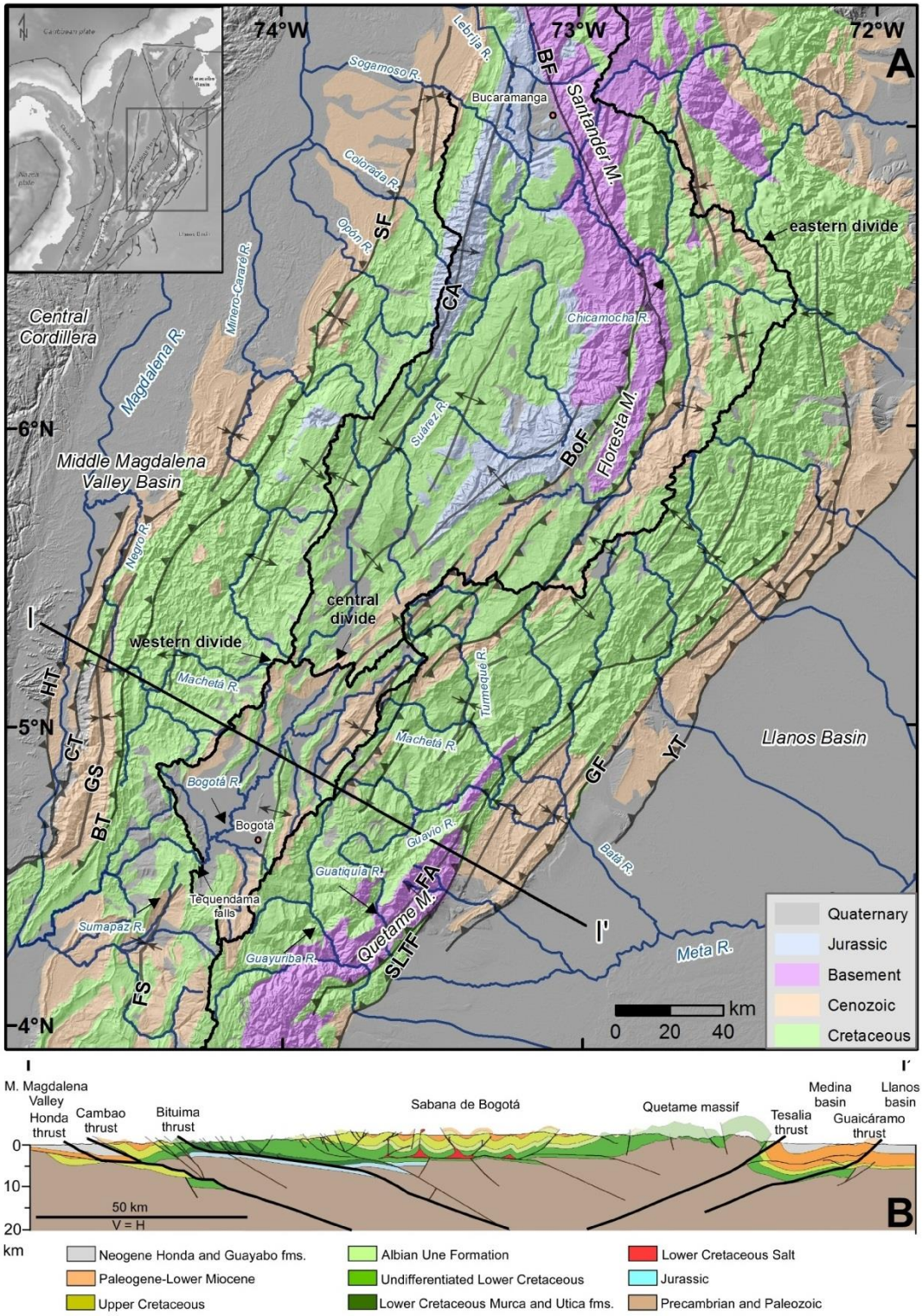

Fig. 1.2. *(A) Geology of the Eastern Cordillera of Colombia compiled from maps produced by Mora et al. (2010), Tesón et al. (2013) and unpublished maps of ICP-Ecopetrol. The fluvial network is represented with blue lines. SLTF: Servitá-Lengupá-Tesalia fault system; FA: Farallones Anticline; GF: Guaicáramo fault; YT: Yopal thrust; BoF: Boyacá fault; BF: Bucaramanga fault; CA: Cobardes anticline; SF: Salina fault; HT: Honda thrust; CT: Cambao thrust; GS: Guaduas syncline; BT: Bituima thrust; FS: Fusagasugá syncline. (B) Structural cross-section of the central part of the Eastern Cordillera (slightly modified from Teixell et al., 2015).Total shortening along this section is 82 km, consistent with values previously reported by Tesón et al. (2013) for the segment of the Eastern Cordillera covered by the map.*

Evidence for active faulting along the foothill thrust system, composed by the Servitá-Lengupá, Tesalia, Guaicáramo, and Yopal thrusts (Fig. 1.2), is provided by deformed terraces and fault scarps in Quaternary alluvial deposits (Taboada et al., 2000; Mora et al., 2010; Hermeston and Nemcok, 2013; Veloza et al., 2015). The amount of orogenic shortening in the Cordillera is still in debate and depends on the style of thrusting adopted and on the role of the pre-orogenic extensional faults. Values of 150-200 km (up to 50%) of shortening have been calculated in thin-skinned models (e.g., Dengo and Covey, 1993; Roeder and Chamberlain, 1995), whereas smaller values of 70-100 km (25-30%) are reported in thick-skinned models (e.g., Colletta et al., 1990; Cooper et al., 1995; Tesón et al., 2013; Teixell et al., 2015). A sequential retrodeformation from Teixell et al. (2015) of the section in Figure 1.2 show a shortening of 27% of the original length, with a total shortening of 82 km between the present-day and the section restored to 70 Ma (Fig. 1.3).

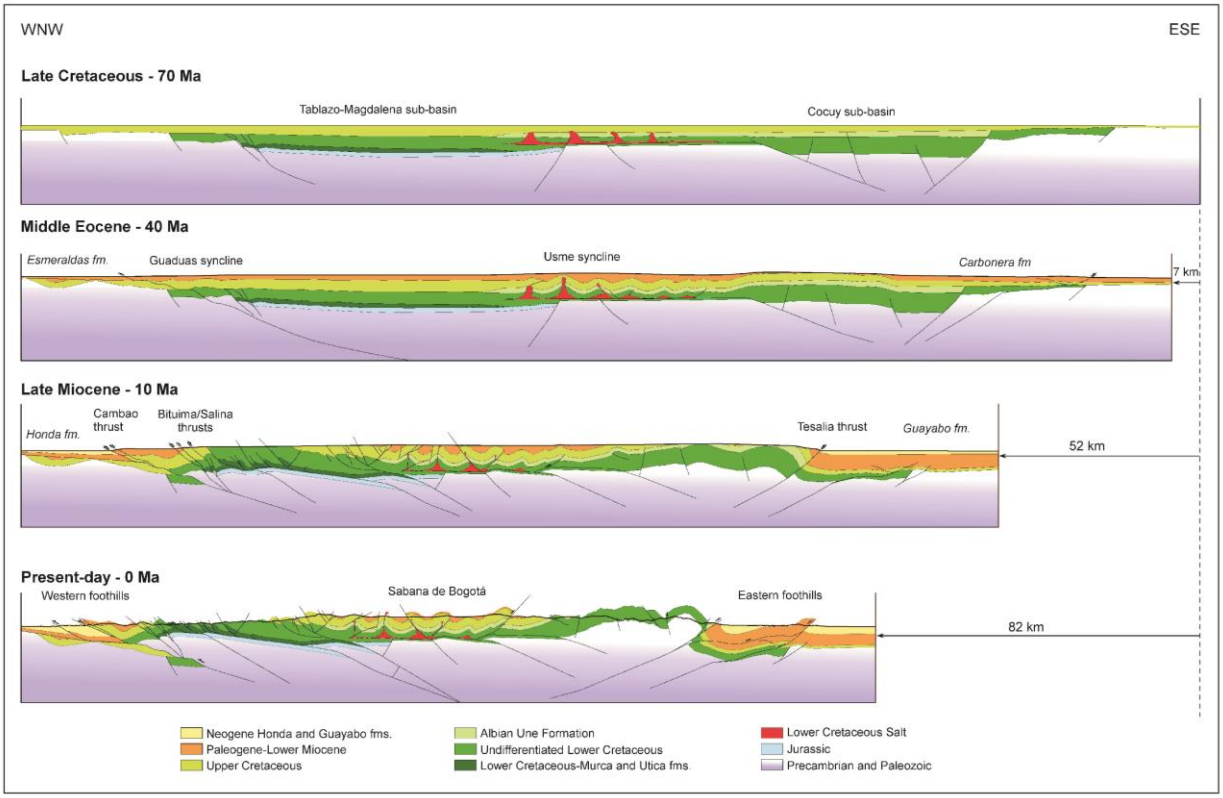

Fig. 1.3. *Restoration in sequential steps of the section indicated in Fig.1.2, taken from Teixell et al., 2015.*

1.1.2. Structure of the Eastern Cordillera

From a structural point of view, the Eastern Cordillera of Colombia is a double-verging thrust system bounded by high angle, thick-skinned inverse faults (Fig. 1.2, 1.3; Campbell and Bürgl, 1965; Julivert, 1970; Irving, 1975). Many of the thrust faults observed in the Eastern Cordillera are derived from the reactivation of former extensional faults of early Cretaceous age, belonging to the main episode of rifting in a back-arc tectonic setting (Cooper et al., 1995; Mora et al., 2006, 2008; Tesón et al., 2013). Two main structural families for the Eastern Cordillera include: i) reverse faults of high angle involving basement, and ii) low-angle thrust faults producing thin-skinned deformation (Kammer and Sánchez, 2006; Mora et al., 2006, 2009). Structural description for each domain is defined as follows:

In the eastern frontal thrust of the Cordillera, the shortening is accommodated by the Guaicáramo system (Santa Maria, Tesalia, Guaicáramo faults), associated to the greatest structural relief and largest displacement for the orogen foothills. In the eastern thrust belt, basement rocks are uplifted by dominant thick-skinned thrust faults and exposed at the surface in the rugged Quetame Massif (Toro et al., 2004; Mora et al., 2006, 2008).

The western foothills are characterized by thrusts sheets with a western vergence involving Cretaceous and Tertiary formations in surface and characterized by dominant thin-skinned deformation (Fig. 1.2.; Cortés et al., 2006; Montes et al., 2005; Sánchez et al., 2012). The western thrust belt does not expose basement to the surface but is still characterized by large thrust displacements, as in the Cambao thrust, which carries a basement wedge in its rear (Gómez et al., 2003; Restrepo-Pace et al., 2004; Cortés et al., 2006; Teixell et al., 2015). Inversion structures in the western flank are attributed to the Lebrija, La Salina, Bituima and Cambao thrusts (Fig. 1.2).

This contrasts with the simple fold belt of the Sabana de Bogotá in the Cordillera interior (Figs. 1.2A, B). The folds of the Sabana have wavelengths around 10 km, consisting in narrow anticlines and relatively wider synclines. Teixell et al. (2015) proposed that many folds in the area were originated as salt walls during the Cretaceous extension and squeezed during the continuous shortening. Since the mid-late Miocene, no major deformation is recorded in the central or axial part of the Eastern Cordillera: the low-relief plateau of the Sabana de Bogotá. Structure of the Sabana de Bogotá consists of a fold belt without major thrusting, dominated in outcrop by late Cretaceous to early Cenozoic rocks (Colleta et al., 1990; Kammer and Mora., 1999; Teixell et al., 2015). Growth strata attest for folding during the Paleogene (Gómez et al., 2005; Teixell et al., 2015).

1.1.3. Stratigraphy

In the syn-rift and post-rift stage, sedimentation in the flanks of the Cordillera were dominated by alternating sandstone and shale formations of dominant lower Cretaceous age (Fig. 1.2) dipping homoclinally or folded in relation with thrust faults. The eastern flank and foothills stratigraphy (Fig. 1.4) is characterized by an alternation of mudstone (e.g., Macanal, Fómeque, Chipaque) and sandstones (Juntas, Une, Guadalupe) formations. The western flank is dominated by thick pelitic formations (e.g., Trincheras, Pacho, Conejo) with intercalations of sandstone or siliceous rock (Murca-Útica, Socotá, Umir-Cimarrona) formations. The oldest rocks exposed in the Sabana are late Cretaceous.

Cenozoic sedimentation occurs in the foothills and in the Sabana, starting before the full growth of the Eastern Cordillera. In the late Maastrichtian-Paleocene, the Guaduas formation is related to the first terrestrial deposits, characterizing an overfilled basin and interpreted, in addition, to the initial stages of tectonic inversion in the orogen (Sarmiento-Rojas, 2001; Bayona et al., 2008). The eastern and western foothills and the Llanos and Magdalena basins are characterized by a continuous Paleogene to Neogene succession. The Sabana de Bogotá synclines preserve Paleocene to lower Oligocene shale and sandstone formations. A sedimentary hiatus occurs during Oligocene-Miocene times. After that, up to 600 m of unconformable Plio-Quaternary fluviolacustrine deposits partially fill the synclinal depressions resulting in the observed low relief (Fig. 1.4; Tilatá and Sabana formations, Julivert, 1963; Andriessen et al., 1993; Torres et al., 2005).

Despite the basement outcrops, no overall difference exists in bedrock strength between the Sabana de Bogotá and the flanks, as both are dominated at the surface by sandstone and shale formations (Fig. 1.4). The axial plateau of the Sabana de Bogotá is dominated by Cretaceous to Paleogene sandstones and shales (Fig. 1.2 and 1.4) that are deformed into open folds whereas the Cordillera flanks and foothills have sandstone-shale alternation with foreland-facing thrust faults with large-displacements (Fig. 1.2B; e.g. Mora et al. 2008 and references therein). Isolated Precambrian-Paleozoic basement massifs with low- and medium-grade metamorphic rocks (phyllites and schists, mainly) are present in the massifs of Quetame, Floresta and Santander (Fig. 1.2; Segovia, 1965; Ulloa and Rodríguez, 1979; Ulloa and Rodríguez, 1982; Parra et al., 2009a).

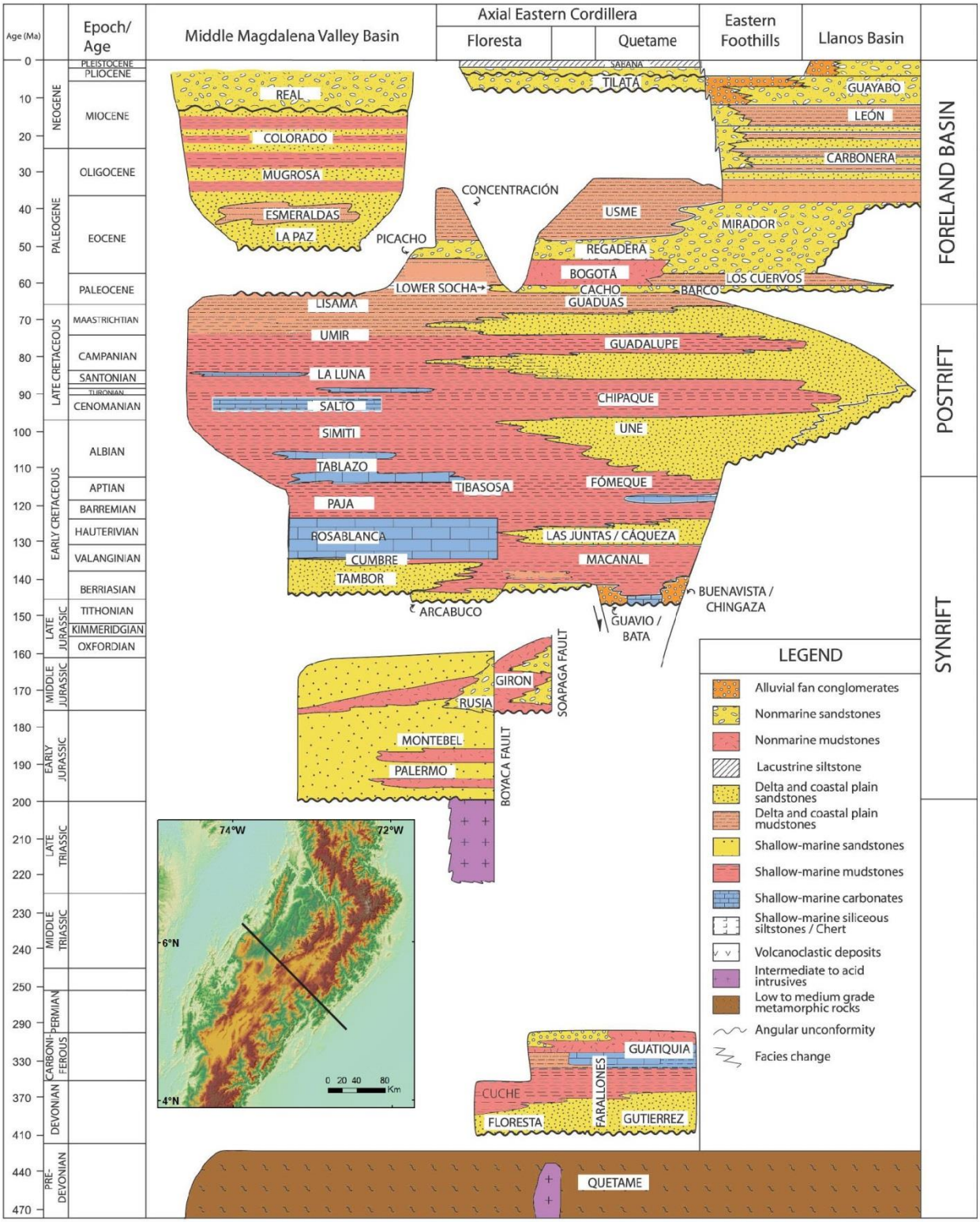

Fig. 1.4. *Regional time-stratigraphic plot for the Eastern Cordillera and the adjacent middle Magdalena Valley and Llanos Basin regions. Inset map indicates the line location of stratigraphic correlation (Fig. 1.3). Slightly modified from Mora et al. (2010), after Cooper et al. (1995), Mora et al. (2006) and Parra et al. (2009).*

1.2. Fluvial and climatic setting of the Eastern Cordillera

1.2.1. Fluvial drainage configuration

From a topographic point of view, the Eastern Cordillera can be divided into i) a central plateau domain in the axial zone; and ii) the Cordillera flanks and foothills. The boundary between the plateau and the flanks is defined by two main drainage divides (Fig. 1.5).

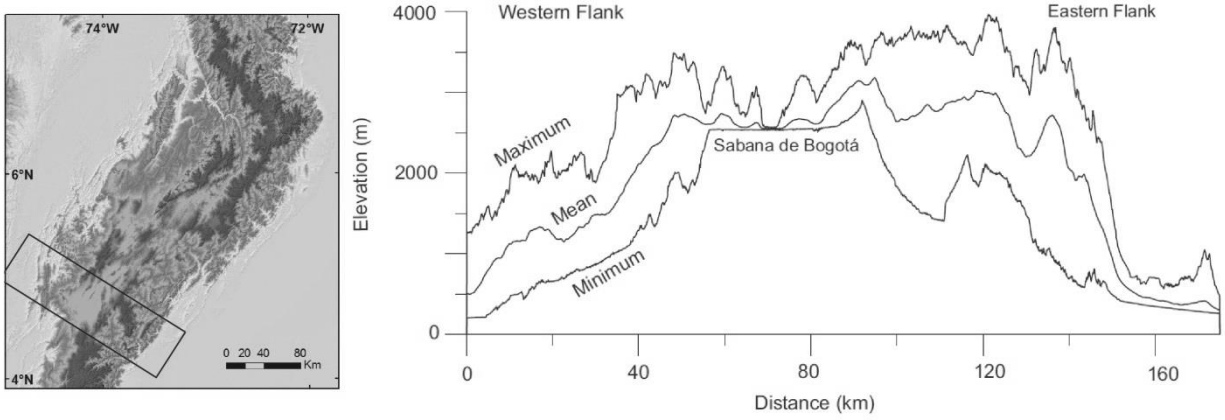

Fig.1.5. *Swath topographic profile across the central segment of the Eastern Cordillera of Colombia showing maximum, mean and minimum elevations for the Sabana and the flanks (from Mora et al., 2008). Inset map shows the swath location.*

The central plateau domain is dominated by a drainage network longitudinal to the orogen following the main folds and thrusts. In this domain we have two different drainage basins that ultimately drain into the Middle Magdalena Valley: the Bogotá river with their tributaries in the low relief Sabana de Bogotá plateau draining to the south and, the Sogamoso basin draining to the north, where the relief increases northwards, and the Lebrija Basin, the northern continuation of the Sogamoso area.

Rivers in the Sabana de Bogotá run approximately NNE-SSW, parallel to fold axes, and preferentially located in synclines (Fig. 1.2). Synclinal valleys are wide and flat, and ridges in between correspond to anticline cores (Fig. 1.6A). Rivers in the Sabana typically show a general meandering pattern (Fig. 1.6C), gentle slopes, and low runoff velocity in accordance with the smooth topography. The Sogamoso basin is characterized by the Suárez and Chicamocha river basins, which flow following main tectonic structures as the Suárez and Bucaramanga fault. Suárez and Chicamocha rivers show a flat area in the upper part of the river profile followed by an incised tract downstream.

In the western flank of the Eastern Cordillera, the main rivers are the Río Negro and Minero-Cararé draining to the Magdalena River at the middle Magdalena Valley. These rivers flow along Cretaceous to Paleogene sandstones and mudstones in a general E-W direction, transverse to the general trend of the Cordillera and perpendicular to the main tectonic structures (Fig. 1.2). However, they also show sharp changes in flow direction with longitudinal reaches separated by transverse reaches in the medium and

lower part of the western flank, displaying a gridiron-like drainage organization which is common in fold-and-thrust belts (e.g., Gupta, 1997).

The eastern flank present a transverse drainage network flowing through Cretaceous sandstone and shale formations with an isolated Precambrian-Paleozoic outcrop named Quetame massif (Fig.1.2) with low and medium grade phyllites and schists (Segovia, 1965; Ulloa and Rodríguez, 1979; Ulloa and Rodríguez, 1982; Parra et al., 2009a). The main rivers are the Guayuriba, Guatiquía and Batá rivers, which drain in a W-E direction to the Meta river at the Llanos Basin. Sharp changes in flow direction with longitudinal valleys in the lower part of the flank are also observed, as in the western flank of the Cordillera.

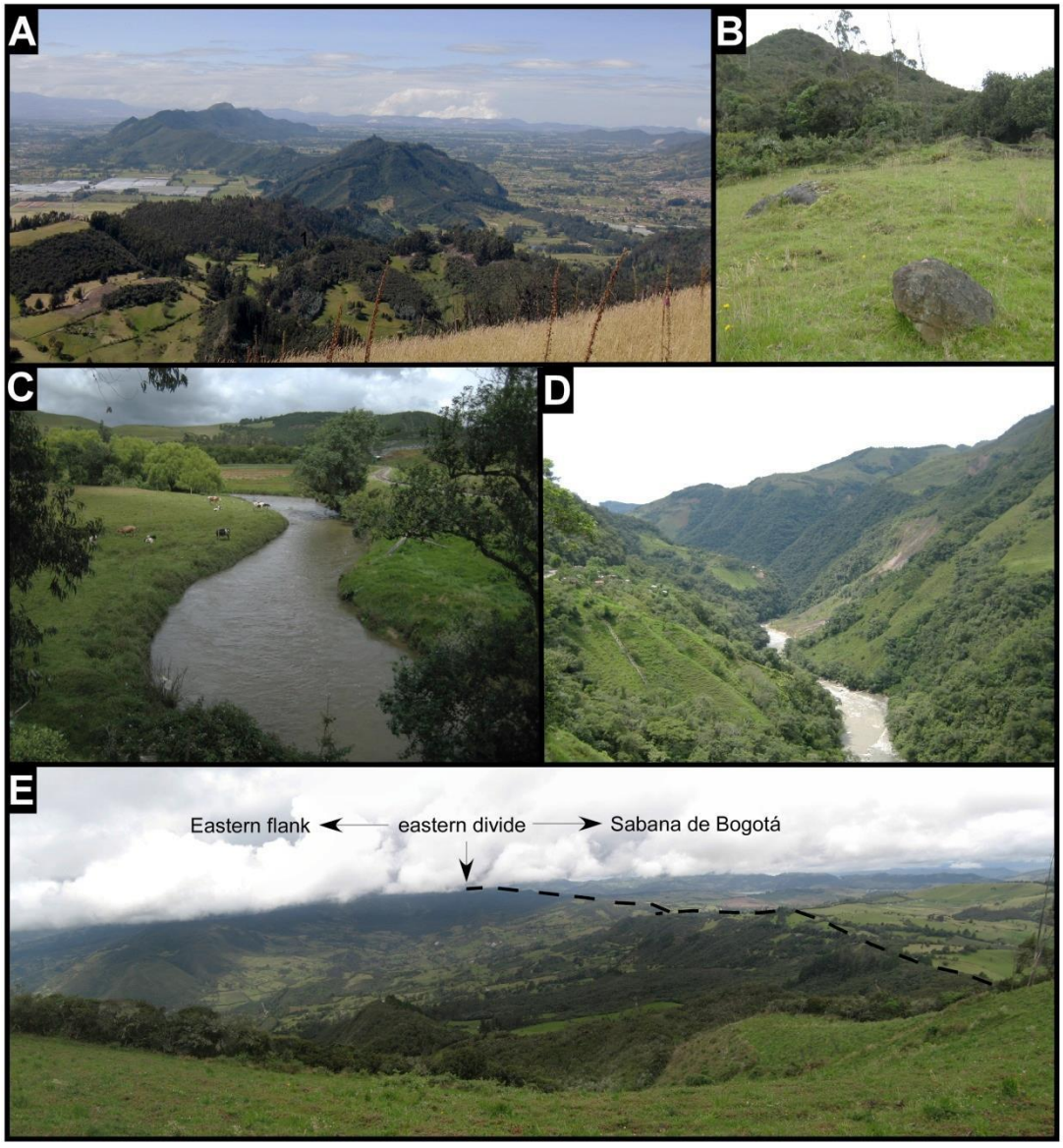

Fig. 1.6. *(A) Field photograph of the Sabana de Bogotá showing the sandstone anticlinal ridge of the Chía Range (middle) and low slopes in adjacent synclinal areas. (B) Rock boulders product of a rockfall located on the eastern divide of the Cordillera, in the Machetá River capture zone (location in Fig. 9). (C) View of the longitudinal river Bogotá flowing in the plateau. (D) View of the transverse river Guayuriba in the eastern flank of the Cordillera with greater slopes and local relief, and common landslides in the hillslopes linked to the high slope angles. (E) Field image of the two topographic domains of the Eastern Cordillera: the Sabana de Bogotá and the upstream part of the Machetá transverse river in the eastern flank (field of view 4 km, view to the south).*

Paleogene drainage in the Eastern Cordillera from paleocurrent data

Paleogene paleocurrent data show a western and southwestern source for a continuous basin in the foreland of the Central Cordillera foreland basin (including the current Magdalena Valley, Eastern Cordillera and Llanos basin) and a drainage network controlled by growing folds and thrusts following a regional slope to the NNE (Laverde et al., 1989; Cooper et al., 1995; Diaz and Serrano, 2001; Gómez et al., 2005a; Bayona et al., 2008; Horton et al., 2010; Nie et al., 2010, 2012; Saylor et al., 2011; Bande et al., 2012; Caballero et al., 2013b; Silva et al., 2013).

During the Paleocene-early Eocene, the drainage was longitudinal (Fig. 1.7), parallel to the growing structures (Brown et al., 1991; Gómez et al., 2005a,b; Bayona, 2008; Bayona et al., 2008; Saylor et al., 2011; Mora et al., 2013; Silva et al., 2013). Fluvial sediments of that age in the Sabana de Bogotá region record paleocurrents to the NNE (Laverde et al., 1989; Bayona, 2008; Bayona et al., 2008; Saylor et al., 2011). The late Eocene-Oligocene still records a mean northward drainage in the Sabana de Bogotá area and in the Magdalena Valley (Diaz and Serrano, 2001; Gómez et al., 2005a; Silva et al., 2013). In the late Oligocene to mid-Miocene interval, important changes occurred in the Magdalena Valley basin: due to deformation in the northern part of the basin, the base level started to rise and forced rivers to divert toward the Llanos Basin across the Eastern Cordillera (Gómez et al., 2005a, b). During the mid-late and late Miocene, the Magdalena Valley paleodrainage returned to the north in relation with continued rising of the Cordillera.

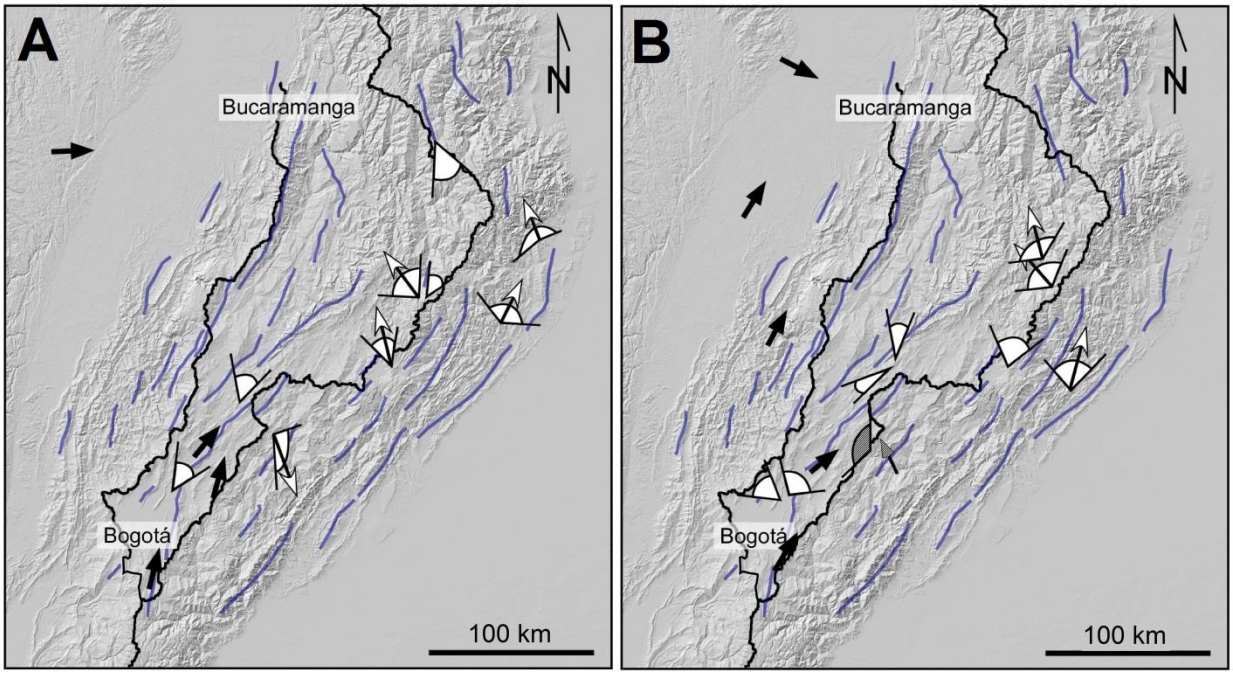

Fig. 1.7. *Summary of paleocurrent data from Paleocene (A) to Eocene (B) in the Eastern Cordillera compiled from Gómez et al. (2005b) (black arrows), Bayona et al. (2008) (white arrows), and Bayona (2008) (line-filled arrows).*

Based on subsidence and exhumation analysis (Parra et al., 2009a,b; Mora et al., 2010) and detrital sediment provenance (Horton et al., 2010), the main emergence of the major thrust faults in the flanks of the Eastern Cordillera started during late Oligocene to early Miocene times. The disappearance of Meso-

Cenozoic detrital zircons (which indicate a Central Cordillera provenance) in the eastern foothills (Horton et al., 2010) indicates that the Eastern Cordillera had already become an effective topographic barrier that separated the Central Cordillera and the axial Eastern Cordillera from the Llanos basin at least before the mid to late Miocene (Horton et al., 2010). This is marked by a contemporaneous conglomeratic influx of the Honda and Guayabo formations (Fig. 1.4) into the middle Magdalena Valley and Llanos basins (Hoorn et al., 1995; Gómez et al., 2003; Parra et al., 2009a).

Since the late Miocene, the Eastern Cordillera was the main source area for Los Llanos and the Central and Eastern Cordillera for the Middle Magdalena Valley Basin, creating a new E-W drainage along the forelands of the chain. There is evidence of recent strong deformation in the most external thrust sheets, by very young apatite fission track ages in the Quetame Massif along the eastern flank (0-3 Ma; Fig. 1.8), which attests to strong exhumation across the Cordillera margins in the latest Neogene and Quaternary (Mora et al., 2008), and by neotectonic evidences (Mora et al., 2013; Veloza et al., 2015).

After a sedimentary hiatus that comprises most of the Oligocene and Miocene, the Sabana de Bogotá accumulated ca. 600 m of fluviolacustrine deposits (Tilatá and Sabana formations, Fig. 1.4; Julivert, 1963; Andriessen et al., 1993; Torres et al., 2005), which partially filled synclinal depressions and contributed to smooth the relief of the plateau as we see it today. In spite of this, Van der Hammen et al. (1973) and Hooghiemstra et al. (2006) inferred low altitudes for the Sabana until the late Miocene and a rapid surface uplift of 1500 ± 500 m between 6 and 3 Ma ago, based on the palynological content of the late Neogene deposits using the nearest living relatives method. However, these data may not be reliable enough because Gregory-Wodzicki (2000) reported errors in paleoaltimetry estimates for the Andes of ±1500 m, implying that the proposed paleoelevation changes of the Sabana de Bogotá may not be accurately resolved by the nearest living relatives method. For this reason, a continuous crustal thickening and surface uplift since the onset of mountain building is not discarded (Babault et al., 2013), as shortening was accumulating in a progressive way (e.g., Moreno et al., 2013; Teixell et al., 2015) and explains the current high elevation of the Eastern Cordillera.

1.2.2. Climate

Climate can be a major control on the evolution of drainage network (e.g. Schumm, 1979; Bull, 1991; Whitfield and Harvey, 2012). A mean annual precipitation map for the Eastern Cordillera of Colombia and adjacent basins (Fig. 1.8) was compiled for the years 1998-2009 using TRMM data (Bookhagen and Strecker, 2008) following the methodology of Bookhagen and Burbank (2010). The map shows a strong gradient of precipitation in the vicinity of the western divide, by which rainfall increases markedly in the western flank of the Eastern Cordillera. In contrast, a similar gradient is not observed across the eastern divide, as the distribution of annual precipitation is approximately homogeneous in the plateau and upper eastern flank. Precipitation is greatest (> 3000 mm/yr) in the middle Suárez Basin (see Suárez river location in Fig. 1.2), in the eastern and western foothills and in the Quetame Massif (Fig. 1.8).

The Sabana de Bogotá presents a sparse record of glaciation during the last 50 ka at altitudes higher than 3500 m (Helmens, 1988, 1990; Helmens and Kuhry, 1995; Helmens et al., 1997). On the basis of moraine deposits, glaciers are described as very small and poorly developed valley glaciers or ice caps, ranging from 0.5 to 8 km^2 and were deglaciated at ca. 12.5 ka (Helmens, 2004). U-shaped valley forms have never been reported (Mark and Helmens, 2005).

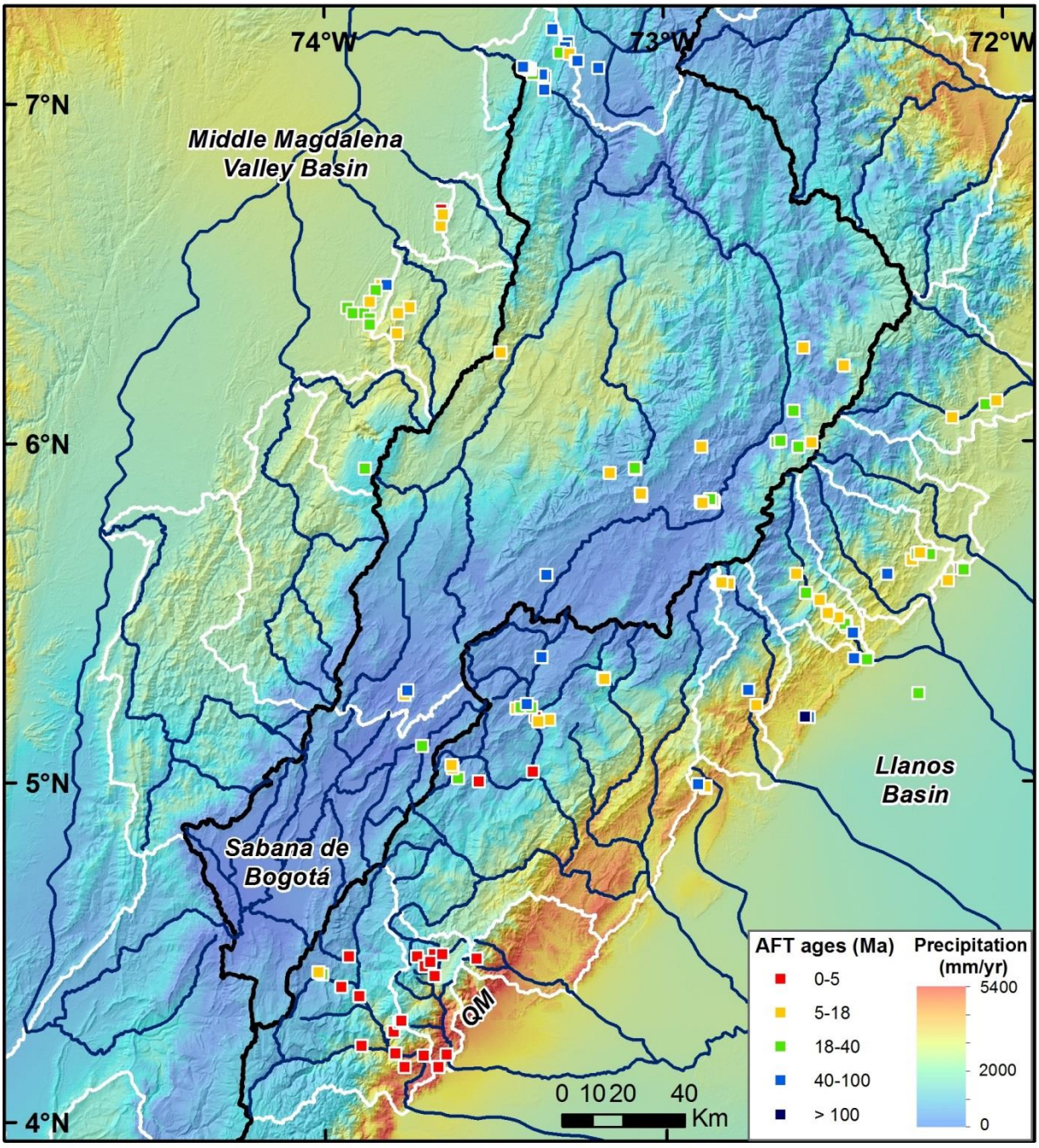

Fig. 1.8. *Mean annual precipitation data for the years 1998-2009 (after Bookhagen and Strecker, 2008) and Apatite Fission Track (AFT) data (Mora et al., 2008, 2010; Parra et al., 2009a) in the Eastern Cordillera of Colombia. QM: Quetame Massif. White lines are the basin boundaries.*

1.3. Starting hypotheses and objectives of the thesis

A detailed study of the drainage dynamics and landscape evolution over recent times (since the main Pliocene inversion stage) is not studied up to date in the Cordillera. This thesis provide a detailed analysis of the drainage rearrangement in recent times and the erosion dynamic quantification in order to avoid the lack of geomorphic works in the Eastern Cordillera and to highlight the interest of the applied methodologies with the aim of characterizing the landscape evolution and the formulation of a drainage model and the relation with the tectonic development.

Given that this PhD project is part of a study of the relationship between tectonic inversion processes and the long-term dynamic of erosion/sedimentation in intracontinental orogens, the obtained results will allow a comparison between them, as for example the High Atlas of Morocco. The hypothesis of a transient drainage from an initial longitudinal stage to transversal was interpreted in a more mature chain as the High Atlas of Morocco. With the contribution of the study in the Eastern Cordillera we approach to a complete cycle with the beginning of a young (less mature) chain as the Eastern Cordillera and a mature chain, as the High Atlas.

The main objectives are related to the structure of this thesis and are summarized in the next points:

A. To characterize the landscape dynamics of the Eastern Cordillera of Colombia, focusing in the drainage rearrangement and to determine the main mechanism that enhances the dynamism of the drainage network (Chapter 2).
B. To quantify the erosion rates along the Eastern Cordillera in order to test the disequilibrium in the fluvial network and the effect of lithology, climate and tectonics in denudation (Chapter 3).
C. Describe the drainage evolution since the building of the Cordillera mountains and to calculate the timing of the plateau capture and the ongoing drainage pattern (Chapter 4).

In order to address the objectives exposed here, a specific methodology is described and discussed in detail in the corresponding chapter, with the aim of highlighting and justifying the agreement of each method to each specific problematic. In this section I summarize the applied methodology for each objective.

In order to characterize the landscape dynamics of the Cordillera, I analyze in first order the topographic digital signal and the fluvial geometry of the Cordillera, and then compare the actual geometry with published data of paleocurrents. The available digital elevation models DEM in the area of study have wrong data introducing a problem that has been solved using topographic maps and correcting all the wrong pixels for a correct flow extraction. With the aim of avoiding the first objective, field work and digital analysis has been done. The digital parameters that I use for avoid this objective are: frequency of elevation and slope along the Cordillera, the steepness index, river and drainage divide longitudinal profiles and a study of geomorphic features that evidence drainage evolution.

Once the topography was well characterized, for the second chapter I tried to quantify the dynamic process using a thermochronologic and geochronologic dating. To extract information about the geomorphic and cooling history in the rivers and know the age of starting of the erosive wave upstream, I used the technique of (U-Th/He in apatites) for 24 rock samples. Sample processing was carried out at the Jackson School of Geosciences of the University of Texas at Austin under the supervision of Dr. Danniel Stockli. Unfortunately, in the picking stage I observed that the content of apatites of sufficient quality was very low and then, the method was discarded. With the aim of gaining insight in the erosion dynamics in the Cordillera, I then used cosmogenic nuclide dating in order to find erosion rates in the catchments, with samples from river sediment. I sampled for three different methods: i) to know the erosion rates, I sampled fluvial sands; ii) for obtain the age of exposure of a terrace and calculate the incision rate, I sampled boulders in one well preserved terrace, and iii) to know the age of abandonment of a fluvial deposit, I use a depth profile methodology. The cosmogenic nuclide samples were processed in the University of Cincinnati under the supervision of Dr. Lewis A. Owen, and measured in the Accelerator Mass Spectrometry in the Purdue Rare Isotope Measurement (PRIME) Laboratory at Purdue University, Indiana, USA.

Finally, with the aim of build a detailed history of the drainage evolution since the inversion of the orogen, we apply a new method: the chi (χ) parameter (Perron and Royden, 2012). The study presented in this chapter has been carried out in collaboration with the Department of Earth Sciences of the ETH-Zürich. With the results obtained with this method, we compare this with all the results and interpretations that we extract from the previous steps.

Chapter 2

Drainage reorganization during mountain building in the river system of the Eastern Cordillera of the Colombian Andes

Published in Geomorphology, 2015

Summary

I describe the topography of the Eastern Cordillera of Colombia and evidence the fluvial dynamic signal on the basis of digital analysis, field observations, and published paleocurrent data. In this way, the Eastern Cordillera of Colombia is characterized by two topographic domains: i) the axial zone, a high altitude plateau (the Sabana de Bogotá, 2500 m asl) with low local relief and dominated by longitudinal rivers, and ii) the Cordillera flanks, where local relief exceeds 1000 m and transverse rivers dominate. On the basis of an analysis of digital topography and river parameters combined with a review of paleodrainage data, we show that the accumulation of shortening and crustal thickening during the Andean orogeny triggered a process of fluvial reorganization in the Cordillera. Owing to a progressive increase of the regional slope, the drainage network evolves from longitudinal to transverse-dominated, a process that is still active at present. This study provides the idea of progressive divide migration toward the inner part of the mountain belt, by which the area of the Sabana de Bogotá plateau is decreasing, the flanks increase in area, and ultimately transverse rivers will probably dominate the drainage of the Cordillera

Key words: Drainage network; Fluvial capture; Drainage evolution; Eastern Cordillera of Colombia

Reference: Struth L, Babault J, Teixell A. 2015. Drainage reorganization during mountain building in the river system of the Eastern Cordillera of the Colombian Andes. Geomorphology 250 : 370–383. DOI: 10.1016/j.geomorph.2015.09.012

2.1. Introduction

In the internal, thickened, and uplifting parts of the orogens, rivers are expected to follow the regional slope and flow perpendicular to the structural trend of mountain ranges, a pattern always matched by numerical models of continental-scale surface processes (e.g., Koons, 1995; Kooi and Beaumont, 1996; Willett et al., 2001; Goren et al., 2014a,b). However, during mountain building, active folds and thrusts can deviate rivers from the regional slope (e.g., Van der Beek et al., 2002). Conceptually, the ability or not of preexisting reaches to incise uplifting structures controls the number of diversions, and by extension it determines the drainage organization, a phenomenon confirmed by modeling (Koons, 1994, 1995; Tomkin and Braun, 1999; Humphrey and Konrad, 2000; Champel, 2002; Van der Beek et al., 2002; Sobel et al., 2003). Additional factors such as bedrock lithology determine spatial changes in strength and erodibility, and climate may control changes in weathering and discharge.

Babault et al. (2012) showed in the High Atlas Mountains of Morocco (a thrust-fold belt formed by tectonic inversion of a continental rift) an evolution from early fold- and fault-controlled longitudinal rivers to a transverse-dominated drainage network during mountain building and crustal thickening in response to a progressive increase in regional slope. This may be a common transient mechanism of fluvial network evolution in mountain belts (Babault et al., 2013).

A fluvial capture implies changes in flow direction, that is, the flow/discharge of the captured drainage basin (victim) is deviated toward the neighbor captor basin with higher erosion potential caused by either higher local precipitation, erodibility, and/or slope (e.g., Brookfield, 1998). Unlike models that show progressive divide migration and small-scale capture events during mountain building (Willett et al., 2001; Pelletier, 2004; Bonnet, 2009; Castelltort et al., 2012; Perron et al., 2012; Goren et al., 2014), the model of evolution from longitudinal- to transverse-dominated drainage network implies captures of large longitudinal drainages and substantial modifications of sedimentary outflux into adjacent basins, potentially influencing clastic systems and petroleum reservoirs. Captures of longitudinal rivers by transverse rivers are episodic and initially localized, whereas the integrated long-term effect of the episodic capture events may be a major drainage reorganization as discussed in this work.

The aim of this chapter is to characterize the fluvial network and the drainage dynamics in the central segment of the Eastern Cordillera of the Colombian Andes, as a case for drainage reorganization. Like the High Atlas, the Eastern Cordillera of Colombia is an example of a thrust-fold belt formed by the inversion of a former continental rift and shows similarities in the fluvial network, with a high-elevation axial area dominated by low-energy longitudinal rivers and with flanking belts of high-relief transverse valleys debouching into the forelands. By means of field observations, morphometric analysis, and a review of published palaeodrainage data, I first document that a longitudinal- to transverse-pattern of fluvial evolution also applies to the Eastern Cordillera and then discuss a main mechanism that may have enhanced drainage reorganization (and captures), together with the potential implications for the downstream basin sediment supply.

2.2. Digital topographic analysis

Comparison of the paleodrainage data summarized above and the present-day fluvial network of the Eastern Cordillera of Colombia suggests that drainage has experienced a process of reorganization over geologic time. I undertook an analysis of the spatial distribution of the local and mean slopes, of the drainage network organization, and of the longitudinal profiles of the main rivers of the Cordillera with the aim of characterizing the river dynamics and the signal of reorganization in the current network. According to Bishop (1995), drainage rearrangement in mountain belts can be produced by beheading during progressive divide migration and by discrete events of capture, which are mechanisms of drainage expansion that result from headward erosion (Fig. 2.1A) The beheading process results in the nonpreservation of early drainages, and thus capture elbows (sharp changes in the river channel direction) and wind gaps (dry valleys with fluvial deposits) in the divide are not preserved. However, low-elevation zones (anomalous depressions) in the topographic profile of a divide may be the topographic expression of the migration of a divide originally located at the crest and later reaching the bottom of an adjacent valley, as reproduced in numerical models (e.g., Willett et al., 2001). Stream capture (piracy) can be identified by distinctive geomorphic features (e.g., Fig. 2.1B). These include the preservation of the early lines of the drainage network, elbows, and knickpoints (Small, 1978; Bishop, 1995).

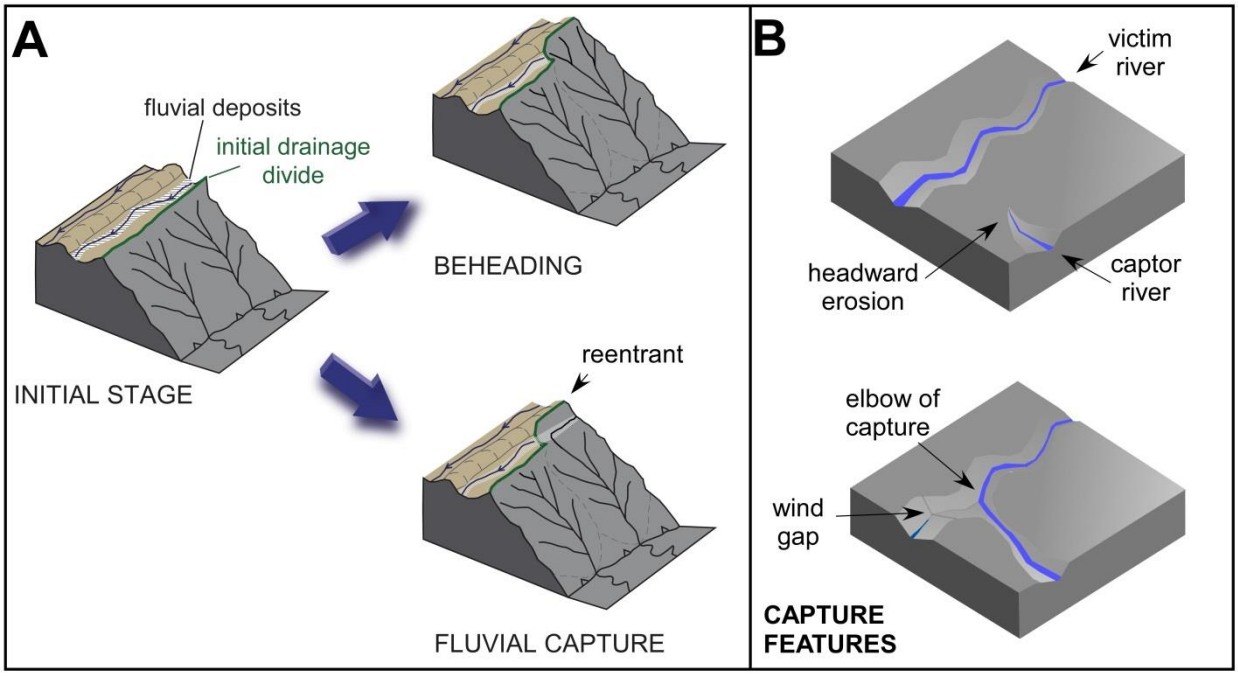

Fig. 2.1. *(A) Diagram showing the process of beheading and fluvial capture from the same initial stage. (B) Fluvial capture processes preserve the initial drainage lines and produce elbows and fluvial deposits in the divide (wind gap). These features do not occur in beheading.*

Elbows and knickpoints cannot be used separately as a diagnostic for captures because changes in rock uplift and river diversion may also produce them. Other features potentially indicating capture events are hanging depressions (wind gaps) or discrete jumps (or reentrants) of a drainage divide, but

they are seldom preserved in rapidly eroding settings like active orogenic belts (e.g., Clark et al., 2004; Prince et al., 2011; Brocard et al., 2012). Wind gaps correspond to segments of captured rivers where water no longer flows and show a width that is impossible to relate with the actual basin drainage area upstream (suggesting that they were created in past times with larger drainage areas). Stratigraphic evidence for captures include abandoned river terrace tracts and the existence of fluvial sediments with larger grain size than the current channel can transport or with lithologies linked to source areas that are now disconnected from the basin.

2.2.1. Methods

In this chapter I analyze the topography in the search of geomorphologic evidence for divide migration and captures as previously mentioned. Beheading and stream captures occur if disequilibrium of erosion exists between two catchments. I highlight potential disequilibrium of erosion by quantifying morphological differences between the axial plateau of the Sabana de Bogotá and the steep Cordillera flanks between latitudes 5º30'N and 4º10'N (see location in Fig. 1.2). I use the 90-m-resolution digital elevation model (DEM) SRTM90v4 (Jarvis et al., 2008) in the analysis. However, in areas where the fluvial channel is narrow (<90 m), the SRTM90 DEM leads to overestimated elevations in gorges, providing wrong data for river parameter extraction. Such errors were corrected using elevations from Instituto Geográfico Agustín Codazzi (IGAC) 1:100,000 topographic maps and then modifying the raster elevation matrix (DEM) pixel by pixel. Morphometric analysis and calculation of the geomorphologic parameters described in the following sections was carried out by using the D8 flow routine (eight-flow direction matrix; O'Callaghan and Mark, 1984; Tarboton, 1997; Mudd et al., 2014). I used that corrected DEM for all the analysis included in the thesis.

I compare the current drainage network geometry with the regional slope obtained by calculating the local slopes of the mean elevations. The mean elevations have been calculated with a moving window of 30 km of diameter. I compare the frequencies of elevations, the local slopes, and the channel slopes between the plateau and the western and eastern flanks of the Cordillera to highlight their topographic difference. In the supplementary data (SD.1) are the longitudinal river profiles of the main rivers draining the Sabana de Bogotá and the Cordillera flanks.

River erosion depends at least on bedrock erodibility, water flow, and slope (e.g., Howard and Kerby, 1983). Analysis of slope-area relationships is often used to reveal spatial trends of erosion and/or rock uplift in channel networks by the mean of the channel steepness index or Ksn (e.g., Kirby and Whipple, 2001; Kirby, 2003; Snyder et al., 2003; Wobus et al., 2006; DiBiase et al., 2010). Although it limitations, the slope-area analysis was usually applied to characterize the bedrock river profiles (e.g. Flint, 1974; Tarboton et al., 1989; Wobus et al., 2006). This limitations referred to i) uncertainty and noisy/artifacts elevation data in the DEMs, causing in scattered slope-area plots and, ii) the measured slope in a topographic map may differ from the reach slope (Perron and Royden, 2012). Therefore, for the

measurement of the normalized channel slopes I prefer an alternative methodology, the chi (χ) parameter. The χ method uses elevation instead of slope as the dependent variable, and a spatial integral of drainage area (χ) as the independent variable with units of distance. Assuming uniform *U* and *K*, and introducing a reference drainage area (A_0) in order to give units of length on both axes and integrating upstream, we applied the following equation with form of a line (Perron and Royden, 2012):

$$\chi = \int_{x_b}^{x} \left(\frac{A_0}{A(x)}\right)^{\frac{m}{n}} dx \qquad \textit{(eq. 2.1)}$$

where x_b is the base level elevation, the parameter χ is the result of the position integral, A_0 is the reference drainage area and *m/n* is the concavity (Willet et al., 2014).

For a given χ distribution, a gradient of this parameter can be obtained (Mx). The value of the channel slope in χ-elevation space (*Mx*) depends on the concavity, and I determine the best concavity with AICc-collinearity tests and χ-plots for each basin following the method developed by Mudd et al. (2014) (see SD.1 and 2). The AICc is a statistical method that selects a model that balances goodness of the fit against model complexity (Akaike Information Criterion, AICc) (Akaike, 1974; Hurvich and Tsai, 1989; Burnham and Anderson, 2002). Assuming that rock uplift is balanced by erosion (steady-state condition) and that uplift, erosion, and erodibility are constant in time and space, the stream power theory predicts that river profile will have a linear χ-plot and *Mx* is proportional to erosion rates (Royden and Perron, 2013; Mudd et al., 2014). However, transient states where uplift rates change spatially or temporally can lead to piecewise (stepped) channel profiles. In this case, I use the collinearity test to identify the concavity (*m/n* ratio) for each river basin that best collapses the tributaries in χ-plots (Mudd et al., 2014).

I generated topographic elevation profiles of the eastern and western main divides, and calculated their mean elevation using an adjacent-averaging smoothing method (over 900 and 550 km distance for the eastern and western divide, respectively). Smoothing with the adjacent-averaging method calculates the average of elevations around each point and replaces the actual elevation of the point with the average value. The location of the divide depressions (low-elevation segments) was compared with the geometry and characteristics of the current drainage network. A fluvial capture leaves depressed zones or gaps in the drainage divide where water does not actually flow (wind gaps). These depressed zones can have fluvial sediments relict of the old fluvial drainage network.

2.2.2. Analysis and results

The differentiation between the topographic domains of the Eastern Cordillera is evidenced by the results of the morphometric analysis. A first differentiation was observed in the geometry of the drainage network for each topographic domain for the central part of the Eastern Cordillera (Fig. 2.1), where the rivers located in the Sabana flow longitudinally to the main structres, and in the flanks, the rivers flow accros the tectonic elements.

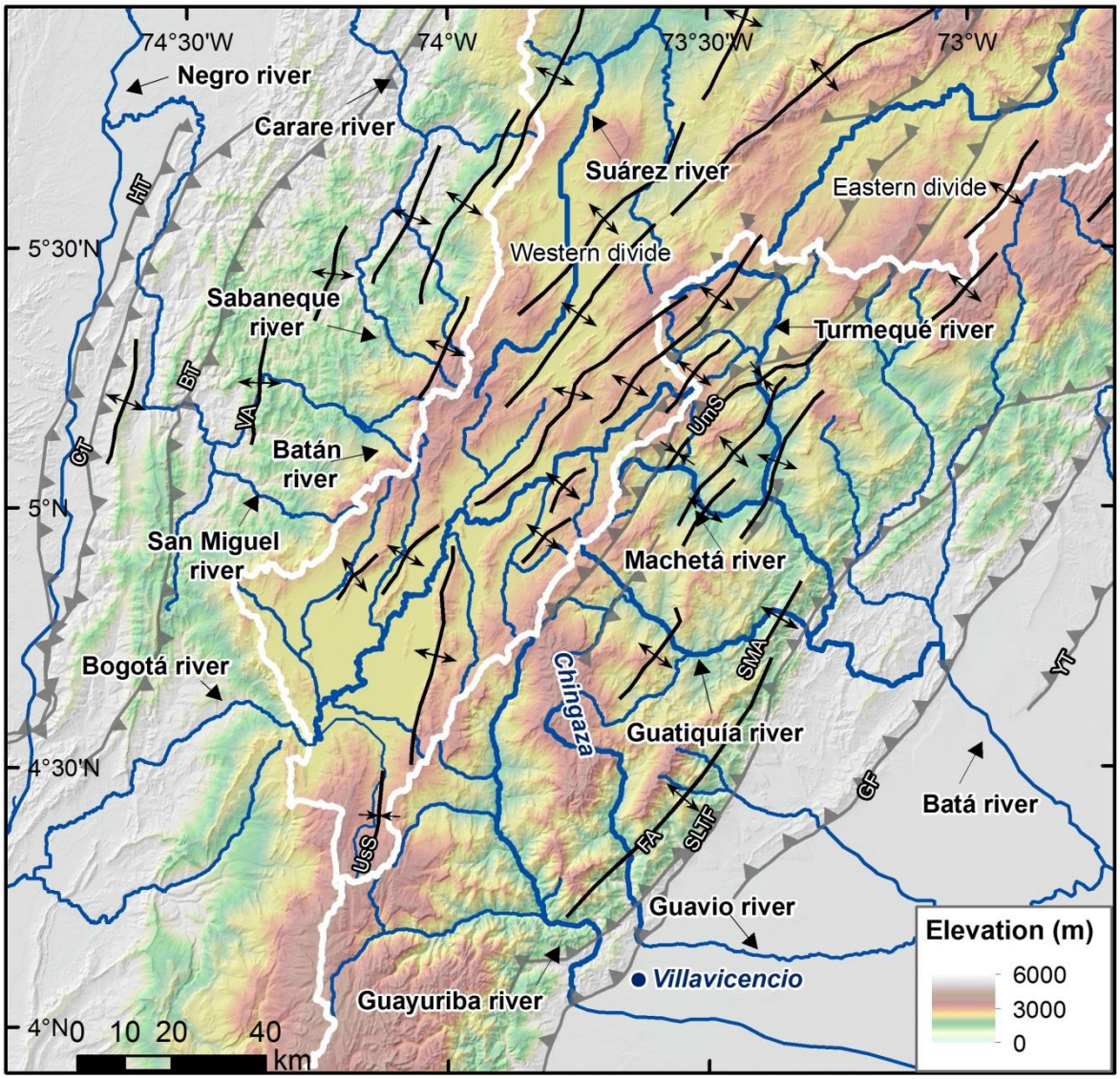

Fig. 2.1. *Main tectonic elements and rivers of the central part of Eastern Cordillera superimposed over digital topography. Thick white lines represent the western and eastern drainage divides between the axial plateau and flanks, and rivers are in blue (the main rivers highlighted by thicker lines). Grey barbed lines represent the main thrusts, and black lines represent the main folds. Rivers in the Sabana de Bogotá run parallel to the main folds, and rivers located in the flanks are transverse to the main tectonic structures. SLTF: Servitá-Lengupá, Tesalia faults; GF: Guaicáramo fault; YT: Yopal thrust; FA: Farallones anticline; SMA: Santa Maria anticline; VA: Villeta anticlinorium; BT: Bituima thrust; CT: Cambao thrust; HT: Honda thrust; UsS: Usme syncline; UmS: Umbita syncline.*

A first differentiation is based on hypsometric and slope frequency curves (Fig. 2.2). The plateau region shows a high frequency in elevation around 2500 m, corresponding to the average elevation of the Sabana plains (Figs. 2.2B and D). This region is also characterized by a high frequency (21%) of slopes of < 3° and secondary maxima close to 8º (14%) (Fig. 2.2C). On the other hand, the flanks of the Cordillera show a wider range of elevation. The eastern flank shows the highest frequency values close to 2300 m, whereas in the western flank they are close to 1300 m. The Cordillera flanks also show a higher local relief, with local slopes greater than 10º. Greater local slope values (>30º) are located in the external parts of the flanks coinciding with the frontal fold-thrust structures (Servitá, Lengupá and

Tesalia faults and Farallones anticline in the eastern flank; Bituima fault and Villeta anticlinorium in the western flank; see location in Fig. 2.1).

The Sabana de Bogotá plateau shows a short range of elevation, giving a high frequency in 2500 m. The Cordillera flanks are characterized by a wider range of elevation values.

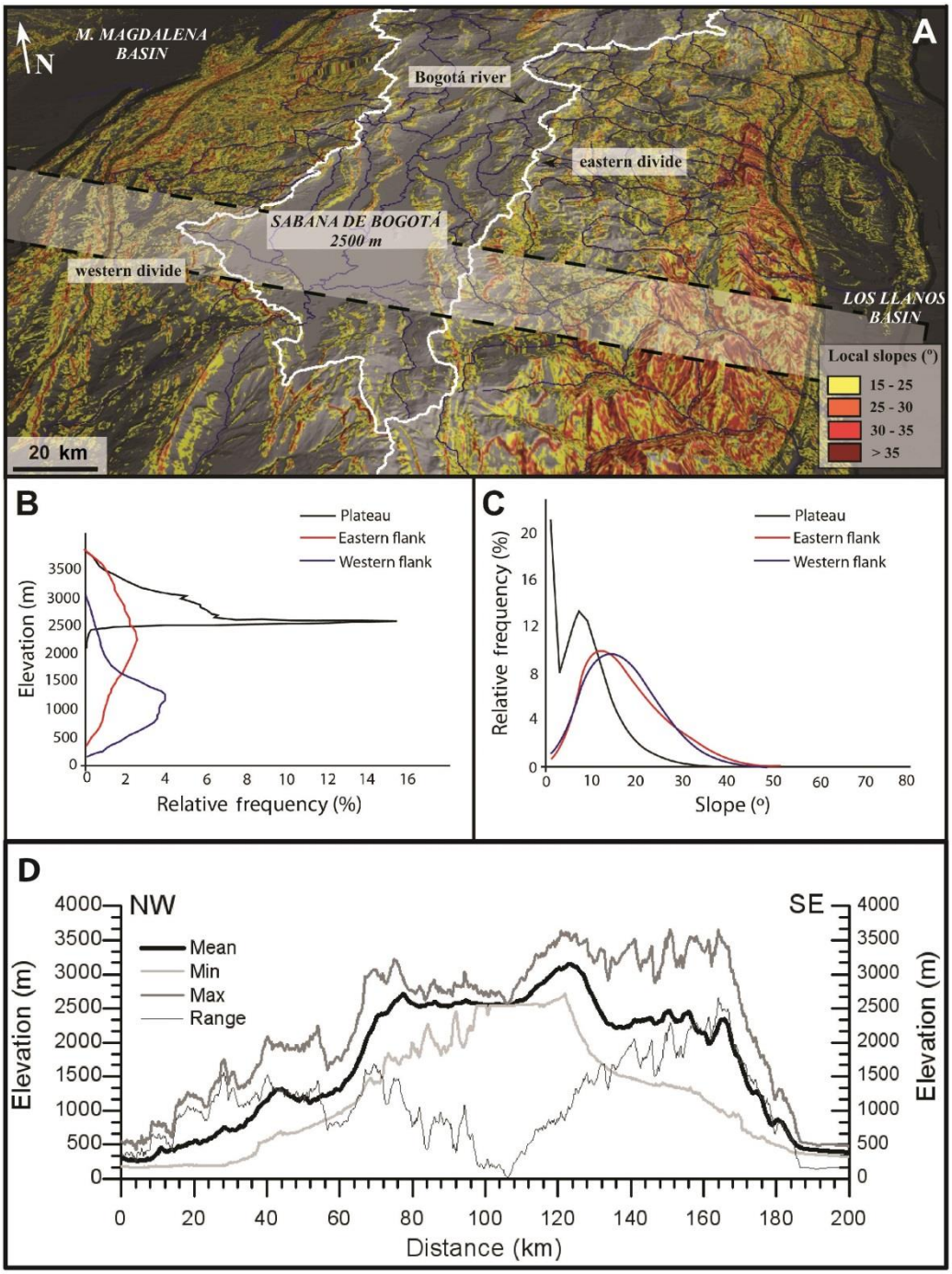

Fig. 2.2. *(A) Oblique view of the Eastern Cordillera indicating local slopes (in colors). The transparent white band indicates the location of the 30-km swath used for the elevation profiles in (D). (B) Plot of the relative frequency of elevations that characterize each topographic domain defined for the Eastern Cordillera. (C) Plot of relative frequency of slopes in each domain. (D) Orogen-transverse topographic profiles of the Eastern Cordillera along the swath indicated in (A), including maximum, minimum, and mean elevations and the elevation range (difference between maximum and minimum).*

The contrast between the plateau and the eastern flank is illustrated in Fig. 2.3, where we plot the long profile of the Guayuriba River in the eastern flank and the profile of the Siecha-Bogotá River in the plateau, including the projections of lateral divides and local relief for each one. The plateau area, represented in Fig. 2.3 by the Siecha-Bogotá river, is characterized by a low-elevation lateral divide and a very low local relief (500 m maximum). In contrast, the Guayuriba basin, in the eastern flank, is characterized by a higher-elevation lateral divide, as well as by a greater local relief (up to 2750 m).

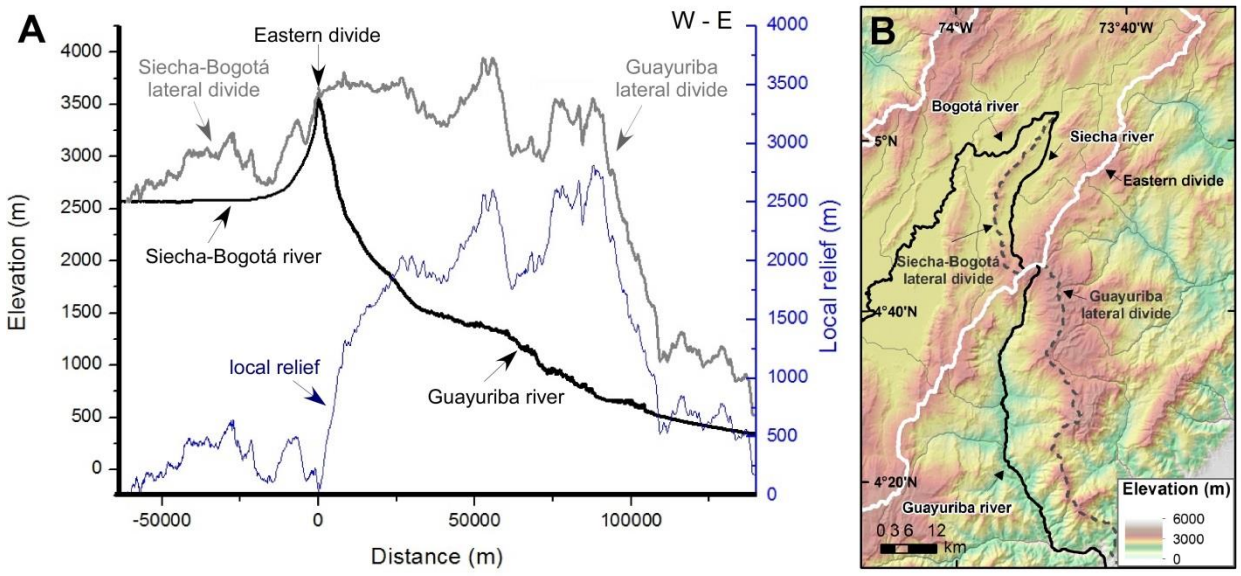

Fig. 2.3. *(A) Longitudinal profiles of the Siecha-Bogotá (Sabana de Bogotá plateau) and Guayuriba (eastern flank) rivers, compared with a projection of their lateral divides and the local relief (difference between maximum and minimum elevations) between rivers and divide ridges. (B) Location map of the rivers and divides shown in (A).*

Mean regional slopes in the Eastern Cordillera illustrate that the Sabana de Bogotá plateau is characterized by a very low mean regional slope of 1º (Fig. 2.4) and rivers follow the main structures longitudinally. Rivers in the eastern flank follow the regional slope, that is, to the east. The eastern flank shows greater mean slope values than the plateau, which becomes greatest in the lower part of the flank (mean values of 2.5º and, 4.5º respectively; Fig. 2.4). The western flank shows high values of regional slope (mean value of 4.5º) immediately west of the western divide where the main rivers are also transverse.

Significant variations in channel slope (expressed by *Mx*, the slope in χ-elevation plots) are not only observed between the Sabana and the flanks. Relevant variations in channel slope occur either along the same river or between different rivers in each domain. The *Mx* values were calculated in function of the best concavity for all basins analyzed. I found a 0.45 concavity as the best value based on the AICc-collinearity test and χ-plots (see supplementary data, SD.2 and SD.3).

The map distribution of the *Mx* index of major rivers (Fig. 2.4) shows generally low values (*Mx* 0-3) in the plateau area, coinciding with the lower regional slope and consistently with the results of digital analysis of local slopes and with field observations: rivers in the plateau show a meandering morphology

(Fig. 1.6C) as well as lower slope and runoff velocity than those in the flanks (Fig. 1.6D). The eastern flank shows *Mx* average values between 5 and 12, with peaks of 20-27. The greatest values are located in areas of recent tectonic uplift (e.g., Farallones and Santa Maria anticlines in the eastern flank; Mora et al., 2008) or in rivers with a drastic slope increase where they leave high-elevation, low-relief upstream areas like the Chingaza region (see Fig. 2.1). The *Mx* values in the higher parts of the western flank (bordering the divide), where rivers are transverse, range around 5-12, and the *Mx* values decrease in the lower part of the flank where rivers are longitudinal (*Mx* 1-4).

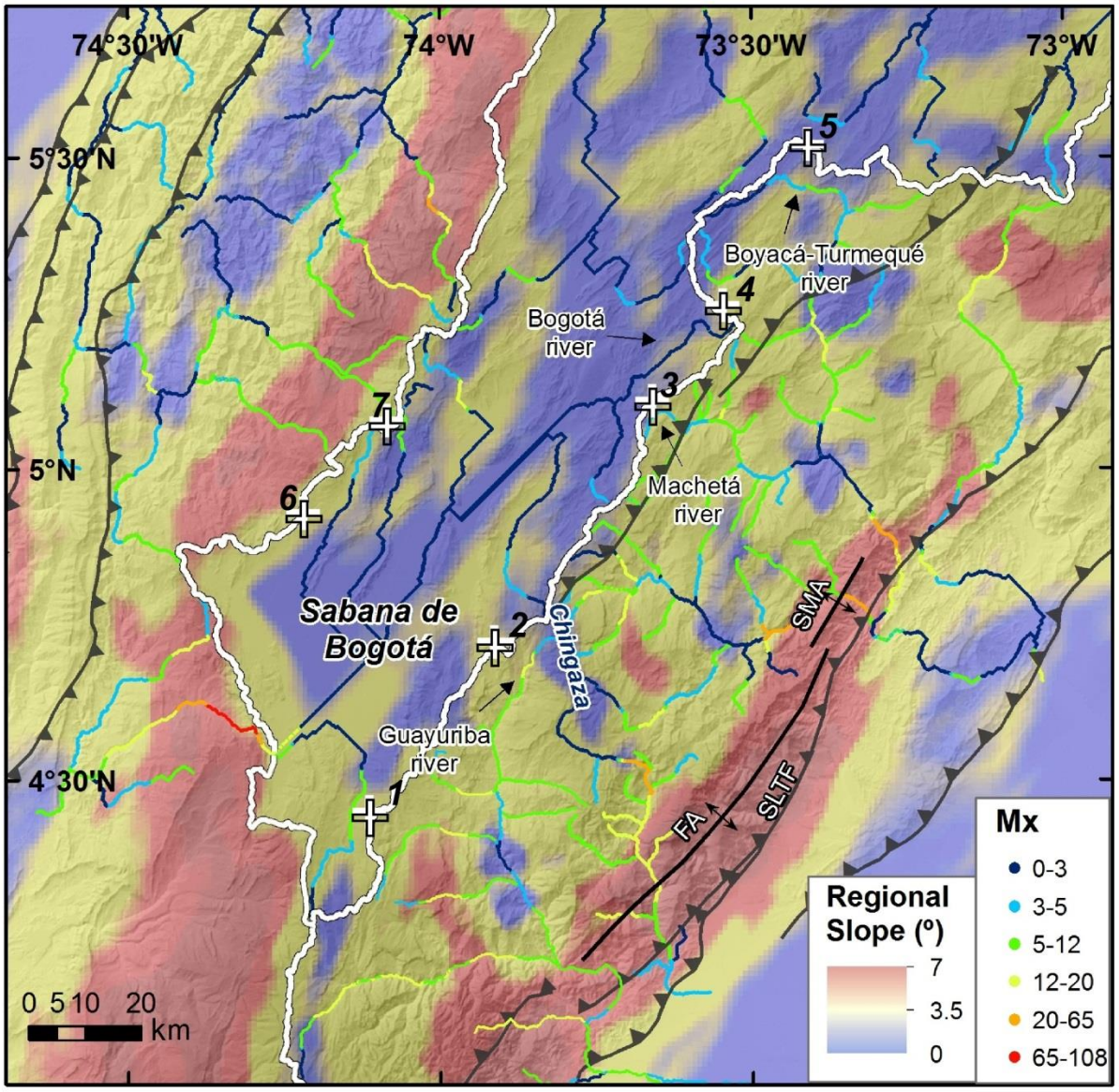

Fig. 2.4. *Map of Mx (slope in χ-elevation plots) values for the analyzed rivers and regional slope (º) calculated with a mobile window of 30 km diameter. The eastern and western divides are indicated by white lines. Note low Mx values in the Sabana de Bogotá and high values in the flanks of the Cordillera. Depressions in the divide ridges are indicated by white crosses and labeled with numbers from 1 to 7 (see text for discussion). FA: Farallones anticline; SMA: Santa Maria anticline; SLTF: Servitá-Lengupá-Tesalia fault.*

Topographic profiles of the two drainage divides separating the axial plateau of the Sabana de Bogotá from the eastern and western flanks (Fig. 2.5) show a series of depressions (low-elevation segments in

the divide) several hundreds of meters deep below the average elevation of the divide ridges. Depressions usually coincide with reentrants of the divide trace into the plateau (Figs. 2.4 and 2.5), i.e., segments of the divide that diverge from the main orientation and project toward the axial plateau of the orogen.

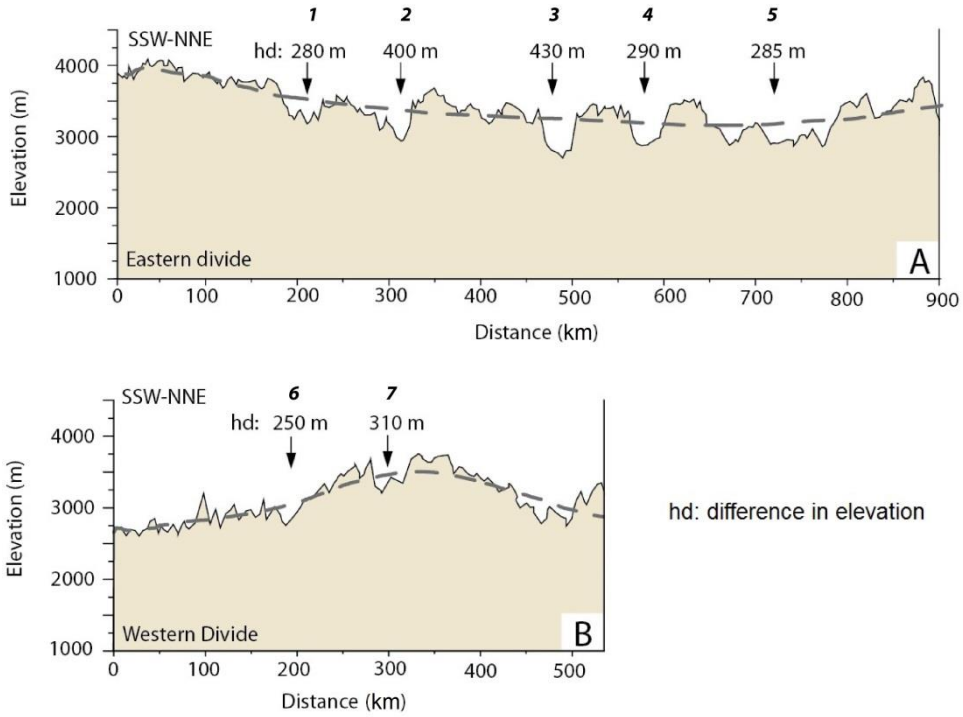

Fig. 2.5. *Profiles of the eastern (A) and western (B) drainage divides that bound the Sabana de Bogotá plateau showing the location of depressions (numbers in italic refer to Fig. 9). Additionally, we indicate the difference in elevation between the lower part of the divide (depressed area) and the mean elevation of the divide (dashed line).*

An illustrative example of a divide depression is observed between the Machetá and Bogotá rivers (see Fig. 2.1 for location). In the headwater of the east-flowing Machetá River, the elevation low in the divide (2700 m) rises only 50 m above the longitudinal river in the Sabana (2750 m) (Fig. 2.6A). Local slopes are higher to the east of the divide (15°) than to the west in the plateau (5°) (Fig. 1.6E). Farther north, the depression in the eastern divide between the Boyacá-Turmequé and Bogotá rivers is only 80 m above the latter (Fig. 2.6B). As in the case of the Machetá River, local slopes are higher to the east (20º) than in the plateau (10º). In addition, the *Mx* of rivers is higher in the flanks than in the plateau (Fig. 2.4), in agreement with the distribution of local slopes. The depressions are associated with elbow geometries with knickpoints in the downstream part of the longitudinal reach in the flank rivers, and I do not observe spatial correlations with the trace of active faults nor with easily erodible bedrock lithologies (Figs. 2.6C and D). Neither of these areas corresponds to zones of fold plunge (which could in principle provide low resistance to incision and favor capture localization). This lack of correlation between divide depressions or reentrants and tectonic structures or specific lithologies is observed all along the eastern and western divides of the Eastern Cordillera.

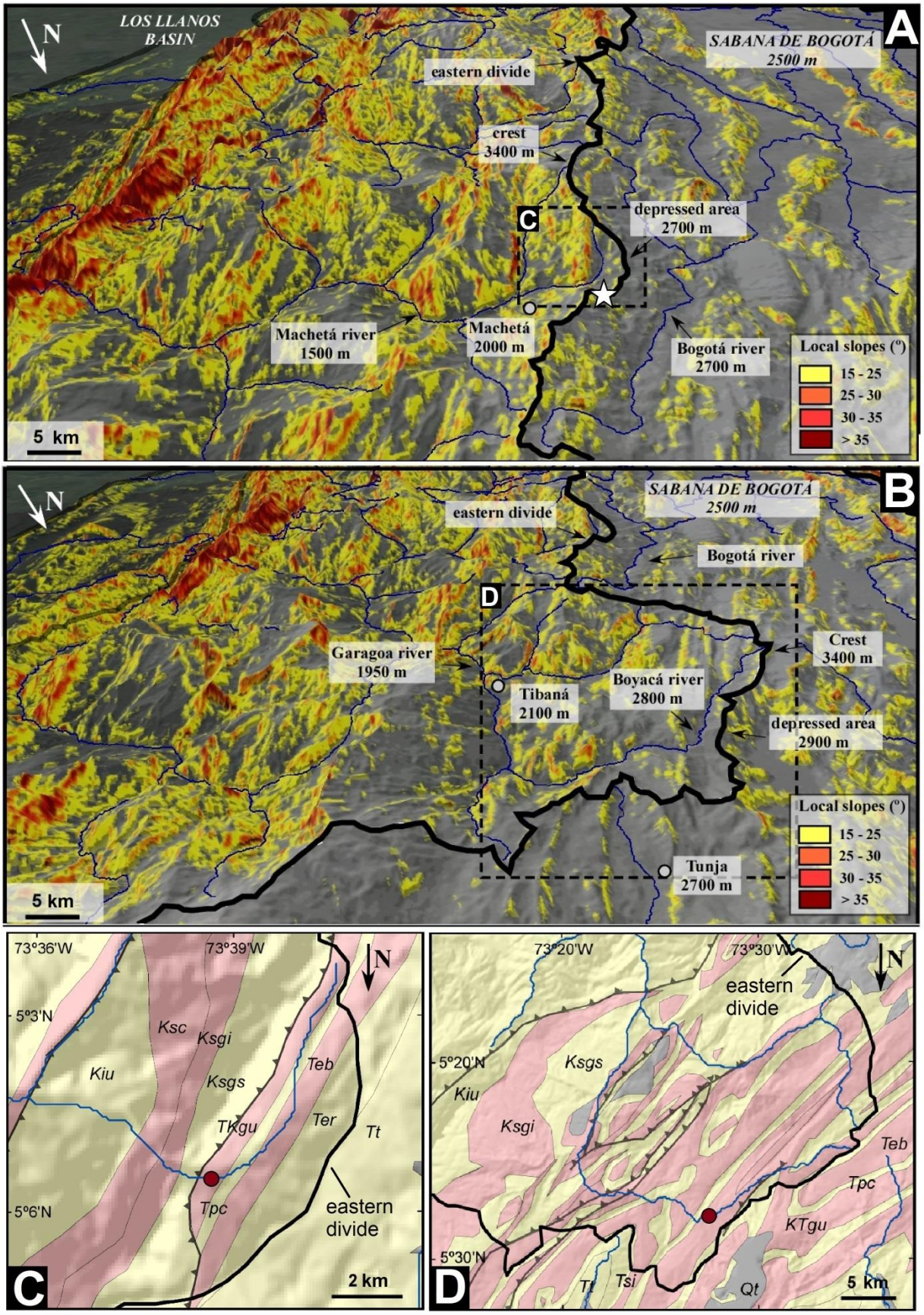
A
LOS LLANOS BASIN
N
SABANA DE BOGOTÁ 2500 m
eastern divide
crest 3400 m
C
depressed area 2700 m
Machetá river 1500 m
Machetá 2000 m
Bogotá river 2700 m
Local slopes (º)
15 - 25
25 - 30
30 - 35
> 35
5 km
B
N
SABANA DE BOGOTÁ 2500 m
eastern divide
Bogotá river
D
Garagoa river 1950 m
Tibaná 2100 m
Boyacá river 2800 m
Crest 3400 m
depressed area 2900 m
Local slopes (º)
15 - 25
25 - 30
30 - 35
> 35
Tunja 2700 m
5 km
73°36'W
73°39'W
N
5°3'N
Ksc
Ksgi
Kiu
Ksgs
Teb
TKgu
Ter
Tt
Tpc
5°6'N
eastern divide
C
2 km
73°20'W
73°30'W
N
eastern divide
5°20'N
Ksgs
Kiu
Ksgi
Teb
Tpc
KTgu
5°30'N
Tt
Tsi
Qt
D
5 km

Fig. 2.6.

2.2.3. River capture and evidence for drainage divide migration

At present, the main rivers flowing in the Sabana de Bogotá plateau are longitudinal and follow synclines constituted by Cenozoic strata, mostly terrestrial in origin. In the Cordillera flanks, the main rivers are transverse to the chain and they are deeply incised across Cretaceous and Paleogene folded series. As summarized above, during Paleocene-Oligocene times, the drainage network was controlled by the emerging folds and thrusts and followed a gentle regional slope to the NNE (Gómez et al., 2005a; Silva et al., 2013).

Incised transverse rivers that cut across the Paleogene folded series in the eastern flank are evidence of a strong contrast between the current flow drainage organization and the paleodrainage deduced from the Paleogene strata. The northern flow direction from palaeocurrent data in these Paleogene series are now incised by an eastern transverse flow. This is the case of the Tertiary Umbita and Usme synclines (Fig. 1.2). The Usme syncline, with a N-S orientation parallel to the mean trend of the orogen, records an Oligocene paleoflow in the same direction. Nevertheless, part of this syncline has been captured by a river of the eastern flank and now drains to the east, which indicates a migration of the main eastern divide toward the inner part of the Cordillera (the plateau) after the Oligocene. The Umbita syncline records a western flow in Paleocene times (see location in Fig. 2.1). This syncline is actually in the eastern flank and dominated by a transverse drainage flowing to the east (Figs. 2.6A and C). Paleogene strata are not preserved in the western flank of the Cordillera, and this line of evidence cannot be applied.

Captures usually leave gaps/depressions in drainage divides (e.g., Bishop, 1995). The topographic profiles of the main divides of the Eastern Cordillera show low-elevation tracts (Figs. 2.4 and 2.5). These depressed tracts coincide with map-view reentrants of the divide trace toward the plateau, suggesting a drainage area transfer from the plateau to the Cordillera flanks, as explained above. In addition, elbows with knickpoints at or above the elbow can be observed in these areas (see Figs. 2.6C and D), and the channel slope map (*Mx* values) (Fig. 2.4) also illustrates a strong topographic contrast across the main divides separating the Sabana plateau from its flanks.

Fig. 2.6. *Local slope and lithology distribution at the Eastern Cordillera of Colombia. Note that they are oriented with North to the bottom of the page for a better appreciation of the topography and drainage. (A) Oblique view showing local slopes in the Eastern Cordillera. A reentrant in the divide associated to a depressed area is indicated in Figs. 9 and 10, testifying to processes of fluvial capture with a difference in elevation of 430 m between the mean altitude of the divide and the bottom of the depression. The occurrence of rounded rockfall deposits (Fig. 3B) is marked by a white star (see text for discussion). (B) Oblique view indicating local slopes in the plateau and in the upstream part of the Boyacá-Turmequé transverse river. The reentrant area is indicated in Fig. 9 and corresponds to a depression in the elevation profile of the divide (see Fig. 10), with a difference in elevation of 285 and 290 m. (C) and (D) Lithologic maps of the depressed divide in (A) and (B), respectively, showing no lithologic or tectonic control on the divide depression and on its trace. Red polygons are shale formations and yellow polygons sandstone formations. The red circle shows the location of a knickpoint. Cretaceous and Tertiary sandstone formations: Kiu (Une Fm), Ksgs (Guadalupe Superior Fm), Tpc (Cacho Fm), Ter (Regadera Fm), Tt (Tilatá Fm), Tsi (Socha inferior Fm). Cretaceous and Tertiary shale formations: Ksc (Chipaque Fm), Ksgi (Guadalupe Inferior Fm), KTgu (Guaduas Fm), Teb (Bogotá Fm) (modified from Toro et al., 2004; Parra et al., 2009b, Mora et al., 2010; and unpublished maps by ICP-Ecopetrol).*

On the other hand, rounded rockfall deposits are locally found on the eastern divide into the Sabana plateau (Figs. 1.6B and 2.6A), where none of the current debris flow corridors observed in the slopes of the surrounding peaks lead to the rockfall deposit. This suggests that the missing crest that fed these boulders must have been eroded away, indicating divide migration toward the plateau.

On the assumption that erosion balances the local base level fall, the Mx value relates to the ratio between erosion rate and erodibility (Royden and Perron, 2013; Mudd et al., 2014). Therefore, the high *Mx* values observed in the Eastern Cordillera flanks suggest greater erosion rates than in the plateau. This may have favored the progressive divide migration toward the plateau and captures of longitudinal rivers previously flowing in the plateau by expanding transverse rivers in the flanks, thus providing an explanation for the contrast between the Eocene paleodrainage organization recorded in the Usme and Umbita synclines, and the current river network. I observe the same distribution of local slopes and channel slopes (*Mx*) between the western flank and the axial plateau, suggesting a similar migration in the western divide toward the centre of the Eastern Cordillera.

In summary, the depressions in the main divides, the occurrence in the flanks of knickpoints in the upstream parts of the longitudinal river profiles (e.g., Chingaza area), the existence of rock landslides with no source near the divide (Figs. 1.6B and 2.6), the observation of elbows in the rivers of the eastern flank with knickpoints upstream, and the contrast between the local slopes and the channel slopes of the main rivers support the view that the drainage network of the Eastern Cordillera reorganizes by progressive divide migration toward the inner part of the chain and by discrete events of capture. This is in agreement with the reorganization inferred from the contrast between the palaeocurrent data of the geological record and the present-day drainage network. The case of the Umbita and Usme synclines (where youngest strata are Oligocene in age) indicates that in those areas such reorganization did not start before the Miocene. As the main divides converge toward the centre of the Eastern Cordillera, and given the scarcity of Cenozoic strata in the Eastern Cordillera flanks, I cannot rule out that reorganization may have started earlier in the external parts of the eastern and western flanks.

2.3. Causes and implications of drainage reorganization

2.3.1. Mechanism causing drainage reorganization

Observations suggest that the drainage network in the Eastern Cordillera evolves from longitudinal-dominated to transverse-dominated, with rivers turning into the direction of the regional slope. The steep transverse rivers must have higher rates of incision than the gentle longitudinal rivers in the plateau to expand their catchment. At least four potential mechanisms that could explain differential erosion between the plateau rivers and rivers in the flanks can be considered.

First, a gradient of precipitation perpendicular to the trend of an orogen can result in divide migration toward the dry side, as has been observed in numerical models (e.g., Willett, 1999; Bonnet, 2009).

Figure 5 shows the annual precipitation for the period 1998-2009 in the Eastern Cordillera, where no precipitation gradient is observed across the eastern main divide. On the basis of evidence as stable isotope geochemistry from fossil and present-day growth bands in mollusks, from palynology, and from macroscopic paleoflora, Mora et al. (2008) suggested that the influence of the erosion processes by global climate change was negligible since the Pliocene in the region. The precipitation pattern appears to have remained similar at least since middle Miocene time (Mora et al., 2008, and references herein), coinciding with the early topographic growth causing the topographic asymmetry of the orogen (Mora et al., 2008). Moreover, an eastward gradient in moisture could not explain the similar contrast of morphology between the western flank and the plateau. Therefore, the reorganization of longitudinal to transverse drainage may not be attributed to an asymmetric precipitation pattern across the eastern divide.

Second, erodibility differences associated with lithological changes can explain spatial variations in erosion rates (e.g., Safran et al., 2005) and can produce local changes in the organization of drainage. In the Eastern Cordillera of Colombia, the depressions along the main divides are not located on less-resistant lithologies, and they occur indistinctly over shale or sandstone formations, from which I can conclude that the reorganization of the drainage is not controlled by lithology.

Third, in some mountain settings at mid-latitudes, different intensity of glacial erosion by valley or cirque glaciers may produce a divide migration toward the hillslopes receiving less insolation (Brocklehurst and Whipple, 2002). The Eastern Cordillera of Colombia is close to the equator so that the reorganization of drainage cannot be controlled by glacial erosion as eastern and western slopes receive the same amount of insolation. Indeed, I see unlikely that the small and poorly developed valley glaciers deduced for the Eastern Cordillera during the Quaternary (Helmens, 2004) contributed to an important difference in erosion between the flanks and the plateau, especially in view of the abundant fluvial geomorphologic features that point for drainage reorganization.

Fourth, longitudinal drainage largely coincides with areas where the regional slopes are low, whereas transverse rivers are related to higher regional slopes. The marked slope contrast between the flanks and the plateau appears to be the sole factor responsible for the higher erosional activity on the flanks. Consequently, I propose that the reorganization of the drainage network in the Eastern Cordillera is the result of increased regional slope. I interpret that the regional slope increase was acquired during orogenic shortening and crustal thickening of the mountain belt. The slope contrast between the axial plateau and the flanks associated with orogenic building promotes fluvial capture of the initial longitudinal drainage area by the transverse drainage system. The longitudinal-to-transverse drainage evolution thus deduced may represent a transient stage in mountain building, as previously discussed for the High Atlas Mountains of Morocco by Babault et al. (2012, 2013). Moreover, the occurrence of precipitation in the eastern flank will enhance the eastern divide migration toward the central part of the Cordillera.

The dynamics of drainage network described here is currently active in the Eastern Cordillera, and I can expect future captures to occur in areas where steep transverse rivers flow close to low-gradient longitudinal rivers located in the plateau, especially if they are separated by a low-elevation stretch of the main divide. As an illustrative example, the Batán river in the western flank threatens to capture the Frío River in the Plateau (zone 7 in Fig. 2.4).

2.3.2. Implications for sediment supply into the adjacent basins

Changes in the sediment supply, sedimentation rate and detrital composition are often considered to be caused by climatic and/or tectonic variations (e.g., Molnar and England, 1990; Stokes et al., 2002; Allen, 2008). Drainage reorganization can exert, alternatively, a control on the sedimentation rates (e.g., Mather, 2000; Stokes et al., 2002; Prince et al., 2011; Antón et al., 2012; Willett et al., 2014). Capture processes involve sudden changes in the drainage areas of the captor river and of the victim river. The captor river gains drainage area and therefore the erosion rate increases connecting an elevated catchment to a lower base level. The remnant drainage basin, the victim, experiences an erosion rate decrease as it loses headwaters and drainage area. These variations must affect the clastic fluxes at the outlets, and modify the spatial and temporal localization of the proximal clastic bodies at the toe of the thrust front. Therefore, with the reorganization of the drainage network in the Eastern Cordillera related to the increase of the regional slope, the transverse rivers located in the flanks increased their drainage areas against the rivers located in the Sabana. In this way, erosion of the captured areas may have enhanced sedimentation rates in the Llanos and Magdalena basins.

Previous works interpreted the distribution of maximum sediment thickness of the late Oligocene to Miocene Carbonera to Guayabo formations (which are coarse-clastic foreland basin deposits derived from the Eastern Cordillera) as associated with the orogenic loads (Parra et al., 2009a,b; Hermeston and Nemcok, 2013; Jimenez et al., 2013). Ipropose that the migration of the orogenic load is not the only mechanism to explain sedimentation rate increases, coarse-clastic inputs, and depocenter migration in the basins adjacent to the Eastern Cordillera. The process of fluvial drainage reorganization in the source areas of the mountain belt may have exerted an additional control.

2.4. Conclusions

The Eastern Cordillera of Colombia presents a clear differentiation into two topographic domains: an axial plateau dominated by gentle longitudinal rivers, with low local relief and slopes, and the flanks, with high local relief and slope dominated by steep transverse rivers. These domains are separated by two main drainage divides in the eastern and western sides of the Sabana de Bogotá plateau.

In the eastern flank of the Cordillera, the change in flow direction between the Paleogene palaeodrainage toward the NNE, parallel to the early tectonic structures, and the current drainage toward the SE, incising across folded Paleogene strata near the eastern divide, argues for drainage reorganization. This chapter highlights the convenience of morphological analysis to characterize

drainage reorganization and supports models of evolution of relief in mountain belts. Morphometric analysis and field observations show depressions and map-view reentrants in the main divides, debris flow deposits with no source near the divide, elbows with knickpoints upstream, and an evident contrast of the local and river slopes across the divides. This evidence indicates that the drainage network reorganizes by progressive divide migration toward the inner part of the chain by discrete events of capture.

I interpret that fluvial reorganization from longitudinal to transverse-dominated drainage in the Eastern Cordillera was triggered by the increase of the orogen regional slope by the progressive accumulation of crustal shortening and thickening. This pattern of drainage evolution is comparable to the drainage evolution described in other orogenic belts such as the Moroccan High Atlas. The evolution from longitudinal to transverse drainage in the Eastern Cordillera of Colombia may lead to a progressive area reduction and eventually a disappearance of the high plateau of the Sabana de Bogotá.

Chapter 3

Plateau reduction by drainage divide migration in the Eastern Cordillera of Colombia defined by morphometry and ^{10}Be terrestrial cosmogenic nuclides

in review in Earth Surface Processes and Landforms, 2016

Summary

Catchment-wide erosion rates were defined using 10Be terrestrial cosmogenic nuclides for the Eastern Cordillera of the Colombian Andes to help determine the nature of drainage development and landscape evolution. The Eastern Cordillera of Colombia, characterized by a smooth axial plateau bordered by steep flanks, has a mean erosion rate of 11 ± 1 mm/ka across the plateau and 70 ± 10 mm/ka on its flanks with local high rates of > 400 mm/ka. The erosional contrast between the plateau and its flanks argues for a main slope contrast factor to explain the drainage evolution of the Eastern Cordillera. The erosion rates together with digital topographic analysis show that the drainage network is dynamic and confirms the view that the drainage divide in the Eastern Cordillera is migrating towards the interior of the mountain belt resulting in progressive drainage reorganization from longitudinal to transverse-dominated rivers and areal reduction of the Sabana de Bogotá plateau.

Key words: Cosmogenic nuclides; Erosion rates; Divide migration; Eastern Cordillera of Colombia.

3.1. Introduction

Rift inversion and/or crustal thickening lead to dramatic topography and drainage network changes in mountain belts that are mainly controlled by major tectonic structures (e.g. Van der Beek et al., 2002). The evolution and development of drainage systems in active orogens has attracted much attention recently, particularly regarding how transverse and longitudinal drainages, and drainage divides evolve (e.g. Willet et al., 2001, 2014; Pelletier 2004; Bonnet et al., 2009; Castelltort et al., 2012; Perron et al., 2012; Goren et al., 2014). Clear examples of drainage rearrangement in relation to progressive mountain building have been described in the inverted rifts of the High Atlas of Morocco (Babault et al., 2012) and of the Eastern Cordillera of Colombia (Babault et al., 2013; Struth et al., 2015). These studies highlight that drainage divides are dynamic features that progressively migrate and result in river capture events. Evidence for differential erosion rates on either side of a drainage divide adds much credence to developing and substantiating drainage evolution models for mountain belts (e.g. Willett et al., 2014). As such, the side of a mountain belt with the greatest erosion will progressively migrate and capture drainages from the side with the least erosion. Theoretically, a dynamic drainage network will evolve towards a steady state, maintaining a steady drainage network and stationary drainage divides (Howard, 1965).

The Eastern Cordillera of Colombia is an example of an orogen with a dynamic drainage network (Babault et al., 2013; Struth et al., 2015). Recent studies have suggested that the increase of regional slopes due to progressive crustal thickening results in fluvial reorganization from longitudinal to transverse dominated drainages in the Eastern Cordillera (Babault et al., 2013; Struth et al., 2015). On the basis of a morphometric analysis, field observations and a summary of paleodrainage data, these studies conclude that drainage reorganization takes place by progressive drainage divide migration toward the axial zone of the orogen by a progressive series of river captures.

In this study, I build on Chapter 2 by using terrestrial cosmogenic nuclides (TCNs) in fluvial sands to determine catchment-wide erosion rates for the Eastern Cordillera to investigate the contrasting erosion dynamics between the Sabana de Bogotá axial plateau and the Cordillera flanks. TCN analysis is combined with a comparative analysis of channel gradients, specific stream power and χ values (the integral of the drainage area). I also examine the role of local tectonics, lithology, and climate conditions as a control on drainage evolution.

3.2. Methods

3.2.1. Analysis of the digital drainage network

Some geomorphic parameters provide information about the erosion trends in channel networks and therefore information about the dynamism of the drainage. The most important parameters are the stream power, the steepness index and the χ parameter. I calculated all of these parameters to

characterize the contrast between the topographic domains of the Sabana plateau and its flanks, and to identify the parameter with the best correlation with the TCN-derived erosion rates. I propose that a correlation between geomorphic parameters and TCN-derived erosion rates may allow a first estimation of erosion rates in areas devoid of TCN data.

As was described in Chapter 2, analysis of slope-area has been frequently used to reveal erosion trends in channel networks defined as steepness index or Ksn (Kirby and Whipple, 2001; Kirby, 2003; Snyder et al., 2003; Wobus et al., 2006; Dibiase et al., 2010). Nevertheless, local slope data in regions of low DEM resolution such as the Eastern Cordillera of Colombia is scattered and results in inaccurate estimates of Ksn. For this reason, we calculate the channel slopes using χ gradient, following the methodology in Chapter 2 (Mx; Perron and Royden, 2013; Mudd et al., 2014). By fixing the concavity we compared the Mx values between different catchments.

Stream power theory predicts that river profiles will have a linear χ-plot and a Mx proportional to the erosion rates, assuming, firstly a steady-state condition, where rock uplift is balanced by erosion, and, secondly that erosion, erodibility and uplift are constant through time and space (Royden and Perron, 2013; Mudd et al., 2014). In reality, U and K can be variable in time and space dependent upon the tectonic and climatic history, and rock types. To solve this problem, we calculated the concavity for all the basins following the method of Mudd et al. (2014) by extracting the steepness index, knickpoints and localize all the known active structures as well as highly erodible lithologies. In the case of stepped channel profiles associated to spatial or temporal changes in uplift rates, we used the collinearity test to identify the best concavity for each catchment (Mudd et al., 2014). This technique allows identification of the magnitude and distribution of the erosion rates.

To extract information about the dynamism of the catchments, we extract the χ map following the method of Willett et al. (2014) with a same base level determined by the area of study and the elevation of the most external tectonic structures (300 m asl) and with a critical drainage area of 1 km^2. The main interest of this analysis lies on mapping differences in χ-coordinate values across drainage divides. Similar χ values on both sides of a drainage divide suggest that the region is in equilibrium, while large differences in χ values across the drainage divide imply river networks in disequilibrium where divide migration or river capture is likely to occur (Willett et al., 2014). Drainage divides generally migrates towards the higher χ values to achieve equilibrium, and hence, catchments with high values are prone to capture and may eventually disappear (Willett et al., 2014). I extracted the χ-map for the entire central segment of the Eastern Cordillera as a proxy for the dynamics of the drainage divides using a modified version of χ that makes a correction factor for the precipitation (Yang et al., 2015), where the χ value is defined by the following equation :

$$\chi(x) = \int_0^x \left(\frac{P_0 A_0}{A(x')P(x')}\right)^{\frac{m}{n}} \mathrm{d}x' \qquad \textit{(eq. 3.1)}$$

where P_0 and A_0 are arbitrary scaling factors for the precipitation rate and drainage area, P is precipitation rate and A is the upstream drainage area and *m* and *n* are empirical and non-integer constants.

Additionally, we calculated an averaged specific stream power (SSP, eq. 3.2, Knighton, 1999) for each catchment following the method described in Godard, (2012) such that:

$$SSP = d \cdot g \cdot Ksn \cdot Q / W \qquad \textit{(eq. 3.2)}$$

where *d* is density, *g* is gravity, *Ksn* is the channel slope, *Q* is discharge and *W* is the channel width.

3.2.2. Cosmogenic nuclides analysis

Sediment samples were collected for ^{10}Be analysis to investigate erosion contrasts between the Sabana plateau and the flanks, including the main streams and major tributaries in the Guayuriba and Turmequé (representing the eastern flank of the Cordillera), Bogotá (Sabana de Bogotá plateau) and upper Suárez catchments. Rivers in the eastern flank and plateau have their headwaters on the same drainage divide, which allows us to make direction comparison between them. Additionally, I analyzed four TCN samples in the low Suárez and Chicamocha catchments (Fig. 3.1, Table 3.1) to examine the effect of a different vegetative cover, bedrock weakness and climate. These four samples are not included in the comparative analysis between the plateau domain and the eastern flank.

The largest the catchment area sampled (above the sampling locality), the higher probability to include mixed fluvial signatures. In such cases, the erosion rate obtained may not be representative of all the reaches of that river, which may have experienced a diverse reorganization history.

Catchments including a relict flat area in the upper part (Chicamocha, Suárez, Bogotá and Turmequé), reflect two different erosion regimes separated by a knickpoint (white stars in Fig. 3.4). As such the upper part the catchment should have lower erosion rates (related to the low relief, slopes, Mx) compared to those downstream of the main knickpoint. The Turmequé catchment constitutes a good example of that, with an ancient plateau domain above the main knickpoint where the erosion rates are low (LUCN-45, 26) and higher in its lower reaches (LUCN-25, 27, 28). I only sampled in the upper part of the Bogotá catchment (LUCN-15, 19, 30, 31, 33) above the Tequendama Falls (see Fig. 3.2 for location) to define the amount of erosion in its lowest erosion rate domain. Finally, for the Suárez catchment, I sampled its gently sloping upper reaches (LUCN-46, 50) and for the steeper lower reaches below the knickpoint (LUCN-53, 55). Only one sample (LUCN-53) was collected in the Chicamocha valley catchment, which was located downstream of the main knickpoint.

I collected ~1 kg of sand for each sample. Catchment areas for each sample were large (>100 km^2) as the recommended by Niemi et al. (2005) and Yanites et al. (2005) to provide a good representation of the ^{10}Be TCN inventory and its erosion rates. To compare the erosion rates between the Sabana and the flanks of the Cordillera, I use the erosion values obtained in the upstream reaches of the flank rivers. These rivers are composed by alternation of sandstone and shale formations in a proportion

which is similar across the different basins and the Sabana so to reduce the possibility of lithological biasing of our samples. I followed the sampling methods of Carretier et al. (2015), who collected fluvial sand from the subcatchments to minimize issues associated with local lithologic variations. The erosion rates determined by ^{10}Be reflect erosion on timescales of tens of thousands of years. Additionally, I sampled rivers across the western flank of the Eastern Cordillera but we could not determine ^{10}Be concentrations because they were dominated by argillaceous rock, which have very little quartz in them that is required for ^{10}Be analysis.

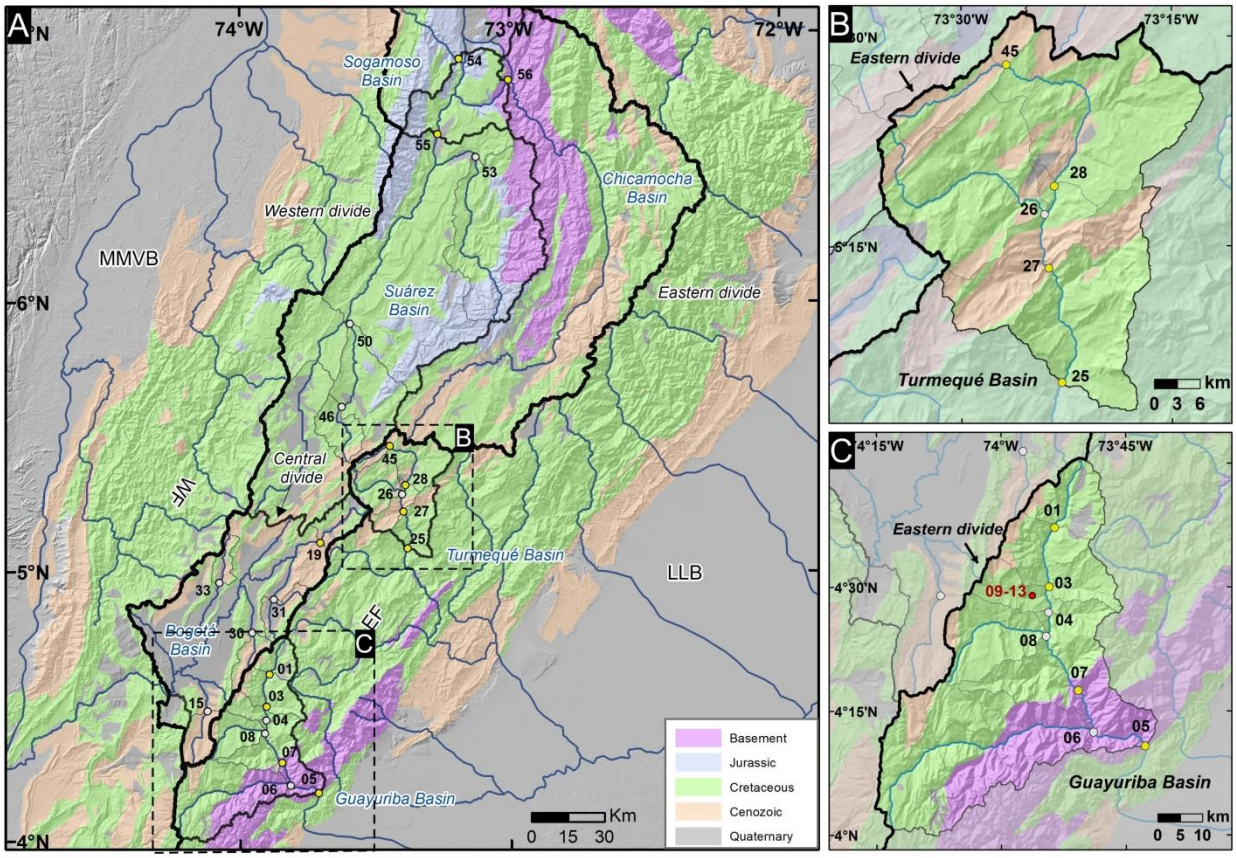

Fig. 3.1. *(A) Location of the fluvial sand samples from the trunk river (yellow) and tributaries (white) collected for ^{10}Be analysis. Detailed locations of sampling sites in (B) the Turmequé catchment and (C) for the Guayuriba catchment. Red point and label shows the location of the terrace boulder samples. LLB: Llanos Basin; MMVB: Middle Magdalena Valley Basin; EF: Eastern flank; WF: Western flank*

Sample Number	Qz wt (g)	^{9}Be carrier weigth (g)	Latitude (^{o}N)	Longitude (^{o}W)	Altitude (m)	^{10}Be/^{9}Be (10^{-15})	# of Be-10 atoms (10^{3} at/g)
LUCN-01	30.4250	0.3504	4.6201	73.8926	2011	205.91±83.26	162.11±6.55
LUCN-03	23.7496	0.3506	4.5006	73.9040	1565	151.52±9.19	152.90 ±9.27
LUCN-04	30.7997	0.3516	4.4491	73.9048	1466	192.99±9.29	150.61±6.47
LUCN-05	29.6340	0.3514	4.1795	73.7116	719	28.07±4.20	22.76±3.40
LUCN-06	28.7791	0.3502	4.2077	73.8151	928	23.22±2.35	19.31±1.96
LUCN-07	30.3416	0.3504	4.2916	73.8455	1237	127.45±8.80	100.61±6.95
LUCN-08	30.0654	0.3510	4.4008	73.9100	1413	165.88±6.76	132.38±5.39
LUCN-15	30.3979	0.3496	4.4830	74.1217	2686	1225.00±19.35	963.09±15.21
LUCN-19	30.7441	0.3556	5.1087	73.7042	2631	1295.97±27.81	1024.71±21.99
LUCN-25	30.5609	0.3499	5.0873	73.3811	1349	213.23±6.60	166.88±5.16
LUCN-26	30.0070	0.3498	5.2879	73.4013	1953	852.14±15.19	679.07±12.11
LUCN-27	24.3370	0.3504	5.2237	73.3964	1797	200.61±5.61	197.45±5.52
LUCN-28	14.6113	0.3512	5.3216	73.3897	2020	135.99±4.53	223.44±7.44
LUCN-30	30.6254	0.3549	4.7742	73.9559	2516	855.50±22.39	677.71±17.73
LUCN-31	30.1409	0.3496	4.8982	73.8769	2607	3850.15±49.01	3052.79±38.86
LUCN-33	30.4318	0.3520	4.9595	74.0777	2621	1958.19±52.60	1548.36±41.59
LUCN-45	30.8061	0.3500	5.4666	73.4464	2762	3068.09±85.63	2382.89±66.50
LUCN-46	17.5983	0.3510	5.6125	73.6243	2113	944.56±20.83	1287.87±28.40
LUCN-50	21.3327	0.3498	5.9204	73.5932	1641	875.76±17.04	981.67±19.10
LUCN-53	29.7526	0.3502	6.5387	73.1259	1108	226.44±5.57	182.20±4.48
LUCN-54	21.8547	0.3506	6.9023	73.1873	354	52.17±6.16	57.21±6.76
LUCN-55	30.3494	0.3496	6.6232	73.2669	506	164.48±4.95	129.52±3.90
LUCN-56	29.8878	0.3495	6.8246	73.0055	555	63.06±2.66	50.41±2.12

Table 3.1. *^{10}Be sample details for rivers of the Eastern Cordillera including location, Be carrier weigth and ^{10}Be concentrations measured. Carrier concentration was 1.023 ppm. See sample location in the map of Fig. 3.*

I also collected five quartzite samples for ^{10}Be TCN surface exposure dating from a rare well-preserved river terrace in the Guayuriba basin (Fig. 3.1C, Table 3.2). The sampled terrace, which lies at ~406 m above the current stream, is not deformed, and there is no evidence of erosion or landsliding. I collected ~500 g rock from the upper surfaces of fresh quartzite boulders. Topographic shielding was calculated by measuring the inclination to the skyline in eight directions following the approach by Balco et al. (2008).

Sample	**Quartz mass (g)**	**^{9}Be carrier weigth (g)**	**Latitude (^{o}N)**	**Longitude (^{o}W)**	**Altitude (m asl)**	**height/width /breadth clast (cm)**	**Thickness (cm)**
LUCN-09	29.765	0.3494	4.4659	73.9325	2133	30/60/80	2
LUCN-10	30.936	0.3503	4.4672	73.9329	2135	40/40/60	4
LUCN-11	28.108	0.3519	4.4675	73.9323	2131	40/180/150	3
LUCN-12	29.743	0.3512	4.4675	73.9322	2129	40/200/400	2,5
LUCN-13	28.115	0.3516	4.4675	73.9317	2125	50/150/120	3

Table 3.2. *Description for the quartzite boulders on a river terrace in the Guayuriba valley with a shielding value of 1 for all the samples. See sample location in the map of Figure 3.1C.*

Quartz isolation, purification, dissolution and preparation of BeO were undertaken in the geochronology laboratories at the University of Cincinnati following the methods of Kohl and Nishiizumi (1992) and described in detail in Dortch et al. (2009). All river sediment and terrace boulder samples were crushed to 250-500 μm for the analysis. Samples were cleaned using HNO_3, HCl and HF and past through a Frantz magnetic separator. Density separation was undertaken using lithium heteropolytungstate followed by an additional HF leach (Brown et al., 1991; Kohl and Nishiizumi, 1992; Cerling and Craig, 1994). For each sample, 15-30 g of clean quartz grains was dissolved in HF and HNO_3 with 350 mg of ^{9}Be carrier. Beryllium was separated using anion and cation exchange columns (Bourlès, 1988; Brown et al., 1992). $^{10}Be/^{9}Be$ ratios were measured by Accelerator Mass Spectrometry in the Purdue Rare Isotope Measurement (PRIME) Laboratory at Purdue University, Indiana, USA.

I took the standard approach and assume that the amount of ^{9}Be in the prepared quartz is negligible. Sometimes this is not true, and quartz may contain some ^{9}Be. This is rare, and almost invariably occurs when the quartz is from a beryl-bearing granite or pegmatite, so that there high traces of Be and/or small amounts of beryl in the supposedly pure quartz sample, as in some parts of the Himalaya (Portenga et al., 2015). However, pegmatites and beryl-bearing granites are not present in our study area. It is therefore highly unlikely that any significant native ^{9}Be is present in our quartz. However, if native ^{9}Be is present then denudation rates calculated from ^{10}Be concentrations will be overestimates, and the calculated erosion rates should be considered as apparent and can be used for comparisons of variation across a region of similar lithologies (Corbett et al., 2013; Portenga et al., 2015).

To model catchment-wide erosion rates from ^{10}Be results I assumed that: i) the sediment volume is proportional to the erosion rate, i.e., the basin is close to the steady-state; ii) all the sediment collected at the sample point was well mixed; iii) the contribution of quartz was homogeneous in the catchment; iv) that there is an isotopic equilibrium within the catchment, i.e., TCNs production in the catchment equals the transport of TCNs out of the catchment; and v) the denudation timescale was significantly larger than the sediment transfer through the catchment (e.g. Lal and Arnold, 1985; Granger et al., 1966; von Blanckenburg, 2005).

The corrected catchment-averaged production rates for ^{10}Be were calculated for each catchment using the SRTM90 digital elevation model, following the method of Dortch et al. (2011) using MATLAB v. 2008 and the scaling factors provided in Lal (1990) and Stone (2000). With this method, the production rate for each pixel is calculated accounting for shielding to make an average for all the pixels in the basin to obtain a spatially average production rate for the entire catchment (Lal, 1991). I use a ^{10}Be half-life of 1.36 ± 0.07 Ma (Nishiizumi et al., 2007).

^{10}Be ages for the river terrace samples were calculated using the CRONUS calculator (http://hess.ess.washington.edu/math/; Balco et al., 2008), using the scale model of Lal (1991) and Stone

(2000) and a sea-level high-latitude production rate of 4.49 ± 0.39 ^{10}Be atoms/g SiO_2/a. These ages will be minimum values and hence the resulting incision rates are maximum values.

3.3. Results

3.3.1. Digital drainage analysis

I analyzed the drainage network for the Eastern Cordillera of Colombia by quantifying the potential capacity of streams to incise (Specific Stream Power - SSP; Godard et al., 2012), channel slope gradients (extending the previous results on Chapter 2) and by mapping the χ-parameter (Willett et al., 2014).

The variation of the SSP values defines two substantially different scenarios in the Eastern Cordillera (Fig. 3.2). The axial zone, which includes the Sabana de Bogotá and the southern part of the Sogamoso basin, is characterized by the lowest SSP values. However, higher SSP values occur on the flanks and in the northern areas of the Sogamoso basin, which argue for higher erosion rates than in the axial zone of the Cordillera.

In this work, I present an extended Mx map for the Eastern Cordillera of Colombia, on the basis of the previous data reported in the Chapter 2 (Struth et al., 2015) that were limited to the area between 4°N and 5°30'N.

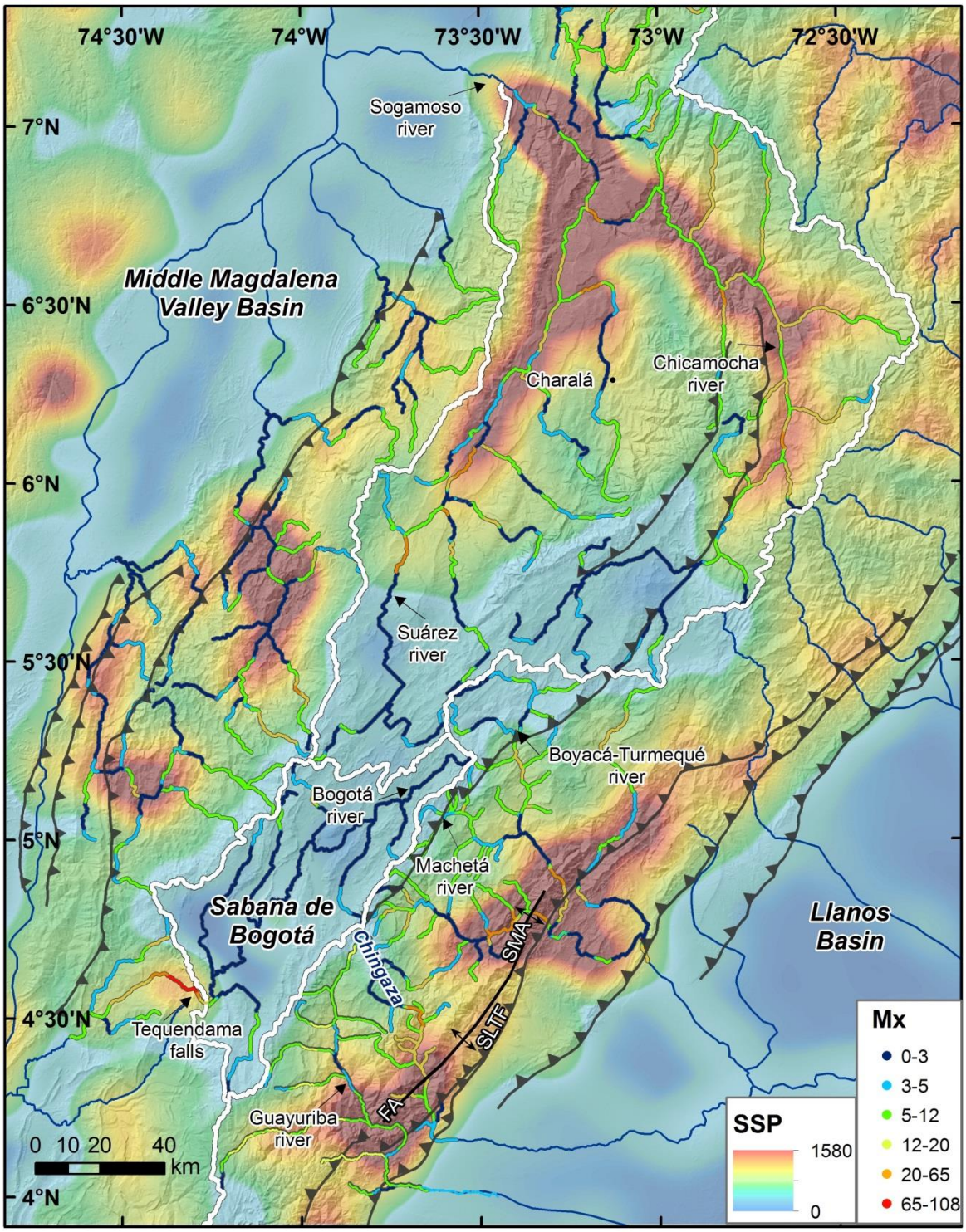

Fig. 3.2. *Distribution of specific stream power (SSP) values and Mx parameter (slope in χ -elevation plots) values for the analyzed rivers in the Eastern Cordillera of Colombia. White lines indicate the eastern and western drainage. χ plots are included in the Supplementary Data.*

Mx values show a map distribution similar to the SSP, with higher values on the flanks and in the northern part of the Sogamoso basin than in the axial zone. In Sabana and the southern part of the Sogamoso basin, the incision capacity is low (low SSP) and values of Mx are also generally low (Mx=0-3). The eastern flank has Mx average values between 5 and 12, with peak values between 20 and 27. The

greatest Mx values are located in areas of recent tectonic uplift such as the Farallones and Santa Maria anticlines (Mora et al., 2008), or where rivers dramatically increase gradient when they exit the high-elevation plains such as at the Tequendama Falls or at Chingaza (see location in 3.2). The upper Sogamoso basin, with northward drainage, has low values similar to the Sabana de Bogotá. The Suárez basin has values between 4 and 7, while the Chicamocha basin has values between 6 and 12. Local high Mx values that occur along the Suárez and Chicamocha rivers are located where deep fluvial incision starts. Mx values in the higher parts of the western flank (bordering the divide), where rivers are transverse, range around 5 to 12, and values decrease to between 1 and 4 in the lower part of the flank where rivers are longitudinal. River profiles in χ space are shown in the Supplementary Data (SD.3).

The χ values calculated for the Eastern Cordillera (Fig. 3.3) are clearly different to those of west and east of the divides, with higher χ values in the axial region of Sabana de Bogotá, near the divide, than along the flanks. A large range of χ values exist within the same domain showing, for example, a strong differentiation between the Sabana de Bogotá (low values near the central divide) and the Sogamoso basin (high values near the divide; Fig. 3.3B1). In addition, χ values indicate disequilibrium between the Turmequé (with low values) and the Chicamocha (with higher values near the divide) basins (Fig. 3.3B2).

In summary, the plateau and flanks domains within the Eastern Cordillera are clearly evident from the geomorphic indices. Low SSP, Mx and precipitation, and high χ values in the headwaters of the rivers characterize the plateau. In contrast, high SSP, Mx and precipitation, and low χ values in the headwaters of the rivers characterize the flanks.

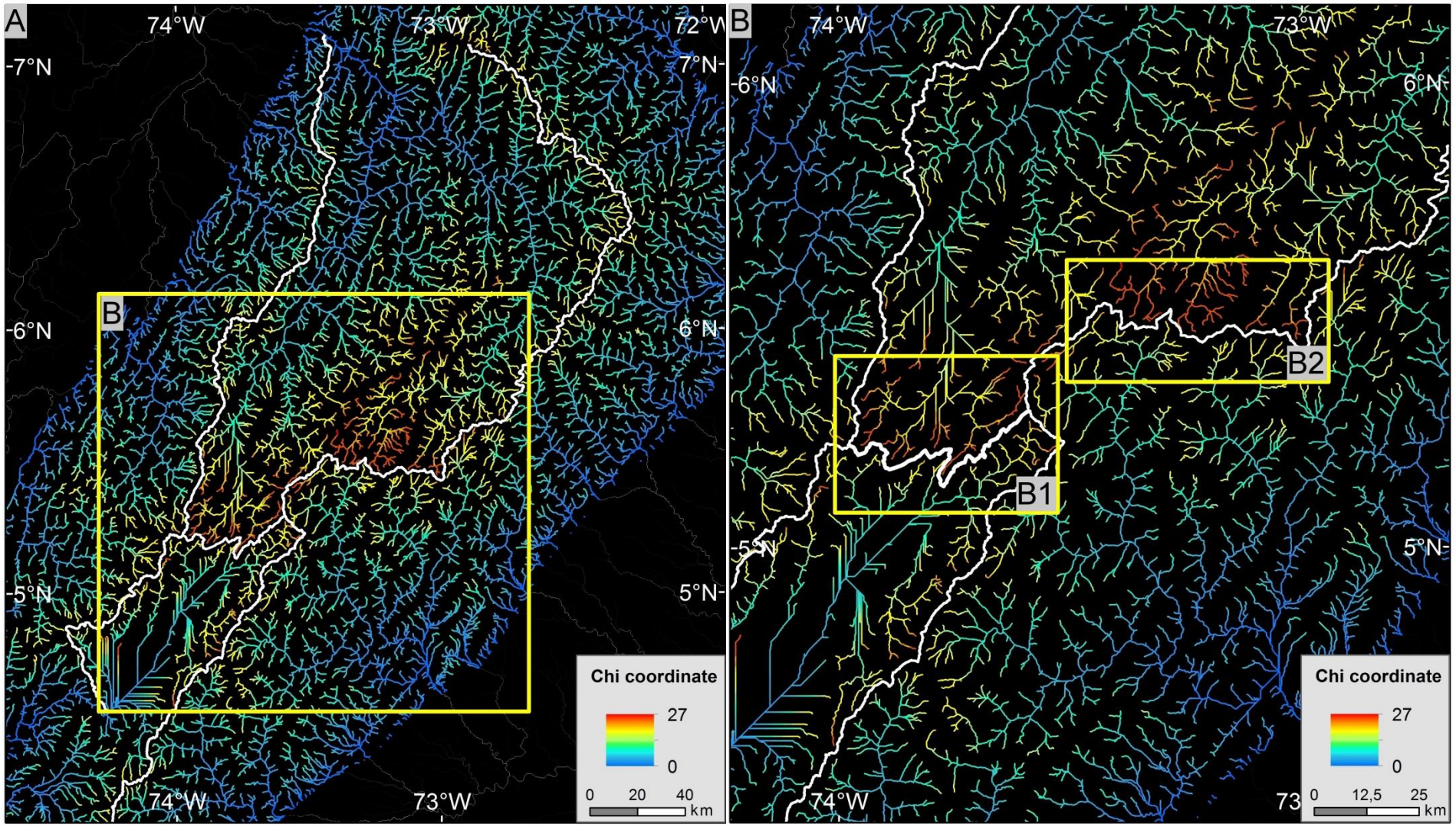

Fig. 3.3. *χ values for the river networks in the Eastern Cordillera. B1 and B2 areas are described in the main text. Discontinuities in χ across divides indicate that the network is not in geometric equilibrium. The waters divides generally move in the direction of higher chi.*

3.3.2. Landscape evolution rates

The large erosional contrast between the plateau and the flanks is highlighted in the distribution of erosion rates (Fig. 3.4). The ^{10}Be analysis shows that the lowest erosion rates occur in the Sabana de Bogotá region with values of < 20 mm/ka (Table 3.3). The ^{10}Be results show that erosions on the flanks are higher than on the plateau.

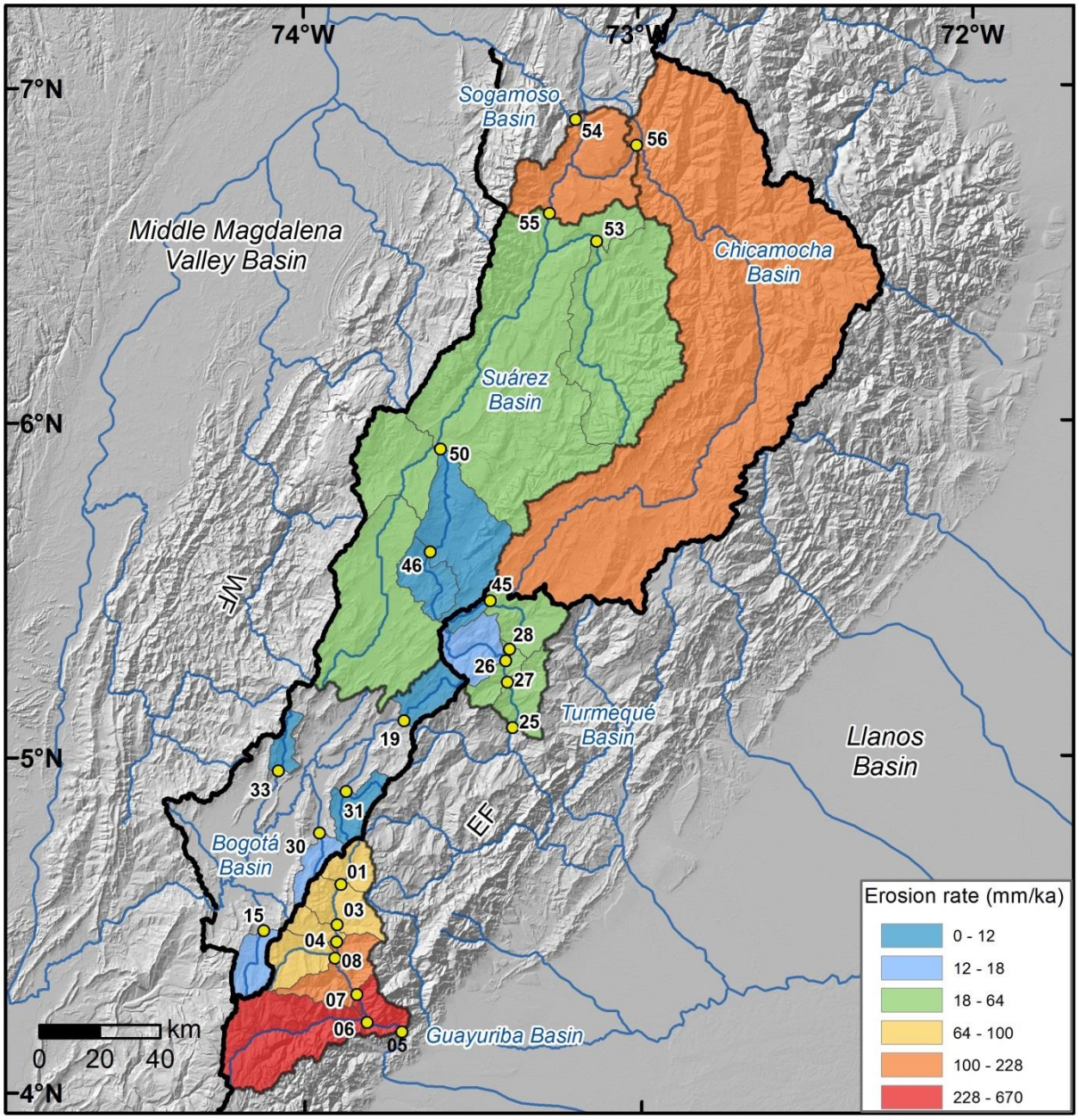

Fig. 3.4. *Map of erosion rates calculated for selected Eastern Cordillera catchments by 10Be terrestrial cosmogenic nuclide analysis of river sediments. Points and numbers indicate fluvial sample with prefix LUCN-XX, yellow for the trunk samples and white for the tributaries. White stars indicate the location of the plateau capture knickpoint in the Suárez, Chicamocha and Bogotá rivers. The main drainage divides are indicated by thick black lines.*

Sample	Sample catchment area (km^2)	Avg. elevation (m)	Standard deviation (m)	MATLAB ^{10}Be P-rate	^{10}Be P-error	^{10}Be concentration (10^5 at/g)	Attenuation length (m)	Erosion rate (mm/ka)	Rainfall rate (mm/a)	SSP (GJ/m2/a)	Mx
LUCN-01	200.5	3071	397	21.3	2.8	1.621 ± 0.065	0.6	79.2 ± 10.9	1331 ± 112	39.28 ± 5.08	7.87 ± 2.77
LUCN-03	526.3	2808	512	18.6	2.4	1.529 ± 0.092	0.6	73.3 ± 10.6	1337 ± 177	51.59 ±14.28	8.18 ± 2.18
LUCN-04	658.8	2760	531	18.2	2.4	1.506 ± 0.064	0.6	72.6 ± 10.1	1318 ± 186	53.56 ± 16.34	8.43 ± 2.45
LUCN-05	2559.7	2726	701	18.1	2.4	0.227 ± 0.034	0.6	479.4 ± 95.8	1678 ± 684	99.71 ± 63.88	9.28 ± 2.93
LUCN-06	1010.1	3054	685	21.5	2.8	0.193 ± 0.019	0.6	670.7 ± 111.9	1648 ± 453	106.27 ± 53.89	9.81 ± 3.33
LUCN-07	1334.5	2610	560	16.7	2.2	1.006 ± 0.069	0.6	100.1 ± 14.9	1445 ± 327	71.90 ± 35.86	8.64 ± 2.61
LUCN-08	293.1	2645	526	17.0	2.2	1.323 ± 0.053	0.6	77.5 ± 10.7	1280 ± 192	57.60 ± 20.30	9.72 ± 2.51
LUCN-15	239.9	3352	278	24.7	3.2	9.630 ± 0.152	0.6	15.4 ± 2.0	1202 ± 149	33.33 ± 2.16	5.08 ± 1.57
LUCN-19	265.3	2910	189	19.4	2.5	10.247 ± 0.219	0.6	11.4 ± 1.5	923 ± 151	17.62 ± 3.77	2.44 ± 1.46
LUCN-25	1291.2	2605	394	16.5	2.1	1.668 ± 0.051	0.6	59.5 ± 8.0	1094 ± 207	39.53 ± 18.37	5.32 ± 2.37
LUCN-26	345.6	2742	286	17.7	2.3	6.790 ± 0.121	0.6	15.7 ± 2.0	982 ± 81	30.12 ± 8.77	3.73 ± 1.42
LUCN-27	977.2	2708	325	17.4	2.3	1.974 ± 0.055	0.6	53.1 ± 7.1	1008 ± 98	31.78 ± 11.81	4.66 ± 1.85
LUCN-28	459.9	2749	325	17.9	2.3	2.234 ± 0.074	0.6	48.1 ± 6.5	997 ± 98	25.94 ± 5.48	4.82 ± 1.59
LUCN-30	162.5	3010	200	20.5	2.7	6.777 ± 0.177	0.6	18.2 ± 2.4	1045 ± 110	21.58 ± 6.12	6.48 ± 1.1
LUCN-31	244.6	2961	264	20.0	2.6	30.527 ± 0.388	0.6	3.9 ± 0.5	1152 ± 180	19.26 ± 5.72	3.35 ± 1.43
LUCN-33	134.9	3072	250	21.2	2.8	15.483 ± 0.415	0.6	8.3 ± 1.1	1054 ± 125	19.54 ± 2.98	3.12 ± 1.83
LUCN-45	64.9	3119	174	21.8	2.8	23.828 ± 0.665	0.6	5.5 ± 0.7	1097 ± 133	20.52 ± 0.57	2.8 ± 0.57
LUCN-46	313.4	2592	305	16.3	2.1	12.878 ± 0.284	0.6	7.6 ± 1.0	1072 ± 90	17.46 ± 3.02	1.89 ± 1.28
LUCN-50	1185.8	2545	401	16.0	2.1	9.816 ± 0.191	0.6	9.8 ± 1.3	1221.61 ± 268.18	34.50 ± 22.07	3.58 ± 3.07
LUCN-53	2083.3	2251	738	14.0	1.8	1.822 ± 0.044	0.6	46.4 ± 6.2	2101.65 ± 577.49	80.70 ± 29.59	5.72 ± 2.12
LUCN-54	20153.1	2441	777	15.9	2.1	0.572 ± 0.067	0.6	167.1 ± 29.6	1618.68 ± 630.75	95.79 ± 91.41	7.01 ± 4.78
LUCN-55	9789.2	2232	650	13.7	1.8	1.295 ± 0.039	0.6	63.8 ± 8.6	1889.11 ± 716.5	78.81 ± 60.33	5.92 ± 4.78
LUCN-56	9307.1	2792	720	19.1	2.5	0.504 ± 0.021	0.6	228.4 ± 31.7	1360.68 ± 399.12	86.02 ± 59.49	8.13 ± 4.72

Table 3.3 *^{10}Be TCN data for samples of the Eastern Cordillera. Also shown are rainfall, SSP and Mx values for each sampled basin.*

The upper half of the Guayuriba catchment is eroding at a rate is ~75 mm/ka (samples LUCN-01, 03, 04, 08; Fig. 6), whereas downstream the erosion rates are ~100, 479 and 670 mm/ka (LUCN-07, LUCN-05 and LUCN-06). Two samples (LUCN-05 and LUCN-06) show that erosion rates are an order of magnitude higher than the rest of the flank samples and record the maximum values of erosion (see discussion below). In the Turmequé catchment, the erosion rates increase downstream from 5.5 mm/ka in the upper part of the catchment in the longitudinal tract (LUCN-45) to 15.7, 48, 53 and 59 mm/ka progressively downstream (LUCN-26, 28, 27 and 25; Fig. 3.4).

The Sogamoso catchment drains the axial plateau of the Eastern Cordillera to the north, and is eroding at a rate of 167 mm/ka (LUCN-54; Fig. 3.4). This catchment is divided into the Suárez catchment in the west and the Chicamocha catchment in the east that are eroding at a rate of 64 mm/ka (LUCN-55) and 228 mm/ka (LUCN-56), respectively. The upper part of the Suárez catchment is eroding at a rate of 8 and 10 mm/ka (LUCN-46 and 50). The erosion rates for the middle part of the Sogamoso catchment is 46 mm/ka (LUCN-53), similar erosion rates for the Suárez catchment.

I calculated exposure ages from the terrace boulders in the Guayuriba basin assuming zero erosion and hence the values obtained must be considered as minimum ages (Table 3.4, Fig. 3.5).

Sample	$^{10}Be/^{9}Be$ (10^{-15})	# of Be-10 atoms (10^{3})	Exposure age (ka)	External uncertainty (ka)	Internal uncertainty (ka)
LUCN-09	3866.38±90.64	310.52±7.27	278	27	7
LUCN-10	3686.99±69.19	285.39±5.35	257	24	5
LUCN-11	7356.65±116.02	627.81±9.93	614	63	11
LUCN-12	8644.81±146.22	697.80±11.80	694	73	14
LUCN-13	7770.53±134.31	664.29±11.48	659	69	14

Table 3.4. *Description and ^{10}Be ages for the quartzite boulders on a river terrace in the Guayuriba valley with a carrier concentration of 1.023 ppm. See sample location in the map of Figure 3.1C.*

However, we can estimate an erosion rate using the oldest boulder age (LUCN-12) and applying the methods included in the work of Lal (1991). The erosion rate obtained from the oldest boulder is ~1 mm/ka and if we assume that all the samples weather at this rate, the initial ages with zero erosion will increase by up 50% up ages up to ~700 ka. However, since we sampled large boulders with no apparent weathering, we can assume that a correction factor for erosion is not really necessary for our ages.

The boulder ages range from 257 to 694 ka. The three oldest samples (LUCN-11 to LUCN-13) clustered particular well given their antiquity, having a mean age of 656 ± 69 ka. I argue that the two youngest ages probably reflect exhumation of the boulders from the terrace and so I do not use those samples in our incision rate calculation. The mean elevation of the three oldest samples is 2129 ± 3 m asl and the elevation in the adjacent valley is ~1723 m asl. Hence an incision rate about 62 mm/ka is calculated based on the mean age of 656 ± 69 ka and a height difference of 406 ± 5 m. This is

comparable with the catchment-averaged erosion rates calculated from river sediment in the flank streams.

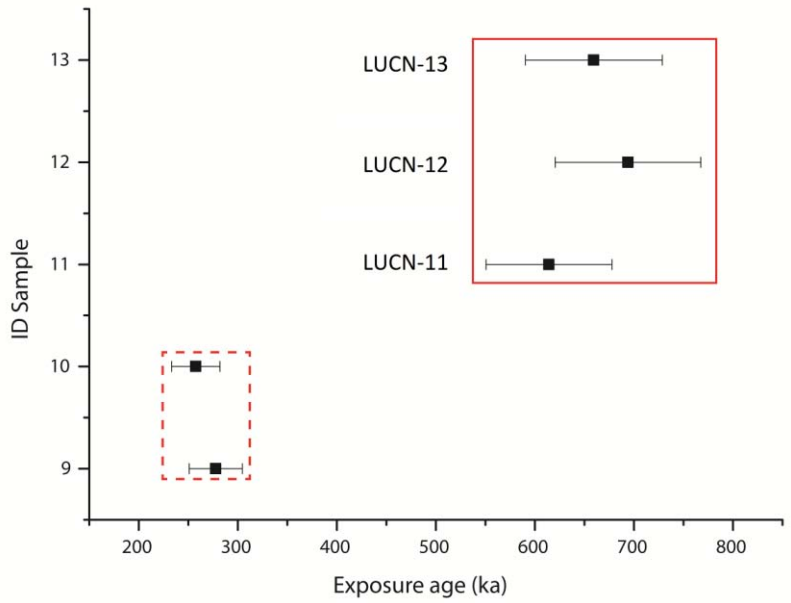

Fig. 3.5. *Be-10 age for the terrace boulders. LUCN-09 and 10 show an exposure age of 267 ± 16 ka (dashed line). LUCN-11, 12 and 13 mark an older mean exposure age of 656 ± 69 ka.*

3.4. Discussion

The calculated erosion rates for the Eastern Cordillera of Colombia and values of SSP, Mx and χ indicate clear erosional contrasts between the axial plateau and its flanks. In addition, there are apparent intra-domain and intra-basin differences between regions.

3.4.1. Drainage network dynamics

For fluvial captures to occur, the rivers across the flanks of the Cordillera need more erosion capacity than the longitudinal rivers in the Sabana plateau (Struth et al., 2015). Higher erosion rates along the flanks (>50 mm/ka) compared to the Sabana (<20 mm/ka) suggest retreat of the main divides and capture of the longitudinal plateau rivers by the transverse flank rivers. I emphasize that catchment size has no influence on the TCN concentrations. The obtained data shows that for similar drainage areas, the erosion rates are higher on the flank than on the plateau. Moreover by choosing large catchments the TCNs concentrations are less biased towards particular lithologies, as might be the case for small catchments than the ones I sampled. The Guayuriba and the Bogotá catchments provide examples of flank catchments with a drainage area of 200 km^2 yielding an erosion rate of 79 mm/ka (LUCN-01), whereas the plateau drainage basins with comparable drainage areas of 163 and 245 km^2 yield erosion rates of 18 (LUCN-30) and 4 mm/ka (LUCN-31), respectively (Fig. 3.4). For a plateau catchment with an area of 240 km^2, an erosion rate of 15 mm/ka (LUCN-15) was determined, which is lower than a similar size catchment (293 km^2) on the eastern flank that has an erosion rate of 77 mm/ka

(LUCN-08). The comparison between the Turmequé and Sogamoso catchments also illustrates this contrast: the sampled catchments for Suárez, with areas of 313 and 1186 km^2, provided rates of 7 (LUCN-46) and 10 mm/ka (LUCN-50), respectively. This is markedly different from the Turmequé flank samples from drainage areas of 460 and 1291 km^2 that have higher erosion rates of 48 (LUCN-28) and 59 mm/ka (LUCN-25), respectively. These results confirm that the main divides in the Eastern Cordillera will migrate towards the axial plateau because rivers in the flanks have more energy (SSP) and erosion capacity (Mx).

A special case is illustrated by comparing the Sabana catchment where sample LUCN-19 (drainage area 265 km^2, erosion rate 11 mm/ka) and the catchment where flank samples LUCN-45 (65 km^2, 6 mm/ka) and LUCN-26 (346 km^2, 15 mm/ka) were collected. The area around these samples was interpreted by Struth et al. (2015) as a capture zone on the basis of topography, featuring a depressed topographic profile and a mapped reentrant toward the west of the main divide, and of the occurrence of knickpoints upstream of an elbow in map view. Similar erosion rates on both sides of the drainage divide in that area argues in favor of drainage capture. In addition, the map of the χ-coordinates shows that the upper area of the Turmequé catchment was part of the plateau area in the past and is now incorporated in the flank domain (Fig. 3.3B1).

At an inter-domain scale, and according to Struth et al. (2015) and Babault et al. (2013), the Eastern Cordillera of Colombia has clear geomorphic differences between its flanks and axial zone, which includes the Sabana de Bogotá and the southern, low-relief part of the upper Sogamoso drainage basin. The comparison of the geomorphic indices and erosion rate results with the drainage divide features arguing for capture. This confirms the view of Struth et al. (2015) who argue for drainage divide migration and then a longitudinal-to-transverse drainage rearrangement in the Eastern Cordillera.

The correlation between erosion rates and Mx values (Fig. 3.7) is better than with the SSP (Fig. 3.6). The SSP is, in first order, a function of the precipitation, slope and drainage area. Calculation of the SSP from a serial of raster measurements and the low-resolution data of the DEM or the precipitation provide equivocal results. Mx is solely a function of the elevation and distance of the river profile, providing a more realistic value to describe the steepness of the river reaches.

3.4.2. Calibration of geomorphic parameters

The links between erosion rates and specific stream power or steepness index has been examined in previous studies (e.g. Kirby and Whipple, 2012; Perron and Royden, 2013, 2003; Safran et al., 2005; Bookhagen and Strecker, 2012). Our data show high erosion rates in samples located on the flanks of the orogen (which possess high SSP) and in the northern parts of the Sogamoso basin, and low rates on the axial plateau (Sabana de Bogotá, upper part of Turmequé basin and southern part of the Sogamoso basin).

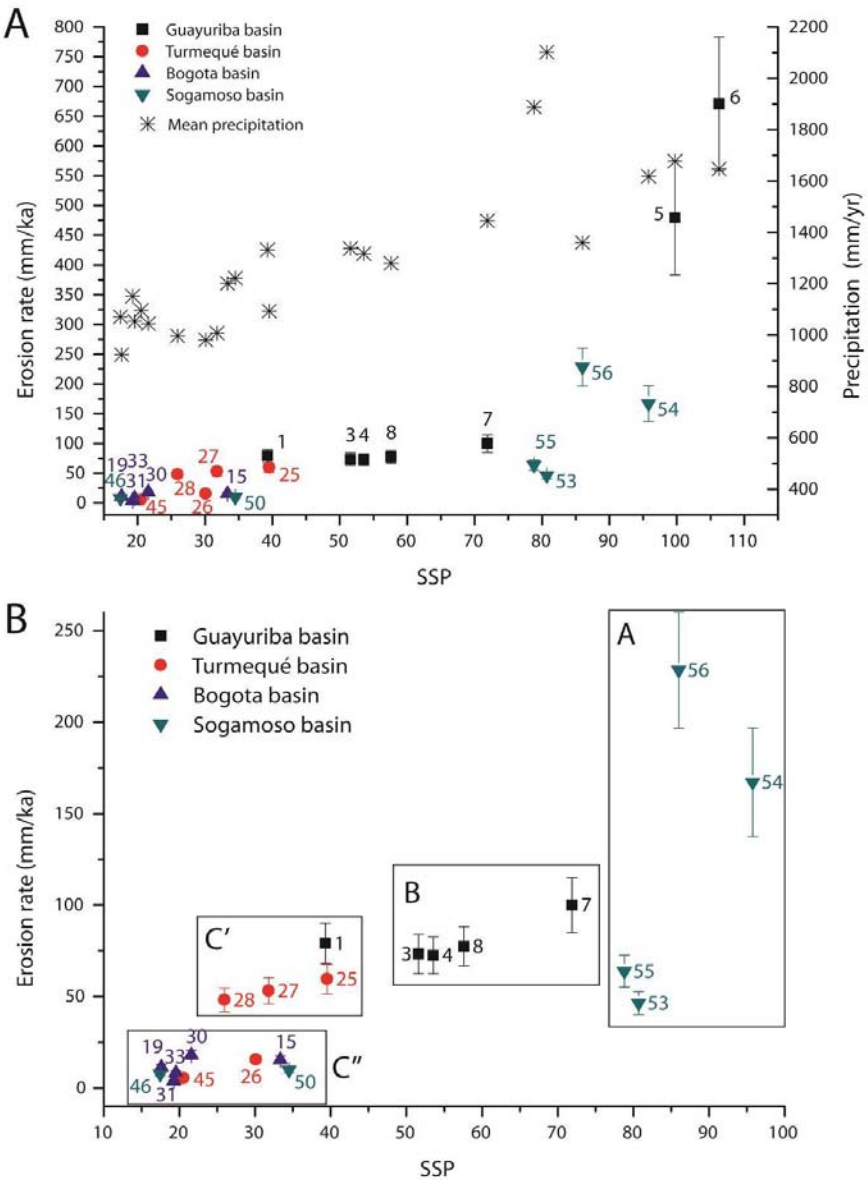

Fig.3.6. *(A) Plots of erosion rate (mm/ka) vs. mean SSP value and precipitation for each sample and basin analyzed in this study. (B) Rescaling of the main graph for better comparison of the individual trends observed for the SSP values, excluding the two highest rate samples, LUCN-05 and 06 (see discussion for the A-C'' groups).*

Geomorphic indices cluster into four groups, A to D (Fig. 3.6B). Group *A* comprises Sogamoso catchment samples from the most incised northern part of that catchment (LUCN-53, 54, 55, 56). Group *B* is associated with flank characteristics with high relief, and group *C* is includes the lowest relief area samples. Group C is subdivided into *C'*, including samples with flank characteristics but with lower relief (LUCN-25, 27, 28 and 01), and *C''*, with plateau characteristics (LUCN-19, 26, 31, 33, 45, 46, 50).

There is positive correlation between erosion rates and the basin-wide average Mx values (Fig. 3.7).

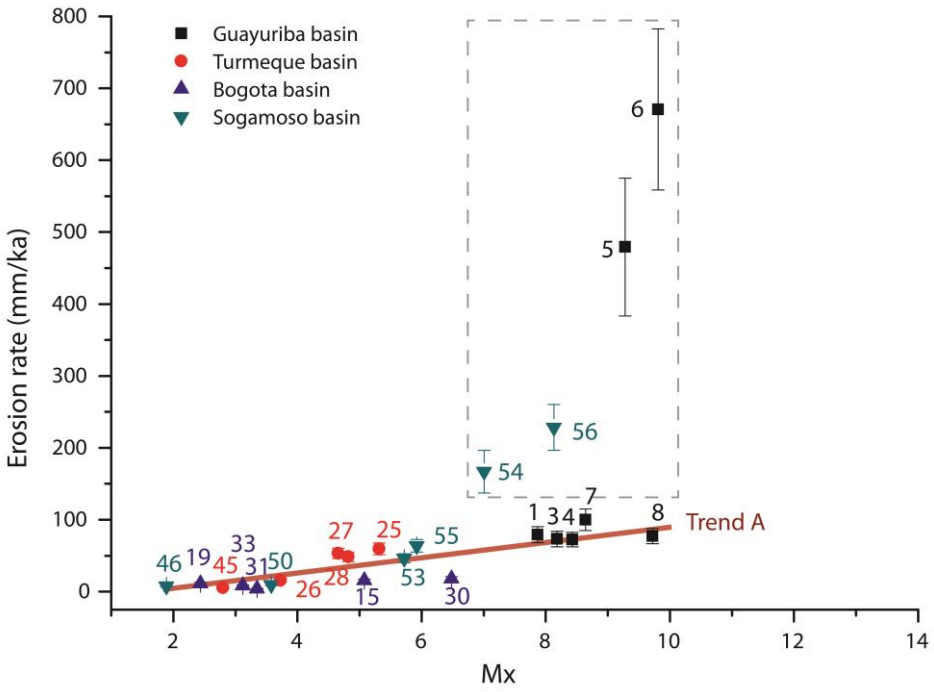

Fig. 3.7. *Erosion rates (mm/ka) plotted against the mean Mx value for each sample and basin analyzed (see discussion for the samples included in Trend A).*

Despite the four samples with different lithologies, climate and uplift conditions (dashed box in Fig. 3.7), a polynomic equation was defined for the rest of samples (Trend A = red line in Fig. 3.7). Trend A reflects samples with similar lithologies and in areas of similar precipitation and uplift.

The equation defining the trend A is polynomic in the form of:

$$E = a_1 \cdot Mx \qquad \textbf{(eq. 3.3)}$$

where a_1 is 12.28.

I propose the use of equation 3.3, related to the Mx parameter, for meaningful comparisons with the erosion rates. This equation is useful to calculate and estimate erosion rates whenever TCN sampling is not possible. Thus this provides a first estimation of the erosion dynamics for a mountain belt with similar lithological characteristics. However, the applicability of equation 3.3 for the shale-rich western flank of the Eastern Cordillera of Colombia might be problematic. This is because the western flank is shale dominated area with more erodible rocks (less resistant) than in the eastern flank (alternation of sandstone and shale formations), and therefore, the incorrect application of the equation in the western side will underestimate the real erosion rate.

3.4.3. Local climatic, lithologic and tectonic effects

In addition to distinguishing between axial plateau and cordillera flanks, I can refine the classification of samples into 4 groups, according to their erosion rates (Fig. 3.8):

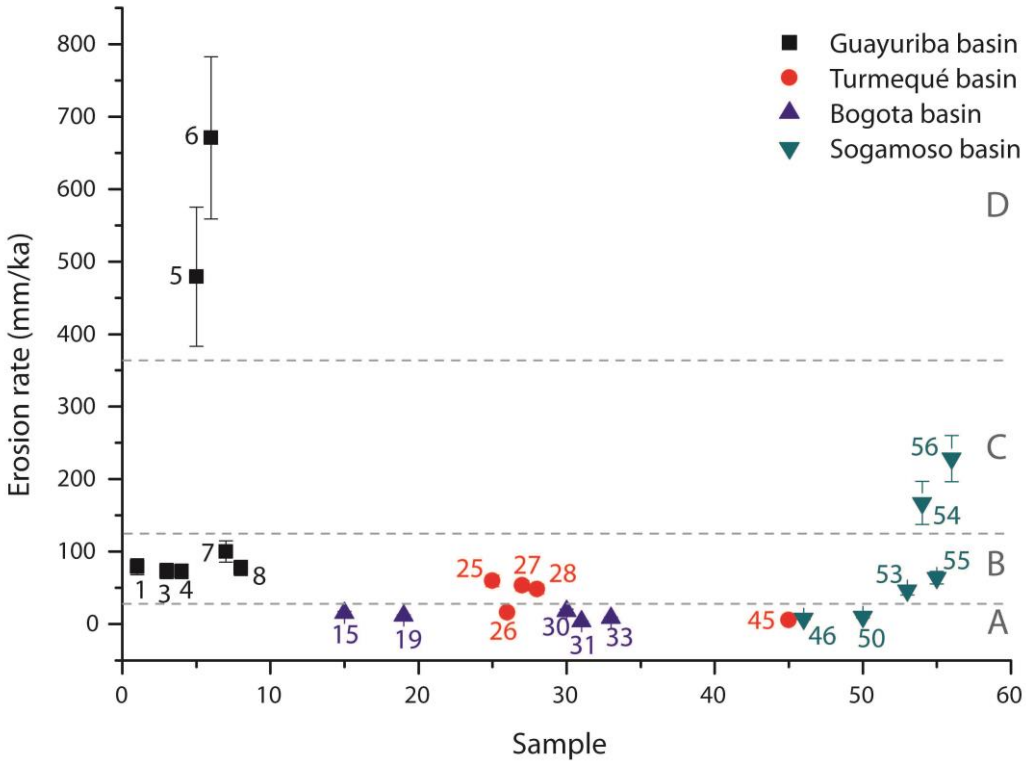

Fig.3.8. *Erosion rates (mm/ka) for each sample. Sample numbers correspond to the ending number of the LUCN-XX numeration.*

Group A represents the plateau domain, with the lower erosion rate values, <20 mm/ka. This area represents the comparatively little tectonically deformed belt of the Cordillera (e.g. Mora et al., 2008, Teixell et al. 2015) associated with longitudinal, structure-controlled fluvial drainage. Samples LUCN-26 and 45 are not located on the plateau, but the low relief of these catchments and the longitudinal trend of the rivers suggest they belonged to the plateau in the past.

Group B samples represent an incised domain, including some of the samples located in the flanks and in the Sogamoso catchment (Suárez River). The samples located in this group reflect high-energy rivers that are transverse to the chain, cutting across tectonic structures.

Group C includes only two samples, LUCN-54 (167 mm/ka, Sogamoso river) and LUCN-56 (228 mm/ka, Chicamocha river; sample LUCN-54 is not taken into account because it is a mix of the sands of LUCN-55 and LUCN-56). The differences between erosion rates for these samples and the neighbors, LUCN-53 (46 mm/ka) and LUCN-55 (64 mm/ka), correlates with a difference in climate, vegetation cover and rock strength. Basement composed of low- and medium-grade metamorphic rocks is exposed in the upper and medium part of the Chicamocha basin (LUCN-56), and the region has little vegetation. In contrast, the Suárez river basin (LUCN-55) mainly traverses alternating Cretaceous sandstone and shale. The basement rocks are weaker than the Cretaceous sedimentary rocks, and as suggested by Castro (1992) and González and Jiménez (2015), the basement is more easily eroded. Moreover, erosion is enhanced because of the lack of vegetation cover in the upper and middle part of the Chicamocha basin.

The Chicamocha valley has an arid microclimate unlike any other part of the Eastern Cordillera. The valley is very narrow and the obtained data from the few pluviometer stations do not reflect the real conditions inside it, resulting in overestimates of precipitation. The Chicamocha valley is bounded by two topographic highs, the Cocuy-Santander massif to the east and the Floresta massif to the west (Fig. 1.2), which forms an orographic barrier and resulting in a rainshadow zone in the Chicamocha valley. The Chicamocha river is characterized by a very high mean Mx (~ 8.13) with steep hillslopes and an erosion rate of 228 ± 32 mm/ka. The Suárez river (sample LUCN-54) mainly flows across Cretaceous formations and the Mx is low (~ 5.92) with an erosion rate of 63.8 ± 8.6 mm/ka. The Chicamocha catchment, with higher erosion rate, has lower precipitation than the Suárez catchment, which is similar to the Sabana de Bogotá. If high precipitation results in large erosion rates, we would, in principle, expect higher erosion rates in the Suárez catchment than in the Chicamocha catchment, but this is not the case. I propose that the high erosion rate in the Chicamocha valley is related to the local "semi-arid" conditions, low vegetation cover and more erodible bedrock, all of which will enhance the erosion capacity. I underline the importance of lithology in determining the magnitude of the erosion within similar topographic domains, as shown in other studies in dynamic settings where higher denudation rates that have been related to high erodibility of the rocks (e.g. Salgado et al., 2008; Chadwick et al., 2013; Bierman et al., 2014; Pupim et al., 2015). Safran et al. (2005) showed that the lithology might play a secondary non-dominating role in catchment-averaged erosion rates in the Bolivian Andes, where high erosion rates were located indistinctly in weak and resistant bedrock, arguing for a first order effect of the uplift, a second order of lithology and non effect of climate. In the Eastern Cordillera of Colombia, the lithology, vegetative cover and climate, has a first order effect in the erosion magnitude.

Group D is composed only by two samples, LUCN-05 and LUCN-06, which yielded strongly different values of erosion compared with the rest of the Guayuriba catchment samples (one order of magnitude higher). Group D samples are located in the Quetame basement massif (that is easily eroded), characterized by higher precipitation values and younger exhumation ages (e.g. Mora et al., 2008, 2010; Parra et al., 2009a) than in the upper part of the basin, as shown by greater erosion and incision (see Fig. 1.8). The combination of these high values of precipitation and exhumation defines a closed feedback erosive cycle, in accordance with the high erosion rates determined for this area.

Up to 150 mm/ka differences in erosion rates for are evident in catchments in the same topographic domain (Fig. 3.4). The difference between the Suárez (64 ± 9 mm/ka) and Chicamocha (228 ± 32 mm/ka) catchments is likely due to a combination of precipitation and lithologic effects. Catchments on the eastern flank also show differences in erosion rates, reflected by the Guayuriba basin with higher erosion rates, relief and incision values than the Turmequé catchment (Figs. 3.4 and 3.9).

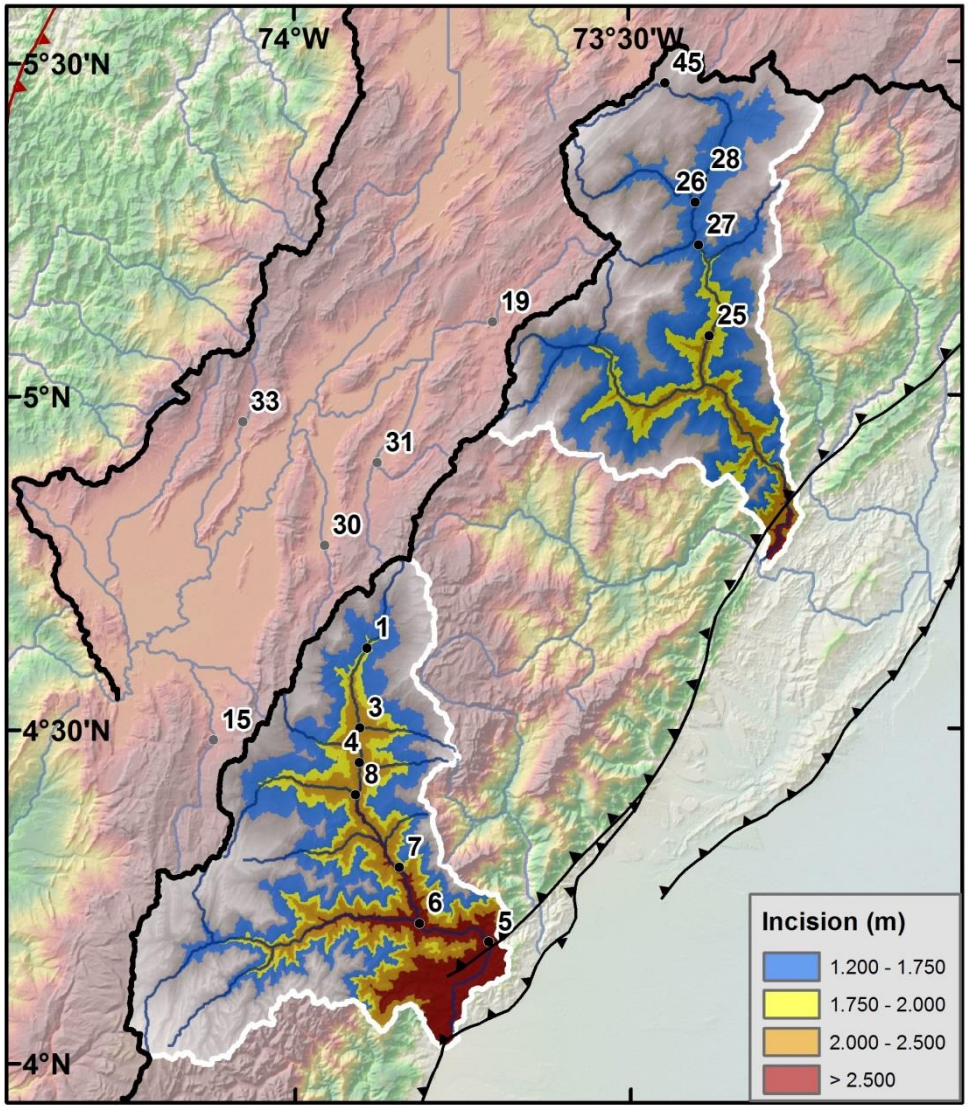

Fig.3.9*. Incision values for the Guayuriba (south) and Turmequé (north) basins calculated by the subtraction of the DEM elevation of the valley floors from the maximum elevation of the lateral ridges. Numbered points indicate samples. Note higher values of incision in the Guayuriba basin compared with the Turmequé basin.*

The difference described above argues for different fluvial dynamics between the Guayuriba and Turmequé catchments. The upper part of the Turmequé catchment has been captured, as suggested by geomorphic work of Struth et al. (2015). Our work adds new analysis using the χ and SSP values suggesting a rearrangement of the axial longitudinal drainage by transverse rivers located on the orogen flanks. The disequilibrium in the χ values at both sides of the eastern divide suggests divide migration toward the inner part of the plateau's interior, which is more evident in the Turmequé catchment than in the Guayuriba catchment, and a northward migration of the central divide. This example supports the view of Struth et al. (2015) who suggested that the Turmequé area was a captured reentrant.

The different geomorphic characteristics of the divide and between the two catchments are interpreted as the result of the competition between the uplift and the erosion. In the Guayuriba catchment, the erosive potential results from the high contrast between slopes during mountain building

and the active tectonics in the basin that has been shown by young thermochronologic ages (Fig. 1.8), arguing for high erosive potential to compensate the high uplift in the foothills of the flanks. In this way, the upstream propagation of erosion and then, the capture and divide migration is less probable than in a catchment with less exhumation, such as for the Turmequé catchment that has a wide reentrant and low-elevated area in the eastern divide.

Struth et al. (2015) interpret the different dynamics between the flanks and the axial plateau of the Eastern Cordillera as a product of mountain building. As such there was progressive increase in regional slope caused by the accumulation of crustal shortening and thickening. This is similar to a model proposed for the Moroccan High Atlas by Babault et al. (2012). Essentially, the contrast in regional slopes results in different erosion rates and topographic dynamics across the Eastern Cordillera. Variations in local precipitation, tectonics and bedrock lithologies within a basin may also influence its erosion dynamics, and may have played a secondary role in the dynamism of divide migration and landscape evolution.

3.5. Conclusions

A smooth axial plateau flanked by steep topographic belts characterizes the Eastern Cordillera of Colombia. TCN data reveal high erosion rates in the high-relief flanks, with a mean value of 70 ± 10 mm/ka (exceeding 400 mm/ka in some catchments), whereas in the low-relief axial plateau the mean erosion rate is of 11 ± 1 mm/ka, arguing for a erosive contrast between the two domains and a migration of the N-S oriented, plateau-flanks drainage divides towards the plateau. The drainage divide moves in response to contrasting denudation rates on the mountain flanks and asymmetric topography. Results of digital morphometric analysis, including specific stream power, channel gradient and χ values distribution confirm drainage divide motion by capture processes and the proposed drainage dynamics for the Eastern Cordillera. Comparison of the TCN-derived erosion rates with the geomorphic digital parameters show positive correlations. High values of SSP and/or Mx are directly related to high erosion rate. Our derived equation (eq. 3.3) stressed as a Mx-erosion rate plot for the Eastern Cordillera may be useful to acquire first-order estimates of erosion rates in areas where there are no TCN data, but with similar lithologic and pluviometric characteristics, which include layered sedimentary rocks in alternating competent and incompetent formations.

Drainage reorganization from longitudinal to transverse-dominated by means of a series of river capture events may lead to a progressive reduction of the extension of the axial plateau of the Eastern Cordillera. This is further supported by erosion rates similar to those of the plateau in longitudinal relicts actually located in flank domains. The erosion contrast between the two morphologic domains of the Eastern Cordillera was primarily driven to the increase in the orogen regional slope by progressive accumulation of crustal shortening and thickening. Local climate, tectonics and lithology play a secondary role in controlling the erosion rates and the basin dynamics at a local scale.

Chapter 4

The Colombian Eastern Cordillera Plateau: a recent fluvial captured area

in preparation

Summary

The aim of this study lies in the extraction of the dynamic state of the drainage network in the Eastern Cordillera of Colombia, by applying a series of χ (chi) parameter calculations. I demonstrate that we can obtain initial information of the dynamic state of a river basin and predict the movement direction of the drainage divide and therefore the degree of expansion or reduction of a basin. The Eastern Cordillera of Colombia shows a drainage reorganization record from an initial longitudinal trend to a transversal domain, on the external and internal parts. In addition, I made an important contribution of the Bucaramanga terrace knowledge providing a vertical profile using terrestrial cosmogenic nuclides (TCNs) to determine the moment of abandonment and the starting of the capture history for the Eastern Cordillera, with an age of 400 ka.

Key words: Chi parameter; Drainage evolution; Cosmogenic nuclides; Eastern Cordillera of Colombia.

4.1. Introduction

In uplifting landscapes, rivers adjust their channel geometry and slopes to changes in uplift rates in order to reach the steady-state conditions, when uplift is balanced by erosion. Recent studies have shown that drainage reorganization by stream captures can be the result of the landscape response to tectonic or/and climate changes.

A new method has been developed to investigate the interactions between catchments in active tectonic areas, the χ analysis (Perron and Royden, 2013; Willett et al., 2014). This method relates to a proxy for steady-state landscapes based on the current geometry of the river network and highlights the dynamic state of the river basins in function of the elevation with the integral of the drainage area. Fluvial captures imply drainage area changes between basins and divide motion. The χ-plots will show these variations along the rivers and then, the disequilibrium in the network, where an area change produces a state of disequilibrium in χ-plots. Therefore, using χ-plots we can extract information about the catchment dynamics and directions of horizontal motion of the drainage divide toward a new stable position.

I applied this method to investigate the evolution of the Eastern Cordillera of Colombia where the transition from longitudinal to transverse drainage network has been interpreted as an evidence of ongoing fluvial reorganization, evolving by progressive drainage divide migration and a series of discrete captures (Struth et al., 2015).

In view of the explained problematic in the Eastern Cordillera, I aim to highlight evidences of the drainage reorganization with the new method of the χ- analysis, including χ-plots and χ-maps. I pursue to demonstrate and validate this method in the Eastern Cordillera. The river reorganization and capture history will be highlighted with the interpretation of the χ-plots with the distribution and study of knickpoints, steepness index and a dating of an abandoned terrace, to estimate the plateau capture timing in the Eastern Cordillera and extract information of the river profiles in the past, current and future times.

4.2. Methodology

Rivers record information about the landscape dynamics, of with influences of climate history, tectonics and lithology. River profiles provide a common test for extracting information about the dynamism of the topography, understanding the deformation history and calibrating erosion models (Whipple, 2004; Wobus et al. 2006; Perron and Royden, 2012).

Following the methodology included in Chapter 3, I analyze the χ gradient with the precipitation correction (eq. 3.2) for the main rivers and tributaries in the Eastern Cordillera, and I extract the longitudinal profiles for the rivers in Fig. 4.2 analyzing the knickpoints. I localize the different knickpoints from the longitudinal profiles and classify them according to the different type and to their position along the river their origin according to the information from the DEM and topographic and geologic maps. Catchments displaying similar number of knickpoints at similar elevation should have

been affected by similar base-level history. Catchments displaying different numbers of knickpoints should indicate local processes of knickpoints generation such as stream captures.

The χ- plots allow identifying perturbations in the profile from the initial linear trend indicating a transient response of the river profile. According to Perron and Royden (2013) and Willett et al. (2014), if a steady-state river gains area by capture (Fig.4.1A), the χ-plot will shift toward lower χ values for a given elevation and above the steady-state trend; the capturing river will experience faster erosion rates; the loser river will be shifted to the right, below the steady trend and experience lower erosion rates. Additionally, not only the capturing river (or aggressor) displays a shift of the χ-plot to the left, but all the tributaries will be shifted toward lower χ values due to this area gain. The slope of the χ plot increases, moving above the steady state trend. The same effect as a capture gain area is produced by either higher uplift rates or less erodible lithologies.

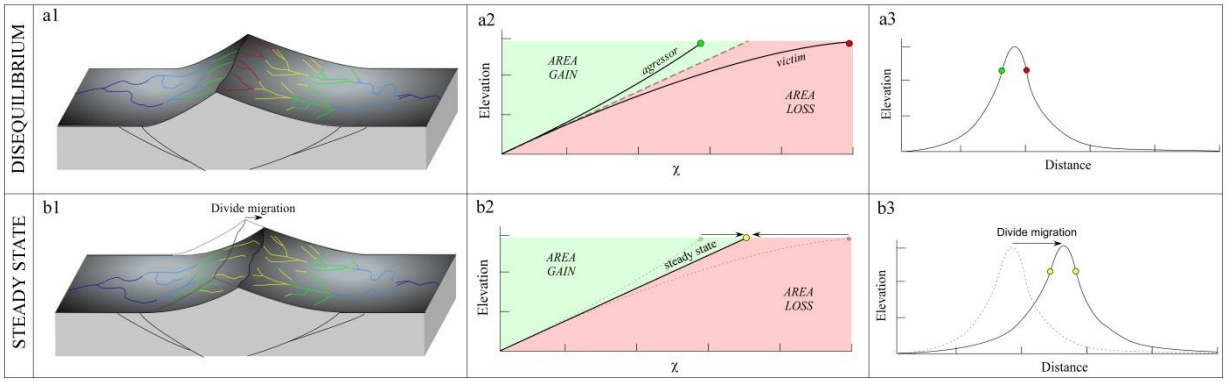

Fig. 4.1. *Effect of the gain or loss of area in chi map (a1, b1), chi plot (a2, b2) and divide profile (a3, b3) (modified after Willett et al., 2014).*

To analyze the fluvial drainage, we extracted the flow direction, downstream flow length and upstream drainage area under a base level of 300 m asl, defined by the elevation of the most external tectonic structures affecting the Eastern Cordillera of Colombia. The value of the critical area for channel initiation (A_c) is 1 km^2 and the scaling area factor (A_0) is 1 m. Therefore I excluded all the pixels with a drainage area less than 1 km^2, because they are considered to be governed by processes of hillslope, landslide or debris flow. The concavity (m/n) was defined following the method of Mudd et al (2014), by calculating it with a variation from 0.3 to 0.6, with a resulting mean value of 0.45 where channels show the best linearity plot (according to Perron and Royden, 2012).

To test the hypothesis that stream captures produce inflections in χ plots, I removed the captured area from the DEM and then recalculated the χ-plots. If recent area gain occurred, the chi-plots of capturing streams should collapse on the trend displayed by the streams which did not capture. I also analyze the distribution of knickpoints and identify geomorphological features that are typical of the stream capture such as wind gaps and elbows of capture.

To extract information about the horizontal dynamics of the river network, I elaborate a χ-map of the Eastern Cordillera of Colombia following the method of Willett et al., (2014). Observing the χ-maps, differences in χ across the drainage divides will suggest disequilibrium and dynamic drainage network rearrangement. Therefore, the analysis of χ values across water divides reveals ongoing drainage network reorganization. Similar χ values at the channel heads on opposite sides of a drainage divide suggest that the river network is near geometric equilibrium, while large differences in χ values across the drainage divide imply that networks geometry is far from equilibrium: identifying contrasts in χ indicates possible divide migration and river capture (Willett et al., 2014). If uplift and bedrock erodibility are spatially uniform, drainage divides generally migrate from low to high χ values to achieve equilibrium and hence, channels displaying high χ values are prone to capture and may eventually disappear (Willett et al., 2014). I calculate the χ-map of the entire central segment of the Eastern Cordillera to investigate the dynamics of the drainage divides.

The described methodology, in addition to the erosion rates in Chapter 3, helps us to understand each basin dynamics and then, extracting the drainage history for the Eastern Cordillera of Colombia.

4.2.1. Cosmogenic analysis

I made a cosmogenic analysis in a terrace located in the Lebrija basin, just near the drainage divide shared with the Sogamoso basin. The location of the terrace and the knowledge of the age might help on the reconstruction of the drainage history of the Eastern Cordillera. I sampled for depth-profile cosmogenic dating (Table 4.1, inset) in a terrace lying at 40 m above the current stream with no evidence of erosion or deformation, and without shielding. I collected a total of 5 samples, with a 1 kg of sand for each one (Table 4.1). The terrace is located on -73.15819W, 6.95242N, with an altitude of 885 m asl. The ^{10}Be carrier concentration was 1.026 ppm.

Sample	Quartz wt (g)	^{9}Be Carrier weigth (g)	Depth (cm)	^{10}Be/^{9}Be (10^{-14})	# of Be-10 atoms (10^{4} at/g)
LUCN-58	27.5127	0.351	50 ± 5	117±4.27	102±3.72
LUCN-59	18.3436	0.35	70 ± 5	59.1±1.19	77.3±1.55
LUCN-61	28.5508	0.3508	105 ± 5	43.2±0.97	36.4±0.81
LUCN-63	28.8631	0.3529	150 ± 5	31.3±1.04	26.2±0.87
LUCN-66	31.1044	0.3517	240 ± 5	31.5±1.20	24.4±9.30

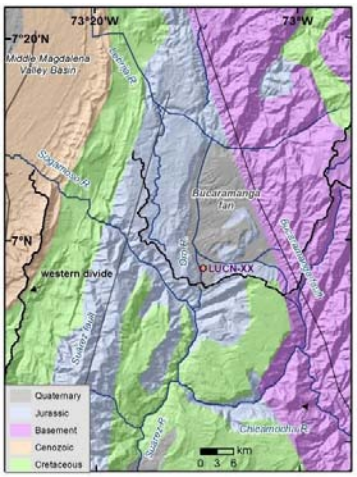

Table 4.1: *^{10}Be sample details including Quartz weight, Be carrier weigth and ^{10}Be concentrations measured. Carrier concentration was 1.026 ppm. See sample location in the inset map from Fig. 1.2 (red point labeled with LUCN-XX).*

The process of quartz isolation, purification, dissolution and preparation of BeO were undertaken in the laboratory at the University of Cincinnati, following the methodology described in Chapter 3. Ratios of $^{10}Be/^{9}Be$ were measured by Accelerator Mass Spectrometry at the Purdue Rare Isotope Measurement (PRIME) Laboratory at Purdue University, Indiana, USA.

The age obtained was calculated with Matlab using the ^{10}Be profile simulator v. 1.2 generating a relative probability density function using the chi-squared values from the Monte Carlo output using the chi-squared likehood function (Hidy et al., 2010; Mercader et al., 2012). For the spallogenic production, I used the new scaling of Borchers et al. (2016), after Stone (2000) after Lal (1991) with a reference production rate of 4.0 atoms/g/a which was scaled to the sampled terrace in basis of latitude and atmospheric pressure providing a new constant value of 4.67160 at/g/a. For the muonic production with a depth of muon effect of 5 m I applied a total muon production of 0.243 atoms/g/a. Following Hidy et al 2010, I used for the fluvial deposit a depth constant bulk density varying between 2.2 and 2.5 g/cm^3. No shielding or cover is applied in the sampled area. A total erosion threshold of 50 cm maximum was used and a neutron attenuation length constant value of 160 g/cm^2. I modelled the erosion rate, inheritance, exposure age as free parameters (stochastic uniform error) in the simulation. I did not found depth profile solutions at 2-sigma level, arguing for a greater geologic scatter in the profile than the AMS measurement uncertainties. I run the simulation with a chi squared value of 10 with the calculation of 1,000,000 profiles.

4.3. Results

4.3.1. Knickpoint distribution from longitudinal profiles

The map of Fig. 4.2A shows the location of the rivers and the knickpoints identified from the profiles. The location and the vertical distribution of the knickpoints illustrated in Fig. 4.2B show some trends that are observed in all the basins of the Eastern Cordillera.

The lowest knickpoints are related to the influence of the most external tectonic structures corresponding to the location of a series of minor knickpoints. Moving upstream from these tectonic structures to the headwaters, I identified and classified structural and lithological knickpoints (red circles in the following figures), knickpoints related to plateau captures (blue circles) and secondary knickpoints (yellow circles, found in the middle of the stream without any apparent relation with the tectonics and lithology; Fig. 4.2). With the aim of highlight the knickpoints associated with captures, I did not plot anthropogenic knickpoints (dams) and the uppermost knickpoints below a threshold drainage area of 1 km^2, where hillslope processes are dominant, landslide or debris flow.

Figure 4.2B summarizes the elevation distribution of each knickpoint in percent units, resulting from the calculation of the relative elevation position for each river. I obtain a distribution where the plateau

captures are in a 100-70% elevated position, the secondary knickpoints are basically between 70-30% and the tectonic-lithologic knickpoint are mainly between 30-0%.

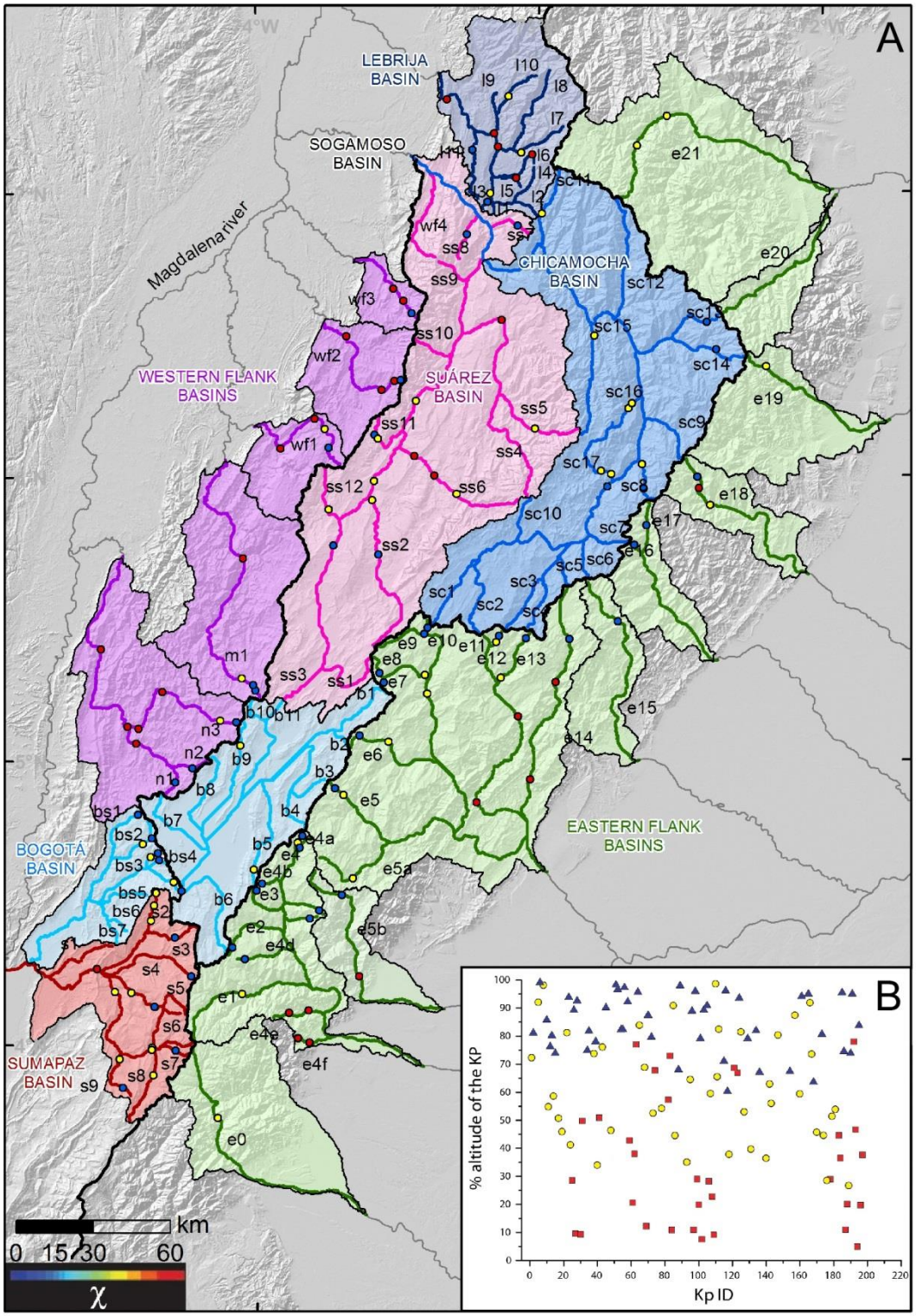

Fig.4.2. *(a) Map with the representation of all the streams analyzed and the respective general basin. (b) Distribution in elevation of the knickpoints with tectonic or lithologic origin (red squares), plateau captures (blue triangles) and secondary knickpoints (yellow points).*

4.3.2. χ-plots

In order to investigate the dynamics between tectonics and surface processes in the Eastern Cordillera, I performed the analysis of transformed river profiles (chi plots) from the SRTM90 DEM of the Eastern Cordillera. Figure 4.3 summarizes the stream and knickpoint location for each basin (A1-E1), the chi plots (A2-E2) and the longitudinal profiles (A3-E3) for all the streams plotted in the Fig.4.2.

In order to compare all the basins in the same plot, I analyzed the chi plots from Figure 4.3 and additionally, selected a representative stream for each basin, containing the main shape and knickpoint distribution (Fig. 5.3A). The chi plot and longitudinal profile of the Lebrija basin (Figure 4.3A), show that all the streams localized in the low elevated flat area remaining parallel to the orogen, collapse in a linear trend, and the rivers with headwaters in the Santander massif with a transverse tract, adopt a steeper shape.

The central part of the orogen, characterized by the Chicamocha, Suárez and Bogotá basins, share a similar knickpoint configuration where the main knickpoint separated a steep lower channel reach from a smooth upper tract corresponding to the plateau in the central part of the orogen: such prominent inflections in the chi plots usually indicate recent river captures (in blue) and are also associated to the presence of wind gaps, abandoned channels or fluvial elbows. The Suárez and Chicamocha rivers drain the internal part of the Eastern Cordillera and display plateau knickpoints in the upper part of the chi plots (Fig. 4.3B). The Chicamocha river (stream sc1, in Fig 4.4A) shows a main knickpoint at an elevation of 2500 m asl separating a less incised area in the upper catchment and a more incised part downstream. In the lower part of the Chicamocha river, a minor knickpoint is observed at 250 m below the main knickpoint and two knickpoints related to the tectonic structures in the lower part of the basin. The Suárez river (ss1, in Fig 4.4A) shows a prominent inflection corresponding to the plateau edge at an approximate elevation of 2600 m asl: this knickpoint separates the low relief topography above the plateau from a more incised part of the lower basin. In the upstream part of the plateau knickpoint I found tectonic knickpoints defining some areas of flat relief. Moving downstream from the main knickpoint, I observed two secondary knickpoints that are not associated with any structural, lithologic, climatic or plateau capture source; in the lower part of the Suarez river I identified two knickpoints corresponding to the external structures. In general, the upper part of the rivers draining the western flank of the Cordillera (Fig. 4.3C) shows several knickpoints related to plateau captures.

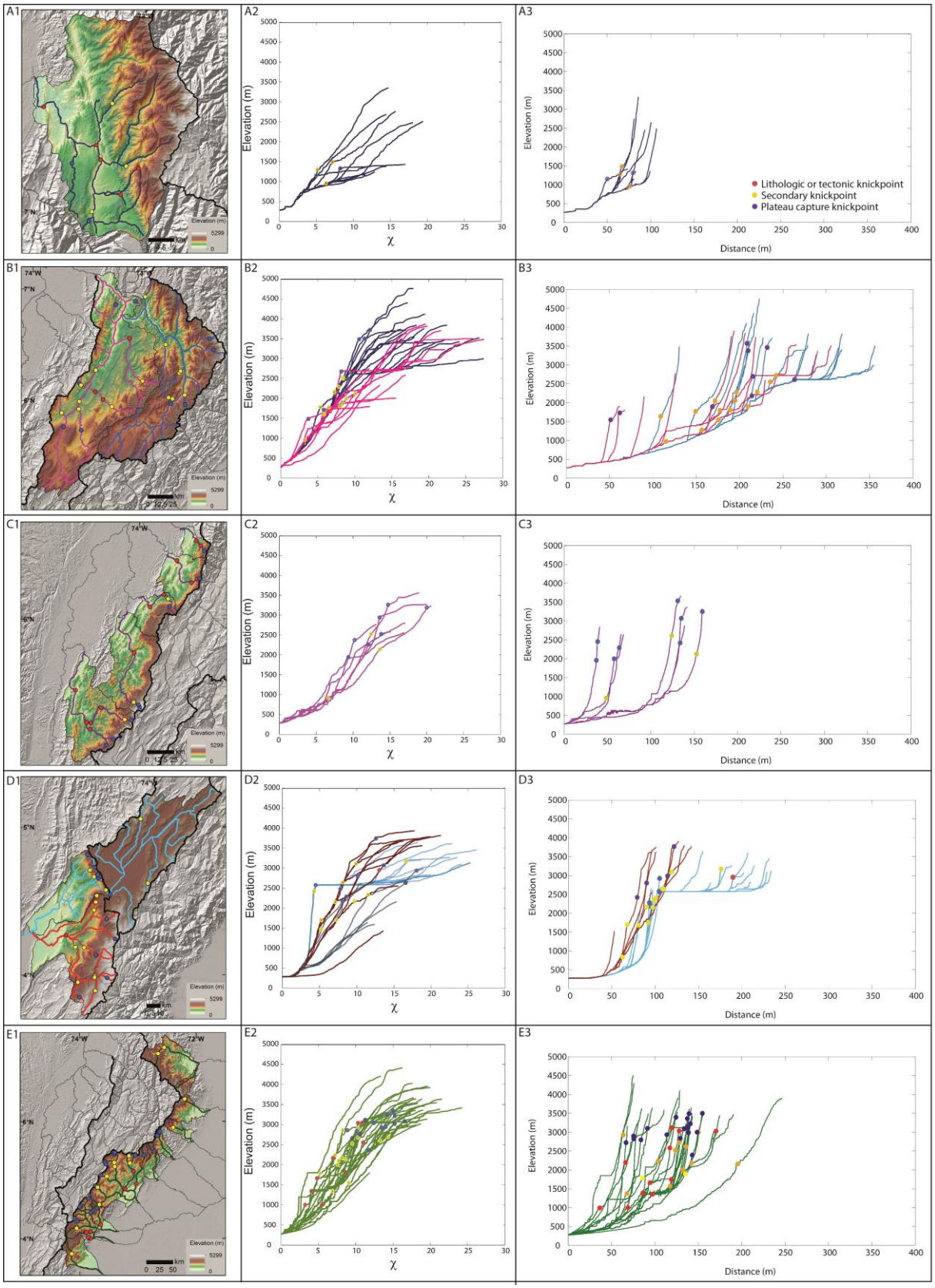

Fig.4.3. *Location of the streams with the knickpoints. The second column corresponds to the obtained chi plots and the third one, to the longitudinal profiles of each basin.*

The Bogotá river shows two relevant inflexions in the plot and map: i) the plateau knickpoint and ii) a secondary knickpoint, just a few meters below the first. Many of the Bogotá tributaries that join to the main rivers in an elevation of 450 m asl show a capture knickpoint in the upper part of the stream (Fig. 4.3D). The s2 stream draining the Sumapaz basin shown in Fig. 4.4, joins the Bogotá river at an elevation of about 260 m asl and presents also flat areas in the headwaters in most of the rivers of the Sumapaz basin (Fig. 4.3D). The s2 stream flows parallel to the Fusagasugá syncline with a direction N-S and shows three knickpoints in the upper basin with no apparent relationship with tectonic or lithologic features, and a knickzone in the lower part associated to tectonic structures.

The rivers draining the eastern flank of the Eastern Cordillera of Colombia also display a flat upper part in their profile (Fig. 4.3E).The stream n1 (fig. 4.4A) shows a prominent knickpoint at an elevation of 3000 m asl and other minor knickpoints in the lower part associated with the inverted external-most structures. The stream e9 (Fig. 4.4A), shows a marked knickpoint at an elevation of 2600 m asl separating the flat area upstream from the downstream part: here we identified a middle knickpoint at 2000 m, a knickpoint corresponding to a dam at about 1400 m and several knickpoints associated with external structures.

In summary, the χ-plots of the Bogotá River draining to the south and the Suárez and Chicamocha rivers draining to the north display very similar configurations: they show a steep and highly incised lower part with structural knickpoints associated with the most external inverted faults along the mountain front of the Cordillera, separated by a marked knickpoint from a higher part relating to the plateau area. Each chi plot shows differences in terms of number of knickpoints. The Bogotá river shows a main plateau knickpoint at 2500 m asl, and just a few meters below another minor knickpoint was observed. In the Sogamoso basin, the Chicamocha river also shows a minor knickpoint below the plateau knickpoint. The Suárez river, shows two marked knickpoints below the main knickpoint and a steeper chi-plot than the Chicamocha river (see Fig. 4.4A for comparison).

The eastern and western flank plots (Fig. 4.3E and C, respectively) also show similarities and present a plateau capture knickpoint in the upper part and structural knickpoints in the lower part of the χ-plot. The western flank rivers show the capture knickpoint, and at lower elevation the χ-plots are in general smooth. In some of the streams draining the eastern flank, the capture knickpoint is usually located at lower elevation than in the western flank. Below the plateau knickpoint, other important knickzones are associated with lithological or structural features.

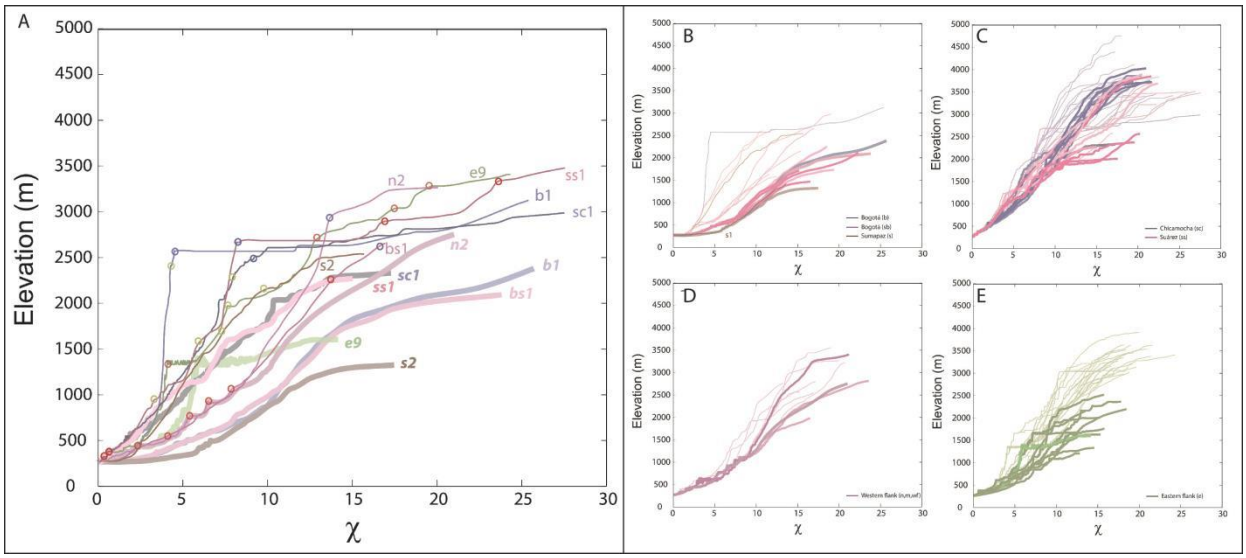

Fig.4.4. *Chi plot (thin lines) of the main stream for each basin with the respective knickpoints related to a plateau capture (blue circle), lithologic, structural, anthropogenic (red circle) or without relation with any of the last mentions (middle knickpoints, green circles). Thick plots are related with the areal remove analysis, (see 3.2.1). (a)Chi plot of the Bogotá and Sumapaz basins (b) Chi plot of Chicamocha and Suarez basins (c) Chi plot of the western flank basins (d) chi plot of the eastern flank basins.*

I checked the hypothesis of plateau captures by removing the upper part of the drainage area. Figure 4.4B shows the chi plots of the Bogotá and Sumapaz rivers removing the presumably captured areas of the plateau. On the resulting chi plots, all streams collapse along a similar trend, in agreement with that of the stream s1, indicating that recent captures did not occur in this stream and that they can be used as a record of the regional trend. The same display occurs in the Suárez and Chicamocha basins (Fig. 4.4C), where constructing the χ-plots without the plateau area leads to the general collapse of the streams. In this case, the trend with less headwater elevation (c.a. 2500 m) corresponds to small tributaries of the Suárez basin that drain to the trunk river in a eastern direction (ss8-10, Fig. 4.2). The western flank (Fig. 4.4D) shows a general collapse in the regional trend, as in Bogotá basin. Finally, the plots corresponding to the eastern flank (Fig. 4.4E) do not collapse on a clear single trend, at variance to Fig. 4.4A-C. The difference lies in the extension of captured area: while large plateau capture areas are related to Magdalena tributaries, the eastern flank only capture little areas of the plateau and then, the effect of the area removal does not give a clear signal as the Magdalena cases. The eastern flank plots indicate capture effect in the lower and medium parts, explaining why removing the upper plateau area they remain scattered in χ.

Observed knickpoints and χ -plot configurations suggest that reorganization is occurring on the western flank of the Eastern Cordillera: the Bogotá, Suárez, Chicamocha are gaining drainage area by plateau captures.

4.3.3. χ-map

Mapping χ over the basin shows high contrasts across the main divides; in general, higher contrast is found in the plateau areas (Fig. 4.5A), indicating that horizontal motion is occurring along the internal divides. An example of the plateau capture is provided by the χ signal in the Turmequé basin, in the eastern flank (Fig. 4.5B). Low values of χ near the divide correspond to the eastern flank and higher values are showed in the axial part of the Cordillera, characterized by the Bogotá and Sogamoso basins. Plateau captures in this area are highlighted by the plateau capture knickpoints (Fig. 4.3E and 4.4) and demonstrated in Chapters 2 and 3 reflecting different reentrant geometry of the divide, elbows of capture, similar slopes and similar erosion rates than in the Bogotá and upper Sogamoso. Therefore, with all these evidences in agreement with the resulting χ-map, I confirm the hypothesis of migration of the eastern divide towards the center of the orogen.

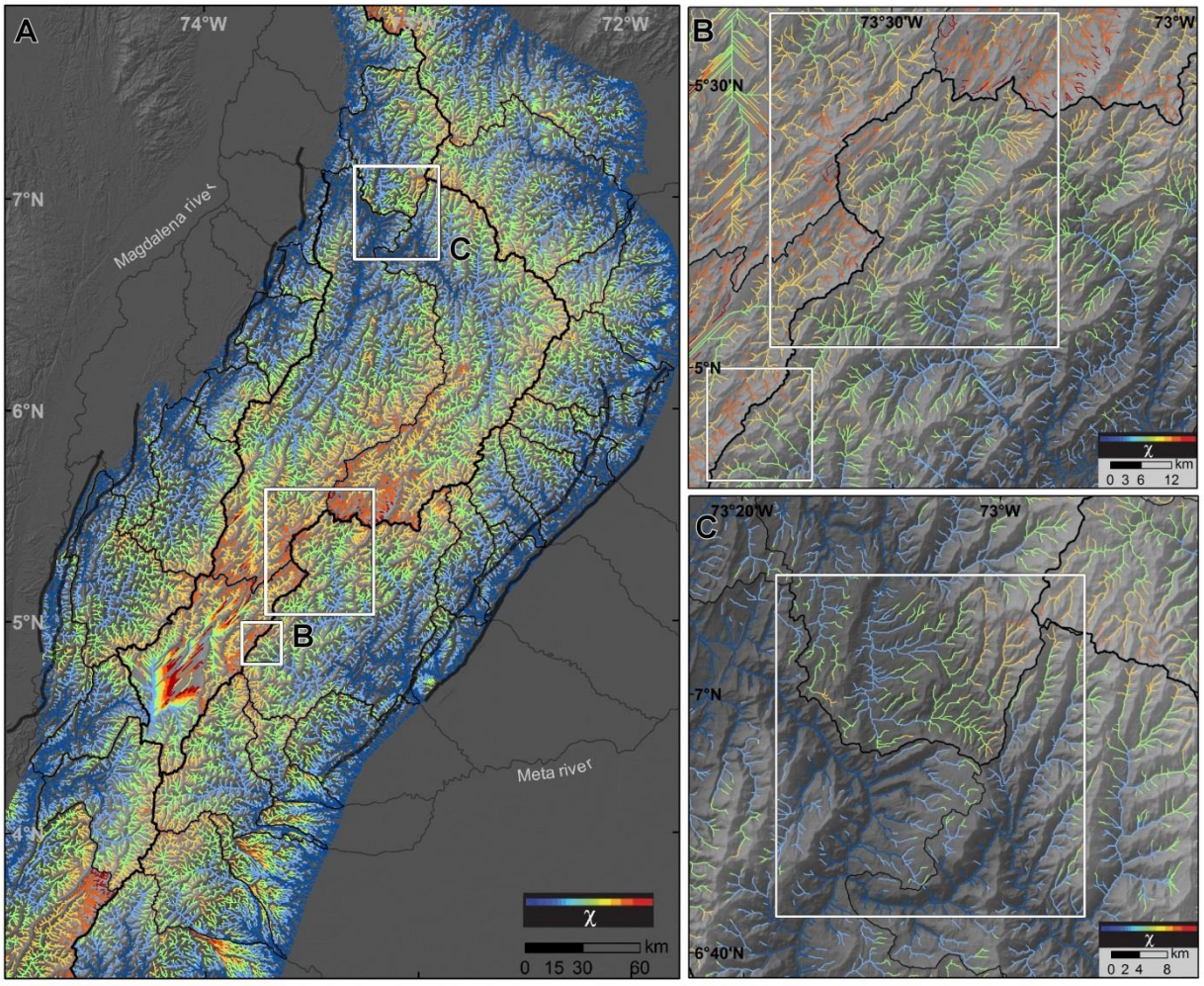

Fig.4.5. *(A) Chi map of the Eastern Cordillera of Colombia. High value contrast across the main drainage divides is notable. The white polygons refeer to zoomings. (B) Detailed chi map for the divide between the eastern flank and the flat central area (including the Bogotá, Suárez and Chicamocha basins). (C) Detailed chi map for the divide between the Sogamoso and Lebrija basins.*

Additionally, I found high χ contrast along the main divides, as shown in the little white box in Fig. 4.5B, indicating an ongoing capture of the longitudinal reach by the transverse river. The divide located between the Lebrija and Sogamoso basins (Fig. 4.5C) defines a chi gradient, where higher values are obtained in the Lebrija headwater elevations, indicating a divide migration to the north and an aggressor pattern of the Sogamoso tributaries.

4.3.4. Cosmogenic profile

The Bayesian results with 2χ error (Fig. 4.6) provide a most probable age for the concentration versus depth profile is 404.5 $^{+191.8}/_{-134.6}$ ka, an inheritance of 11.46 $^{+9.5}/_{-9.91}$ 10^4 atoms/g and an erosion rate of 0.08 $^{+0.04}/_{-0.08}$ cm/ka (see SD.4).

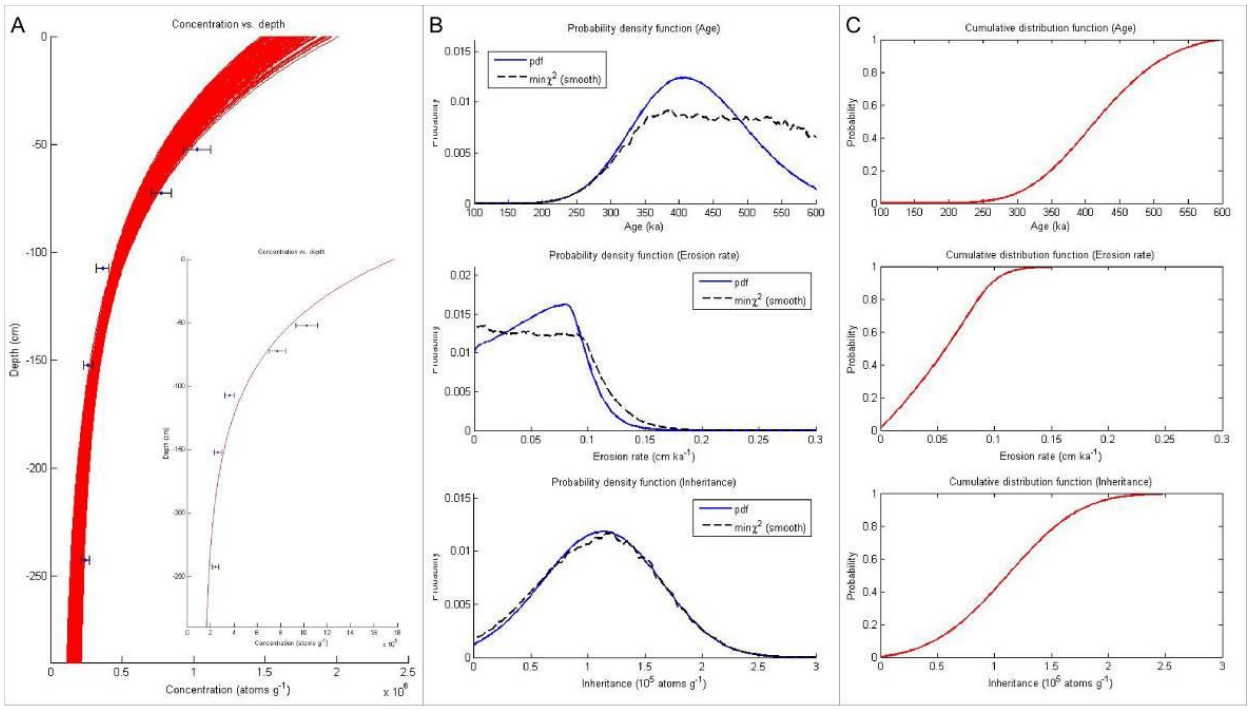

Fig.4.6. *Simulation depth profile results including the concentration versus depth plot of 2s profile solution with the best fit (A), the Probability density function (B) and Cumultaive distribution function (C) for the three free parameters: exposure age, erosion rate and inheritance.*

4.4. Discussion

The Eastern Cordillera of Colombia record a series of fluvial captures arguing for a drainage rearrangement (as was discussed in Chapters 2 and 3) with wind gaps, rockfall boulders in the divide and elbows of capture, as well as with calculations of erosion rates showing high contrasts across the main divide.

The number and distribution of the knickpoints reveal important information about the drainage network history. I observed that all basins have different knickpoint signature, with a major knickpoints in

different elevations or without them, meaning that the current network was developed before the mountain building. Otherwise, all streams would record same number and location (elevation) of major knickpoints.

The knickpoints analyzed can be related to changes in the base level and can be associated with captures in the same basin in the past. In this way, tributaries with a high quantity of knickpoints along the profile will be interpreted as earlier streams which had more time to register capture events along the trunk stream. Tributaries with minor number of knickpoints or without them are interpreted as formed in more recent times, and have not recorded past capture events.

The χ−plots can inform about the drainage pattern of gain/loss after the plateau capture (with the plateau areal remove), the current dynamics (adding the χ−map) and the ongoing drainage pattern.

Several fluvial captures occurred in the Eastern Cordillera of Colombia. The most important, which involucres the plateau captured areas are in the north of the Cordillera, the Suárez and Chicamocha captures and, in the south, the Bogotá capture. In what follows I reconstruct the relative timing of captures for the northern and southern plateau. Finally I explain a new model of drainage rearrangement for the Eastern Cordillera of Colombia.

4.4.1. Northern plateau capture: Suárez and Chicamocha basins

The northern part of the axial zone of the Eastern Cordillera is drained to the north by the Lebrija river, and the Suárez and Chicamocha rivers that finally flows to the west and joins the Magdalena river. The basins of the Suárez and Chicamocha rivers are deeply incised in the lower and intermediate parts, shaping impressive canyons along the trunk streams between latitudes 6-7ºN. This area was probably an ancient low-relief area delimited by two main thrusts, the Suárez fault to the west and the Bucaramanga fault to the east (see location in Fig.1.2). The drainage network flows parallel to the structural trends. The Suárez river flows parallel to the Suárez fault and finally drains to the Magdalena River after turning its course to the west with a sharp elbow. The Chicamocha River shows the same pattern: it follows the Bucaramanga fault along an N-S direction and finally shows a sharp elbow towards the Suárez River. The analysis performed on the digital elevation model helped to identify topographic evidences of the ongoing capture processes. The abrupt changes of flow direction do not correspond to structural trends, lithology or precipitation gradients. In the case of fluvial captures, I expected to find some evidence that highlighted the process: the described elbows, abandoned river valleys and fluvial terraces in the divide and different steepness of the opposite channels across the divide. I also expected high χ contrast across the divide in the χ-map and χ-plots with prominent inflections and different steepness revealing this process.

The χ-map shown in Figure 4.5 reveals χ contrast across the current divide between the Sogamoso and the Lebrija basin. Figure 4.7 summarizes, from Figure 4.3, the plot of elevation along the distance for the

Suárez (Fig. 4.7B) and for the Chicamocha river (Fig. 4.7C). I plot the elevation vs. distance of the drainage divide (Fig. 4.7D) following the methodology used in Chapter 3, highlighting three main depressions at lower elevation (of 500 m of difference between the depression and the mean elevation of the divide), in agreement on the elbow locations and the hypothetic ancient Suárez (marked with a number 2, Fig. 4.7A, D) and Chicamocha (number 3). The depression labelled with the number 1 relates to the ancient continuation of a southeast valley, following the main mechanism that for the Suárez and Chicamocha captures.

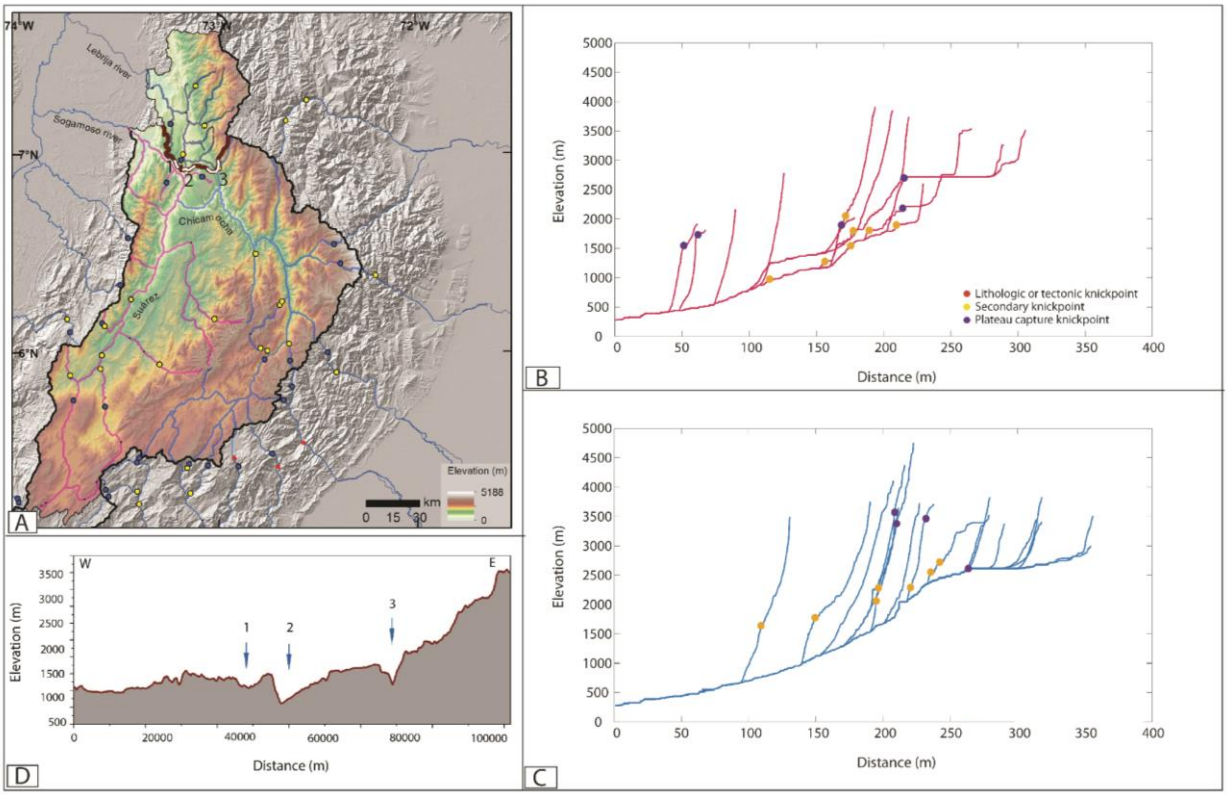

Fig.4.7. *Detailed results for the longitudinal profiles of the Suárez and Chicamocha river basins. Sogamoso and Lebrija basins with the location of the knickpoints and the divide between the basins in red (A). Longitudinal profiles of the analyzed rivers in the Suárez basin (B) and Chicamocha basin (C) and, elevation profile of the red drainage divide (D).*

A few terraces were found near the main divide in the Lebrija basin. I sampled one for dating and it provided an age c.a. 400 ka. Some works inquiry about the origin and significance of the thick Bucaramanga fan (300-400 m, see Fig.3 for location), an important quaternary sediment accumulation at the foot of the Santander Massif (De Porta, 1959; Julivert, 1963). The deposit age is estimated between 3 and 1 Ma (Jiménez et al., 2014). This thick fan is currently disconnected from important fluvial drainages upstream with sufficient transport capacity to explain the thickness. Previous works attributed its origin to the eastern drainage, draining from the Santander Massif (Ingeominas 2001, Jiménez et al., 2014) but the drainage area is not enough to explain the amount/volume of accumulated sediment volume. Therefore, the possibility of an ancient drainage of a Suárez-Chicamocha draining to the north, as proposed by Julivert, (1958), supplying sediments to the Bucaramanga fan, can explain the thick deposit.

From the knickpoint and χ-analysis we can obtain information about the capture history of these two basins. From figure 4.7 with the longitudinal profiles of the two rivers and the location of the knickpoints, we need to observe the number of "secondary" knickpoints just below the main capture knickpoint and then, compare between them. The Suárez trunk stream (Fig. 4.7B) has two major secondary knickpoints meanwhile the Chicamocha (Fig. 4.7C) does not have any. According to Giachetta et al. (2015), a large number of knickpoints in the chi profiles can be associated with a record of a large number of discrete capture events in the older part of the drainage. The larger number of knickpoints observed in the Suárez river profile compared to the Chicamocha river, support the hypothesis that the drainage network of the former is older and recorded capture events occurring in the latter.

Therefore, in the early stages of drainage network development in the northern part of the Eastern Cordillera, the Suárez and Chicamocha drained to the north following the mean faults that delimitated the ancient flat area, providing sediments to the Bucaramanga area. With the onset of plateau uplift, the regional slope increased along the flanks of the Eastern Cordillera and led to an increase of potential energy of the tributaries of the Magdalena River. At a given time, a Magdalena tributary (Sogamoso) finally captured the Suárez River producing a sharp elbow towards the Magdalena trunk river and producing a wind gap along the new divide. Based on our depth profile of the terrace in the wind gap related to the Suárez ancient course, the age of this capture is about 400 ka. After this capture, the incision propagated upstream by headward migration, providing more erosional potential to the tributaries of the Suárez river compared to the adjacent streams (Chicamocha basin). During this phase of river profile adjustment to the new base level, a tributary of the Suárez finally captured the Chicamocha river basin and the drainage network reached its current configuration. The knickpoints found along the Suárez river well fit in this model of drainage network evolution: the lower one (at an elevation of 1400 m) is probably related to the recent capture of the Chicamocha river.

4.4.2. Southern plateau capture: Bogotá basin

The southern part of the axial zone of the Cordillera is drained by the Bogotá river basin to the south, which joins finally the Magdalena river. The Bogotá river and its tributaries in the Sabana de Bogotá are rivers that follow the main structures longitudinally to the orogen, with low runoff velocity and meandering geometry, and the obtained erosion rates in Struth et al., (2016) indicate a very low denudation. The Bogotá river shows an important plateau capture at an elevation of 2550 m asl. A few meters below it (400 m), there is a secondary knickpoint. Downstream the plateau knickpoint, there is a stream length that appears very incised, where the river falls c.a. 1500 m, from the initial 2550 m altitude of plateau outlet (the Tequendama falls, see location in Fig. 3.2). The plateau abandonment marked by the plateau knickpoint and the presence of a capture elbow reinforce the capture interpretation of the Bogotá plateau river by a Magdalena tributary.

Figure 4.8, summarized from Figure 4.3, shows the plot of elevation vs. distance for the Bogotá rivers (Fig. 4.8B) and for the Sumapaz river (Fig. 4.8C). I plot elevation along the distance of the drainage divide (FIG. 4.8D), highlighting eight depressions at lower elevation, where the number 5 is related to the Bogotá plateau outlet. Depressions from 1 to 4 reflect little plateau captures from Bogotá tributaries and depressions 6-8 reflect little plateau captured areas from Sumapaz tributaries.

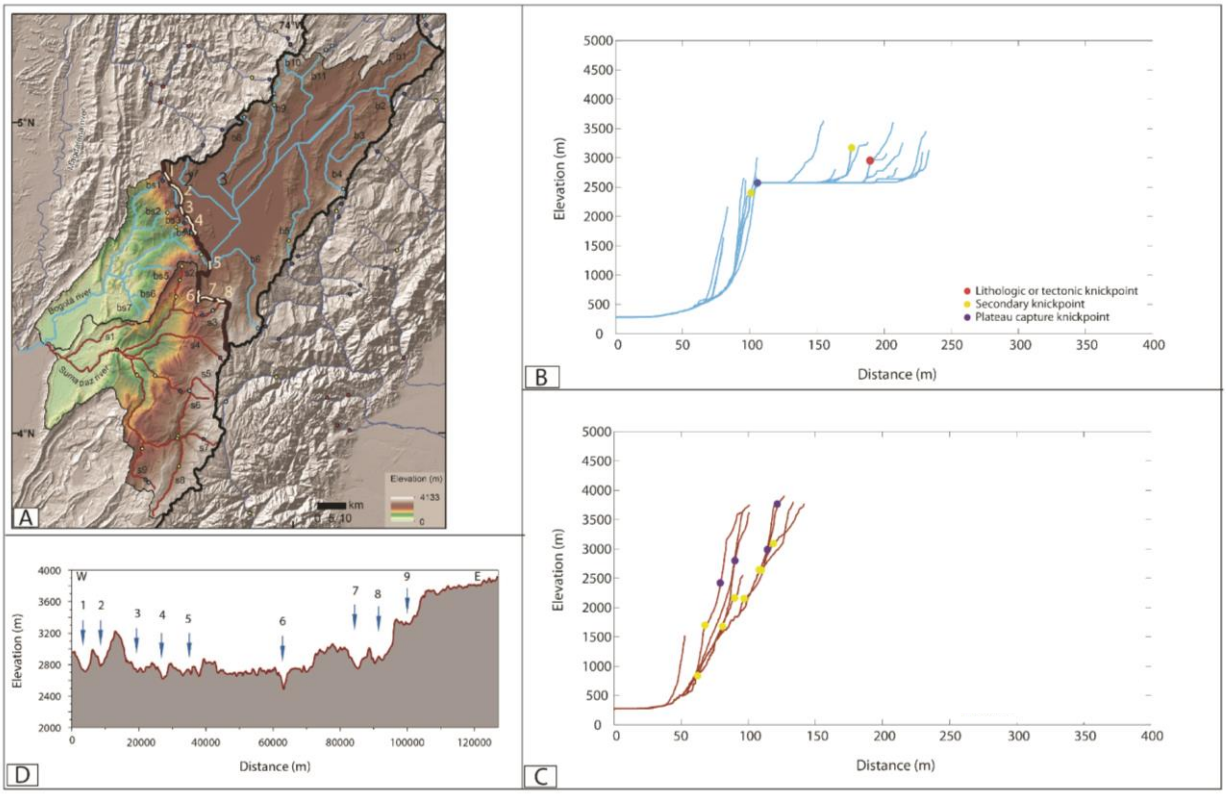

Fig.4.8. *Detailed results for the longitudinal profiles of the Bogotá and Sumapaz river basins. Bogotá and Sumapaz basins with the location of the knickpoints, drainage divide (red thick line) and depressions location (white tracts) (A). Longitudinal profile of the rivers of the Bogotá basin (B) and Sumapaz basin (C). Elevation profile of the divide and location of the main depressions (D).*

Important capture evidences are found in the southernmost Sumapaz basin (Fig. 4.9), defined by the Fusagasugá syncline structure (see location in Fig. 1.2). First, this syncline show a recent incision signal based on the observation of well-preserved terraces now incised in the middle of the tectonic structure (Fig. 4.9, pale pink polygon). Secondly, following the axis of the syncline to the north, we can observe in the watershed divide an impressive wind gap, with a preserved meandering shape (Fig. 4.9B and C), arguing for an ancient drainage to the north, towards the Sabana, indicating a probable connection between them. In addition, the χ- map shows that for the northern part of the Fusagasugá basin, χ values are higher than for the Bogotá tributaries, arguing for a divide migration to the south.

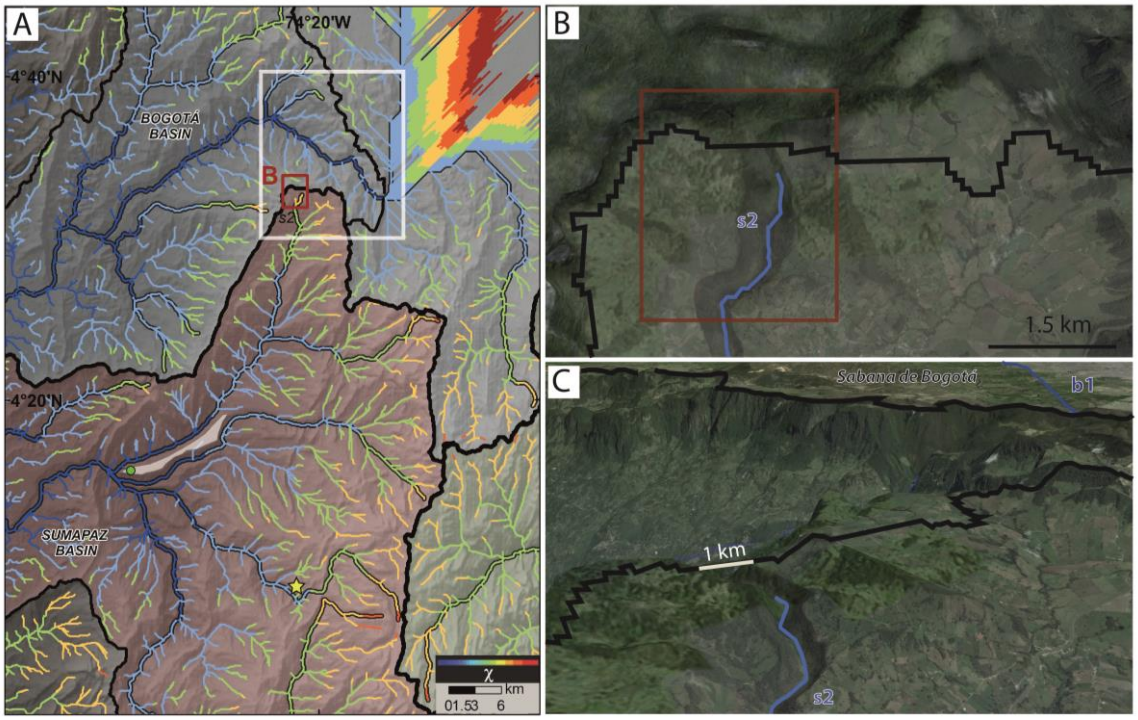

***Fig.4.9**. Detail of the Sumapaz and Bogotá drainage divides (see location in Fig. 4.2). (A) χ map for the detailed area showing higher χ values in the Sumapaz basin and lower ones in the Bogotá, just in the wind gap location indicated with a red box. White box highlights the irregular shape of the divide and the yellow star indicates the location of a non-dissected landslide (B) Detail of the relict meandering valley of the s2 stream. (C) Oblique view of the wind gap, with a width of 1 km and 160 m high. Source of B and C: Google maps, DigitalGlobe.*

In order to highlight the capture of the Sabana by a transverse river (tributary of the Magdalena), I focus in the results of the plateau area removal (Fig.6). I observe that for the Bogotá basin, without the plateau, all the streams collapse in the same trend, representing the regional trend of river profiles before capture.

All this evidence in the same area, allows to interpret a complex history characterized by two important capture events related to the Sabana de Bogotá: i) an initial Magdalena tributary reached the Fusagasugá syncline (Sumapaz basin), capturing the associated longitudinal drainage. The increasing erosion in the Sumapaz river finally results in the first Sabana capture. By the extensive area gain from the Sabana capture in the Sumapaz river, all the Magdalena tributaries experienced the gain area and increment their erosive capacity, resulting in a second capture of the Sabana plateau by a different Magdalena tributary and providing the current Bogotá fluvial network. Due to this erosive capacity, these tributaries started to incise and capture the high plateau areas and then, one of those captured laterally the Sabana de Bogotá again, and a sharp capture elbow, leading a wind gap in the northern divide of the Sumapaz basin, and resulting in the current form of the Bogotá boundary downstream of the main plateau capture knickpoint.

The capture hypothesis can be tested by different drainage areas to the S2 stream (Fig. 4.10). In order to confirm the lost connection between the Sabana and the Sumapaz drainages, I can estimate the area needed for the s2 stream (see location in Fig. 4.2A) to be linearized and collapsed on the regional trend of it basin; this will be the minimum area loss for the post-plateau capture of the S2 river.

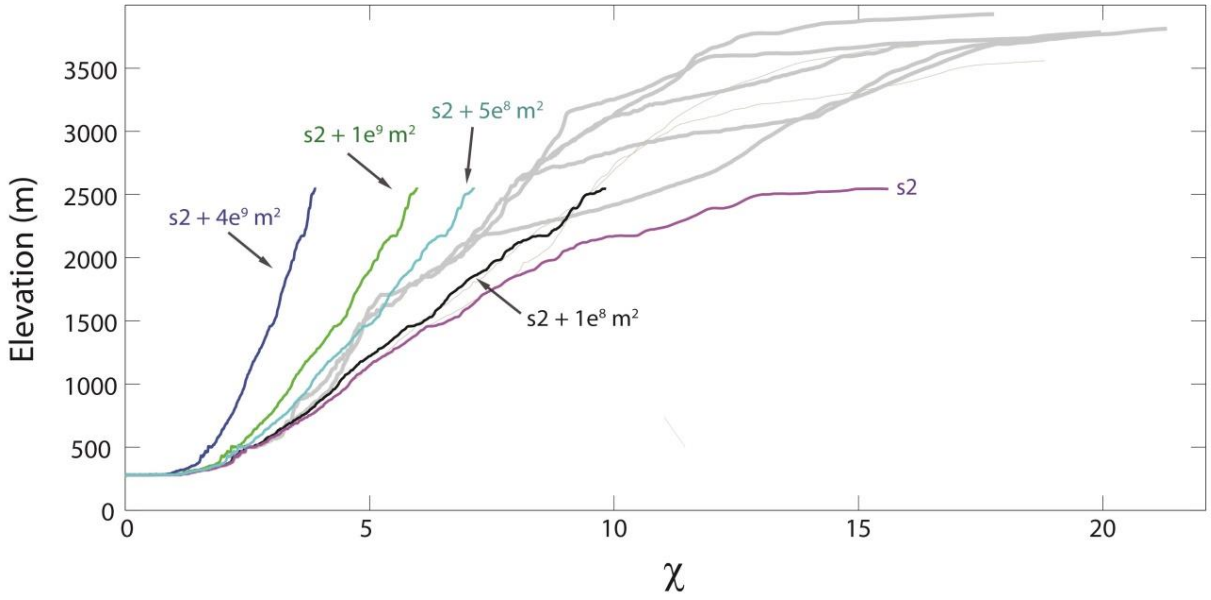

Fig.4.10. *Drainage test on the s2 chi plot. Different areas added to the s2 stream are indicated in the figure. The gray lines are the plots of the Sumapaz tributaries.*

The results of figure 4.10 indicate that the minimum upstream drainage area to make s2 collapse the regional trend is between the addition of $1e^9$ and $5e^8$ m^2. Therefore, I can conclude in an ancient connection of the Sumapaz with the plateau. I should like to highlight that the current area of the Sabana de Bogotá area is about $4e^9$ m^2, an area which fits with the necessary extension for make the s2 stream to collapse with the tributaries.

4.4.3. A model of drainage network evolution

From the evidence presented for the northern and southern plateau captures, I propose a new model of drainage rearrangement of the Eastern Cordillera of Colombia, taking into account to the observed knickpoints, the χ analysis, the geomorphic evidence, the erosion rates and the paleodrainage reconstruction.

The current drainage network and its reorganization derive from a previous fluvial configuration and compartmentalization, which evolved with time. In a pre-inversion stage (Campanian to Maastrichtian), the southern and northern part of the Central Cordillera were uplifted, sourcing clastic deposition in the current western side of the Magdalena Valley Basin. In the Paleocene- Early Eocene, the Central Cordillera was still actively uplifting (the current Magdalena Valley Basin too), being the source area for an eastern drainage to the former graben of the Eastern Cordillera, and to the Amazon craton. Early Cenozoic deposits in the Eastern Cordillera show paleocurrent data indicating a western sediment source, with a drainage network controlled by the emerging structures (flowing longitudinally) and following the regional slope to the north (Laverde et al., 1989; Cooper et al., 1995; Diaz and Serrano, 2001; Gómez et

al., 2005a; Bayona et al., 2008; Horton et al., 2010; Nie et al., 2010, 2012; Saylor et al., 2011; Bande et al., 2012; Caballero et al., 2013; Silva et al., 2013).

In the Late Eocene, the Floresta massif started to be exhumed, and the pattern of NE-SW of actively structures continued in this time. The axial zone of the Eastern Cordillera was characterized by small anticlines that grew and erode contemporaneously with syntectonic deposition in the adjacent synclines (Silva et al., 2013). During the late Oligocene-early Miocene, in association with the most widespread mountain building in the Eastern Cordillera began the thrust-induced exhumation along the eastern flank of the Eastern Cordillera, and the coeval units were preserved in the axial zone, now bounded by exhuming structural highs: the Farallones Anticlines to the east, the Villeta Anticlinorium to the west and the Floresta Massif to the north, and was topographically closed to the south as well. Additionally, the Quetame Massif began to exhume and isolated the axial basin from the Llanos foreland (south of 6º), as indicated by a decrease in Zr in the eastern foothills. Similar to the axial zone of the Eastern Cordillera, the Magdalena Valley was probably another partially closed basin during the entire Oligocene (Caballero et al., 2012a). During the early and middle Miocene, the exhumation became faster in north of 6ºN and the entire Eastern Cordillera was submitted to exhumation. At this time, the tectonic activity was greater than river incision, arguing for a structural control factor for drainage. Since the late Miocene, Neogene deposits were exposed to the erosion along both foothills, due to faster denudation and topographic growth and no depositional record in the axial Eastern Cordillera due to a complete exhumation.

In summary, the drainage pattern in the Eastern Cordillera generally remained axial and parallel to structural features during Paleogene times. During the Pliocene to present, faster deformation rates and topographic building were recorded in the Eastern Cordillera. At this time the Magdalena Valley reopened to the north, where the proto-Magdalena was connected with all the transverse drainage streams from the Central and Eastern Cordilleras. The Sabana basin remained closed (Caballero et al., 2012b; Silva et al., 2013).

At the Sabana de Bogotá (intermontane basin of the Bogotá river), a fluvio-lacustrine sediment infill started c. 3.2 Ma, followed by shallow-water and swamps with some fluvial activity (c. 3-1.5 Ma). Between 1.5 and 0.028 Ma, the sedimentation was in almost uninterrupted lacustrine conditions. The most recent sediments reflect a fluvial paleoenvironment deposited by the Bogotá river and its tributaries (Torres et al., 2005). A controversy in this basin lies in the nature of the current outlet of the Bogotá river and the timing of basin opening.

At this time, the Eastern Cordillera is characterized by two steep flanks with steeper transverse rivers flowing to the Magdalena (W) and Meta (E) rivers, and a high flat elevated area (the Sabana de Bogotá) with an internal drainage. We observe two big basins incorporating flat areas in the headwaters: the Sogamoso and Bogotá basins, both associated with capture events.

With the Cordillera uplift, the flank streams increased the potentially energy. Initially, the small tributaries compete with the external longitudinal tectonic structures, and finally they cut them and began to experience an upward erosion wave cutting all the longitudinal structures and capturing the longitudinal stream associated. The chronology of this erosion wave in each one of the streams was interpreted by knickpoint distribution and χ analysis.

Consequently I argue for an erosion wave that originated in the northern parts of the Magdalena River basin and propagated upstream toward the south, where its tributaries were the "agressors" in the capture history of the Eastern Cordillera of Colombia. A common feature of all the tributaries of the Magdalena in the Eastern Cordillera is the existence of knickpoints of tectonic origin at low elevations on the chi plots, evidencing the capture of the longitudinal streams in the most external parts of the inverted rift by the transverse tributaries. First, the Sogamoso tributary captured the Suárez around 400 ka ago (based on the dating of the abandoned terrace), and an erosion wave started to propagate trough the drainage network of the inner Cordillera, where eventually a tributary captured the adjacent longitudinal valley of present-day Chicamocha river. As the erosion wave propagated southward, all the tributaries of the Magdalena increased energy and began to incise and capture the external longitudinal streams, propagating further upstream and threatening the Sabana by fluvial captures of the high elevated longitudinal rivers. The mean divides started to retreat, moving in direction of the interior of the plateau, as recorded in the erosion rates (chapter 3). The erosion continues moving upwards providing more erosive capacity to the rivers located in the southern part of the Magdalena Valley, where one of the tributaries (the s2 stream) reached the Fusagasugá syncline (the Sumapaz basin) and captured the longitudinal drainage. The erosion increase in the Sumapaz basin resulted in an important capture of the Sabana de Bogotá and subsequently to the end of the endorheic conditions, with a new flow towards the Magdalena Valley. From the large captured area of the Sabana, all the Magdalena tributaries shifted in the χ plot to the aggressor zone, providing an increase of energy for all the Magdalena streams. Finally, one of them captured the Sabana of Bogotá again, resulting in the current Bogotá river (b1). This capture event is evidenced by the main knickpoint and capture elbow in the Bogotá river, by the meandering wind gap in the Sumapaz divide, by the area calculation and by an anomalous basin shape of the Bogotá basin downward of the main knickpoint (white box in Fig.4.9). OSL analysis from Hoyos et al. (2015) provide an age of 38.9-8.7 ka for the terrace deposits in the Sumapaz basin (Fig. 4.9), enhancing our interpretation of a recent capture on the basis of flat relicts poorly eroded or the presence of undissected landslides (Fig. 4.11).

Fig. 4.11. *Undissected landslide (white polygon) indicating a very recent current fluvial configuration. In addition, we can observe an ongoing fluvial capture of the longitudinal valley by the transverse river. See location in fig.4.9, yellow star. Source: Google, DigitalGlobe.*

Figure 4.11 shows the location of an undissected landslide (about 2 km long and 0.7 wide) arguing for a recent fluvial reorganization. In addition, in this figure we can observe an ongoing fluvial capture of the longitudinal course located at the east side of the landslide.

On basis on the results and interpretations here presented, I propose the reopening of the Magdalena Basin and the subsequent decrease of the base level as the main precursor of the propagating incision wave to the south in the Magdalena Valley. In this way, the basins connected with the Magdalena river reflect an "aggressor" pattern in contrast to the basins from the Meta river (eastern flank).

4.5. Conclusions

This work confirms the dynamic state of the fluvial drainage network of the Eastern Cordillera of Colombia, on the basis of the χ-parameter and topographic, sedimentologic, and geochronologic evidence. The dynamism of the drainage network follows an evolution pattern from an initial longitudinal-dominated drainage to a transverse-dominated one. A new model of drainage rearrangement for the Eastern Cordillera of Colombia is described, taking into account the knickpoint distribution, the chi analysis, the geomorphic evidence, and published erosion rates and paleodrainage data. The evolution of the fluvial network of the Cordillera was triggered by fluvial captures, which I interpret as caused by the reopening of the Magdalena basin and the subsequent decrease of the base level. This was the precursor of the propagating incision wave that moved southwards along the Magdalena Valley. The first

main longitudinal basin captured was the Suárez basin around 400 ka ago (based on the dating of the abandoned terrace), propagating the erosion wave inside the Cordillera, resulting in the capture of the Chicamocha basin. As the erosion wave propagates southward along the Magdalena Valley, all the tributaries of that river increased their energy and began to incise and capture the external longitudinal streams, and one of them finally captured a big area: the Sumapaz basin. After the capture, the incision began to move upwards reaching eventually the endorheic Sabana de Bogotá basin. At the same time, all the Magdalena tributaries experienced enhanced erosion resulting, again, in a capture of the Sabana leading to the current fluvial configuration. This capture is evidenced by a wind gap in the Sumapaz divide, the steeper knickpoint at the plateau outlet (the Tequendama falls), and by the calculation of area loss for the Sumapaz river. The Sabana capture events are very recent, indicated by published ages of 38.9-8.7 ka for a terrace in the Sumapaz basin. Therefore, the Magdalena basin play the main role of aggressor in contrast to the basins located in the eastern flank (joining the Meta river), which acted as losers.

The dynamics of drainage network described here is still active in the Eastern Cordillera, and we can expect future captures to occur in areas where steep transverse rivers flow close to low-gradient longitudinal rivers of the Sabana de Bogotá plateau, especially if they are separated by a low-elevation stretch of the main divide.

Conclusions

This thesis addresses the interrelation between the fluvial drainage and the tectonic evolution of the Eastern Cordillera of Colombia, based on a multidisciplinary approach including digital topographic analysis and geochronology. This multidisciplinary approach allowed to evidence the dynamic state of the topography and quantify the erosive signal in the drainage basins in order to highlight the fluvial dynamism, and to describe the evolution pattern of the fluvial drainage network since the initial stages of orogenic inversion of the former Eastern Cordillera rift.

The most important findings of this study are summarized below:

5.1. River dynamics from topographic analysis and terrestrial cosmogenic nuclides

- Two topographic domains are distinguished in the Eastern Cordillera of Colombia: an axial plateau and the adjoining flanks. The plateau (Sabana de Bogotá) is characterized by gentle longitudinal rivers that follow the main tectonic structures, low local relief and slopes and by a terrestrial cosmogenic nuclide data revealing low erosion rates (<20 mm/ka). The flanks are characterized by high local relief and slope, and are dominated by steep transverse rivers that cut across the tectonic structures, with a higher erosion rate (>50 mm/ka).
- The dynamic state of the fluvial network of the Eastern Cordillera is evidenced by morphometric analysis, published palaeocurrent published data and field observations suggesting that the drainage network in the Cordillera evolves from longitudinal-dominated to transverse-dominated via fluvial captures, with rivers turning into the direction of the regional slope perpendicular to the orogenic trend. These evidences indicates, in addition to the contrasting erosion rates between the flanks and the Sabana, that the N-S oriented drainage divide migrate toward the inner part of the Cordillera by discrete events of capture, leading into a progressive plateau area reduction.
- Certain geomorphic parameters provide information about the erosion trends in channel networks and therefore inform about the dynamism of the fluvial drainage. Comparing the most relevant of those (SSP, Mx and χ) with the erosion rates, I found that the Mx parameter is the best fit parameter with the best correlation, allowing by extension a first estimation of erosion rates in areas without cosmogenic data (equation 3.3, Chapter 3), i.e. it can provide a first estimation of the erosion dynamics for a mountain belt with similar pluviometric and lithologic characteristics (alternation of sandstone and shale formations).
- A review of published paleocurrent data showed a change in sediment dispersal in the eastern flank of the Cordillera: a Paleogene palaeodrainage toward the NNE, parallel to early tectonic structures, is now replaced by a SE-directed drainage, incising across Paleogene strata, arguing for drainage reorganization.

- The fluvial reorganization evolves from longitudinal to transverse-dominated drainage triggered by the regional slope increase by the progressive accumulation of crustal shortening and thickening, what has been reported to the Moroccan High Atlas. Local climate, tectonics and lithology play a secondary role in controlling the erosion rates and the basin dynamics at a local scale.
- The thesis contributes with the first exposure age terrace dating in the Eastern Cordillera of Colombia, with a sampled terrace in the Guayuriba basin (eastern flank, 406 m above the Guayuriba river) with an age of 655 ka, indicating an average incision rate of 62 mm/ka.
- Changes in drainage areas by captures must affect the clastic fluxes at the outlets, and modify the spatial and temporal localization of the proximal clastic bodies at the toe of the thrust front in the contemporaneous sedimentary basins. The process of fluvial drainage reorganization in the source areas of the mountain belt may have exerted an important control in sedimentation rates and depocenter migration in the forelands adjacent to the Eastern Cordillera, in addition to thrust loading.

5.2. A new model of drainage network evolution

- A new model of drainage rearrangement for the Eastern Cordillera of Colombia is presented taking into account the knickpoint distribution, the chi analysis, geomorphic evidences, erosion rates and paleodrainage.
- The model proposes that the evolution of the fluvial network was triggered by a series of fluvial captures along the Eastern Cordillera with an origin in the reopening of the Magdalena basin as the main precursor of the propagating incision wave to the south along the Magdalena Valley, which eventually reached the Eastern Cordillera.
- A common characteristic of all the tributaries of the Magdalena in the Eastern Cordillera is the existence of small knickpoints at low elevation on the chi plots evidencing the capture of the longitudinal streams in the most external parts of the growing mountain belt by the transverse tributaries. Number and elevation distribution of the knickpoints in a basin can inform us about the relative timing capture.
- The first capture by the Sogamoso river (a Magdalena tributary), which captured the Suárez basin 400 ka ago (based in the abandoned terrace), resulted in the onset of the propagation of the erosion wave inside the Eastern Cordillera. One of the Suárez tributaries eventually captured the adjacent longitudinal valley: the Chicamocha basin.
- The continued upward propagation of the erosion wave increased energy to the Magdalena tributaries, resulting in the capture of the longitudinal valleys located in the most external part of the western flank of the Cordillera, with the consequent incision along that flank and the threat to the longitudinal streams of the Sabana. The increased erosion and incision in these flank rivers results in a fluvial captures of the high-elevation longitudinal rivers in the Sabana and hence, the main divides started to retreat and move in direction of the center of the plateau, as suggested by the recorded

erosion rates. This fluvial evolution is in agreement with the hypothesis of longitudinal to transverse fluvial evolution.

- Eventually, the Magdalena tributaries located between 5-4º N began to incise with more energy and one of them finally reached the longitudinal drainage of the Fusagasugá syncline (Sumapaz Basin) and later captured the endorheic Sabana de Bogotá, as evidenced by the area calculation and the meandering wind gap. Terrace dating in the Sumapaz basin gave an age of 38.9-8.7 ka, based in OSL (Hoyos et al., 2015), supporting the interpretation of a young capture. This capture enhanced several erosion waves propagating in all the Magdalena tributaries, and one of them eventually capture the Sabana, resulting in the steeped long profile of the Bogotá river, producing large knickpoint, the wind gap in the Sumapaz syncline, and an anomalous shape of the Bogotá basin downward of the main knickpoint.
- The dynamics of drainage network described in this thesis is currently active in the Eastern Cordillera of Colombia. We can expect future captures to occur in areas where steep transverse rivers flow close to low-gradient longitudinal rivers located in the plateau, especially if they are separated by a depression in the main divide, and a continental reduction of the plateau of the Sabana de Bogotá.

References

Akaike H., 1974. A new look at the statistical model identification. IEEE Trans. Autom. Control, 19, 716–723, doi:10.1109/TAC.1974.1100705.

Allen, P.A., 2008. From landscapes into geological history. Nature, 451, 274–276, doi: 10.1038/nature06586.

Alvarez, A.J., 1983. Geología de la Cordillera Central y el occidente Colombiano y petroquímica de los intrusivos granitoides mesocenozoicos. Boletin Geologico Ingeominas, 26, Bogotá.

Andriessen, P.A.M., Helmens, K.F., Hooghiemstra, H., Riezebos, P.A., Van der Hammen, T., 1993. Absolute chronology of the Pliocene-Quaternary sediment sequence of the Bogota area, Colombia. Quaternary Science Reviews, 12, 483–501, doi: 10.1016/0277-3791(93)90066-U.

Antón, L., Rodés, A., De Vicente, G., Pallàs, R., Garcia-Castellanos, D., Stuart, F.M. Braucher, R., Bourlès, D., 2012. Quantification of fluvial incision in the Duero Basin (NW Iberia) from longitudinal profile analysis and terrestrial cosmogenic nuclide concentrations. Geomorphology, 165-166, 50–61, doi:10.1016/j.geomorph.2011.12.036.

Babault, J., Teixell, A., Struth, L., Driessche, J. Van Den, Arboleya, M., Tesón, E., 2013. Shortening, structural relief and drainage evolution in inverted rifts: insights from the Atlas Mountains, the Eastern Cordillera of Colombia and the Pyrenees. Geological Society of London, Special Publications, 377, 141–158, doi: 10.1144/SP377.14.

Babault, J., Van Den Driessche, J., Teixell, A., 2012. Longitudinal to transverse drainage network evolution in the High Atlas (Morocco): The role of tectonics. Tectonics, 31, doi: 10.1029/2011TC003015.

Balco, G., Stone, J.O., Lifton, N. A., Dunai, T.J., 2008. A complete and easily accessible means of calculating surface exposure ages or erosion rates from 10Be and 26Al measurements. Quaternary Geochronology, 3: 174–195, doi: 10.1016/j.quageo.2007.12.001 .

Bande, A., Horton, B.K., Ramírez, J.C., Mora, A., Parra, M., Stockli, D.F., 2012. Clastic deposition, provenance, and sequence of Andean thrusting in the frontal Eastern Cordillera and Llanos foreland basin of Colombia. Bulletin of the Geological Society of America, 124, 59–76, doi: 10.1130/B30412.1.

Bayona, G., Cortés, M., Jaramillo, C., Llinas, R., 2003. The Tertiary Fusagasugá Succession: a Record of the Complex Latest Cretaceous-Pre- Miocene Deformation Between the Magdalena Valley and Sabana de Bogotá. VIII Simposio Bolivariano de Cuencas Subandinas, Cartagena; 180–193.

Bayona, G., 2008. Geocronología, termocronología, bioestratigrafía y procedencia de unidades paleógenas en la zona axial de la Cordillera Oriental; Aportes al modelamiento del sistema petrolífero en las cuencas adyacentes. ICP-Ecopetrol report.

Bayona, G., Cortés, M., Jaramillo, C., Ojeda, G., Aristizabal, J.J., Reyes-Harker, A., 2008. An integrated analysis of an orogen-sedimentary basin pair: Latest Cretaceous-Cenozoic evolution of the linked Eastern Cordillera orogen and the Llanos foreland basin of Colombia. Bulletin of the Geological Society of America, 120, 1171–1197, doi: 10.1130/B26187.1.

Bierman, P.R., Coppersmith, R., Hanson, K., Neveling, J., Portenga, E.W., Rood, D.H., 2014. A cosmogenic view of erosion, relief generation, and the age of faulting in southern Africa. GSA Today, 24, 4–11, doi: 10.1130/GSATG206A.1.

Bishop, P., 1995. Drainage rearrangement by river capture, beheading and diversion. Progress in Physical Geography, 19, 449–473, doi: 10.1177/030913339501900402.

Bonnet, S., 2009. Shrinking and splitting of drainage basins in orogenic landscapes from the migration of the main drainage divide. Nature Geoscience, 2, 766–771, doi: 10.1038/ngeo666.

Bookhagen, B., Burbank, D.W., 2010. Toward a complete Himalayan hydrological budget: Spatiotemporal distribution of snowmelt and rainfall and their impact on river discharge. Journal of Geophysical Research: Earth Surface, 115, 1–25, doi: 10.1029/2009JF001426.

Bookhagen, B., Strecker, M. R., 2008. Orographic barriers, high-resolution TRMM rainfall, and relief variations along the eastern Andes. Geophysical Research Letters, 35, 1–6, doi: 10.1029/2007GL032011.

Bookhagen, B., Strecker, M.R., 2012. Spatiotemporal trends in erosion rates across a pronounced rainfall gradient: Examples from the southern Central Andes. Earth and Planetary Science Letters, 327-328, 97–110, doi: 10.1016/j.epsl.2012.02.005.

Borchers, B., Marrero, S., Balco, G., Caffee, M., Goehring, B., Lifton, N., Nishiizumi, K., Philips, F., Schaefer, J., Stone, J., 2016. Geological Calibration of spallation production rates in the CRONUS Earth project. Quaternary Geochronology, 31, 188-198, doi: 10.1016/j.quageo.2015.01.009.

Bourlès, D.L., 1988. Etude de la géochimie de l'isotope cosmogénique 10Be et de son isotope stable 9Be en milieu océanique. Application à la datation des sediments marins.

Brocard, G., Willenbring, J., Suski, B., Audra, P., Authemayou, C., Cosenza-Muralles, B., Moran-Ical, S., Demory, F., Rochette, P., Vennemann, T., Holliger, K., Teyssier, C., 2012. Rate and processes of river network rearrangement during incipient faulting: The case of the Cahabon River, Guatemala. American Journal of Science. 312, 449–507, doi: 10.2475/05.2012.01.

Brocklehurst, S.H., Whipple, K.X., 2002. Glacial erosion and relief production in the Eastern Sierra Nevada, California. Geomorphology, 42, 1–24, doi: 10.1016/S0169-555X(01)00069-1.

Brookfield, M.E., 1998. Evolution of the great river systems of southern Asia during the Cenozoic India-Asia collision: Rivers draining southwards. Geomorphology, 22, 285–312, doi: 10.1016/j.geomorph.2008.01.003.

Brown, E.T., Brook, E.J., Raisbeck, G.M., Yiou, F., Kurz, M.D., 1992. Al in quartz: Implications for exposure age dating. Geophysical Research Letters, 19, 369, doi: 10.1029/92GL00266.

Brown, E.T., Edmond, J.M., Raisbeck, G.M., Yiou, F., Kurz, M.D., Brook, E.J., 1991. Examination of surface exposure ages of Antarctic moraines using in situ produced 10Be and 26Al. Geochimica et Cosmochimica Acta, 55, 2269–2283, doi: 10.1016/0016-7037(91)90103-C.

Brown, E.T., Edmond, J.M., Raisbeck, G.M., Yiou, F., Kurz, M.D., Brook, E.J., 1991. Examination of surface exposure ages of Antarctic moraines using in situ produced 10Be and 26Al. Geochimica et Cosmochimica Acta, doi: 10.1016/0016-7037(91)90103-C.

Bull, W.B. ,1991. Geomorphic Responses to Climatic Change. Oxford University Press: New York.

Burnham, K.P., Anderson, D.R., 2002. Model Selection and Multimodel Inference: A Practical Information-Theoretic Approach, 2nd ed., 488 pp., Springer-Verlag, New York, ISBN:0-387-95364-7.

Caballero, V., Parra, M., Mora, A., Lopez, C., Rojas, L.E., Quintero, I., 2013b. Factors controlling selective abandonment and reactivation in thick-skin orogens: a case study in the Magdalena Valley, Colombia. Geological Society, London, Special Publications, 377, 343–367, doi: 10.1144/SP377.4 .

Caballero, V., Mora, A., Quintero, I., Blanco, V., Parra, M., Rojas, L.E., Lopez, C., Sanchez, N., Horton, B.K. Stockli, S., Duddy, I., 2013a. Tectonic controls on sedimentation in an intermontane hinterland basin adjacent to inversion structures: the Nuevo Mundo syncline, Middle Magdalena Valley, Colombia. Geological Society, London, Special Publications, 377, 315–342. doi: 10.1144/SP377.12.

Campbell, C.J., H. Burgl, 1965, Section through the Eastern Cordillera of Colombia, South America: Geological Society of America Bulletin, 76, 567-590.

Carretier, S., Regard, V., Vassallo, R., Martinod, J., Christophoul, F., Gayer, E., Audin, L., Lagene, C., 2015. A note on 10Be-derived mean erosion rates in catchments with heterogeneous lithology: examples from the western Central Andes. Earth Surface Processes and Landforms, 40, 1719-1729, doi: 10.1002/esp.3748.

Castelltort, S., Goren, L., Willett, S.D., Champagnac, J.D., Herman, F., Braun, J., 2012. River drainage patterns in the New Zealand Alps primarily controlled by plate tectonic strain. Nature Geoscience, 5, 744–748, doi: 10.1038/ngeo1582.

Castro, E., 1992. Estado actual de investigación en la cuenca del río Chicamocha, Departamentos de Santander y Boyaca. Ministerio de Minas y Energía. Instituto de investigaciones en geociencias, minería y química. Oficina regional nororiente.

Cerling, T.E., Craig, H., 1994. Geomorphology and In-Situ Cosmogenic Isotopes. Annual Review of Earth and Planetary Sciences, 22, 273–317, doi: 10.1146/annurev.earth.22.1.273.

Chadwick, O.A., Roering, J.J., Heimsath, A.M., Levick, S.R., Asner, G.P., Khomo, L., 2013. Shaping post-orogenic landscapes by climate and chemical weathering. Geology, 41, 1171–1174, doi: 10.1130/G34721.1.

Champel, B., 2002. Growth and lateral propagation of fault-related folds in the Siwaliks of western Nepal: Rates, mechanisms, and geomorphic signature. Journal of Geophysical Research, 107, doi: 10.1029/2001JB000578.

Clark, M.K., Schoenbohm, L.M., Royden, L.H., Whipple, K.X., Burchfiel, B.C., Zhang, X., Tang, W., Wang, E., Chen, L., 2004. Surface uplift, tectonics, and erosion of eastern Tibet from large-scale drainage patterns. Tectonics, 23, TX1006, doi:10.1029/2002TC001402

Colletta, B., Hebrard, F., Letouzey, J., Werner, P., Rudkiewicz, J.R., 1990. Tectonic style and crustal structure of the Eastern Cordillera (Colombia) from a balanced cross-section. Petroleum and Tectonics in Mobile Belts, 81–100.

Cooper, M.A, Addison, F.T., Alvares, R., Hayward, A.B., Howe, S., Pulham, A.J., Taborda, A., 1995. Basin development and tectonic history of the Llanos basin, Colombia. Petroleum Basins of South America. AAPG. Memoir No. 62, 10, 659–666.

Corbett, L.B., Bierman, P.R., Rood, D.H., 2013. Optimizing sample preparation for high precision, low-detection limit analysis of in situ 10Be: Strategies and new data. Geological Society of America Abstracts with Programs 45.

Coutand, I.,Whipp Jr., D.M., Grujic, D., Bernet, M., Fellin, M.G., Bookhagen, B., Landry, K.R., Ghallet, S.K., Duncan, C., 2014. Geometry and kinematics of the Main Himalayan Thrust and Neogene crustal exhumation in the Bhutanse Himalaya derived from inversion of multithermochronologic data. Journal of Geophysical Research, Solid Earth, 119, 1446-1481, doi: 10.1005/2013JB010891.

Cortés, M., 2004. Evolution Structurale du Front Centre-Occidental de la Cordillere Orientale de Colombie. Ph.D. Thesis, Université Pierre et Marie Curie, Paris, 350pp.

Cortés, M., Colletta, B., Angelier, J., 2006. Structure and tectonics of the central segment of the Eastern Cordillera of Colombia. Journal of South American Earth Sciences, 21, 437–465, doi:10.1016/j.jsames.2006.07.004.

Dengo, C.A., Covey, M.C., 1993. Structure of the Eastern Cordillera of Colombia: Implications for trap styles and regional tectonics. American Association of Petroleum Geologists Bulletin, 77, 1315–1337.

De Porta, J., 1959. La Terraza de Bucaramanga. UIS. Boletin de Geología 3, 5-13.

Diaz, L., Serrano, M., 2001. Observaciones sobre el Terciario del Piedemonte. Reporte Presentado a Occidental de Colombia Por Ariana Ltda.

DiBiase, R.A., Whipple, K.X., Heimsath, A. M., Ouimet, W.B., 2010. Landscape form and millennial erosion rates in the San Gabriel Mountains , CA. Earth and Planetary Science Letters, 289, 134–144, doi: 10.1016/j.epsl.2009.10.036.

Dortch, J.M., Owen, L.A., Haneberg, W.C., Caffee, M.W., Dietsch, C., Kamp, U., 2009. Nature and timing of large landslides in the Himalaya and Transhimalaya of northern India. Quaternary Science Reviews, 28,1037–1054, doi:10.1016/j.quascirev.2008.05.002.

Dortch, J.M., Owen, L.A., Schoenbohm, L.M., Caffee, M.W., 2011. Asymmetrical erosion and morphological development of the central Ladakh Range, northern India. Geomorphology, 135, 167–180, doi:10.1016/j.geomorph.2011.08.014.

Duque-Caro, H., 1990. Neogene stratigraphy, paleoceanography and paleobiogeography in northwest South America and the evolution of the Panama Seaway. Palae, 77, 203–234.

Giachetta E., 2015. Personal communication.

Godard, V., Burbank, D.W., Bourls, D.L., Bookhagen, B., Braucher, R., Fisher, G.B., 2012. Impact of glacial erosion on 10Be concentrations in fluvial sediments of the Marsyandi catchment, central Nepal. Journal of Geophysical Research: Earth Surface, 117, F03013, doi: 10.1029/2011JF002230.

Gómez, E., 2002. Tectonic controls on the Late Cretaceous to Cenozoic sedimentary fill of the middle Magdalena Valley Cuenca, Eastern Cordillera, and Llanos Cuenca, Colombia: Ph.D. thesis, Cornell University, New York, 619 p.

Gómez, E., Jordan, T.E., Allmendinger, R.W., Cardozo, N., 2005b. Development of the Colombian foreland-basin system as a consequence of diachronous exhumation of the northern Andes. Bulletin of the Geological Society of America, 117, 1272–1292, doi: 10.1130/B25456.1.

Gómez, E., Jordan, T.E., Allmendinger, R.W., Hegarty, K., Kelley, S., Heizler, M., 2003. Controls on architecture of the Late Cretaceous to Cenozoic southern Middle Magdalena Valley Basin, Colombia. GSA Bulletin, 131–147, doi: 10.1130/0016-7606(2003)115<0131:COAOTL>2.0.CO;2.

Gómez, E., Jordan, T.E., Allmendinger, R.W., Hegarty, K., Kelley, S., 2005c. Syntectonic Cenozoic sedimentation in the northern middle Magdalena Valley Basin of Colombia and implications for exhumation of the Northern Andes. Bulletin of the Geological Society of America, 117, 547–569, doi: 10.1130/B25454.1.

González, J.V., Jiménez, G., 2015. Análisis estructural y características microtectónicas de un segmento de la falla Bucaramanga en los alrededores del corregimiento Umpalá, Santander. Universidad Industrial de Santander, Bucaramanga.

Goren, L., Willett, S.D., Herman, F., Braun, J., 2014. Coupled numerical-analytical approach to landscape evolution modeling. Earth Surface Processes and Landforms 39, 522–545, doi: 10.1002/esp.3514.

Goren, L., Fox, M., Willett, S.D., 2014. Tectonics from fluvial topography using formal linear inversion: Theory and applications to the Inyo Mountains, California. Journal of Geophysical Research: Earth Surface, 119, 1651-1681, doi: 10.1002/2014JF003079.

Granger, D.E., Kirchner, J.W., Finkel, R., 1996. Spatially Averaged Long-Term Erosion Rates Measured from in Situ-Produced Cosmogenic Nuclides in Alluvial Sediment. The Journal of Geology, 104, 249–257, doi: 10.1086/629823.

Gregory-Wodzicki, K.M., 2000. Uplift history of the Central and Northern Andes: A review. Geological Society of America Bulletin, 112, 1091–1105, doi:10.1130/0016-7606(2000)112<1091:uhotca>2.0.co;2.

Gupta, S., 1997. Himalayan drainage patterns and the origin of fluvial megafans in the Ganges foreland basin. Geology, 25, 11–14.

Helmens, K.F., 1988. Late Pleistocene glacial sequence in the area of the high plain of Bogotá (Eastern Cordillera, Colombia). Palaeogeogr. Palaeoclimatol. Palaeoecol., 67, 263–283.

Helmens, K.F., 1990. Neogene-Quaternary Geology in the high plain of Bogotá, Eastern Cordillera, Colombia (stratigraphy, paleoenvironments and landscape evolution). Dissertas Botanicae, 163, pp 202.

Helmens, K.F., 2004. The Quaternary glacial record of the Colombian Andes. In: Ehlers, J; Gibbard P L (eds), Quaternary Glaciations-extent and chronology, Part III: South America, Asia, Africa, Australasia, Antarctica. Developments in Quaternary Science, 2c, 115–134, doi:10.1016/S1571-0866(04)80117-9.

Helmens, K.F., Kuhry, P., 1995. Glacier fluctuations and vegetation change associated with Late Quaternary climatic oscillations in the area of Bogotá, Colombia. Quat. South America Antarctica Peninsula, 9, 117–140.

Helmens, K.F., Rutter, N.W., Kuhry, P., 1997. Glacier fluctuations in the eastern Andes of Colombia (South America) during the past 45,000 radiocarbon years. Quaternary International 38-9, 39–48.

Hermeston, S., Nemcok, M., 2013. Thick-skin orogen-foreland interactions and their controlling factors, Northern Andes of Colombia. Geological Society, London, Special Publications, 377, 443–471, doi: 10.1144/SP377.16.

Hidy, A.J., Gosse, J.C., Pederson, J.L., Mattern, J.P., Finkel, R.C., 2010. A geologically constrained Monte Carlo approach to modeling exposure ages from profiles of cosmogenic nuclides: An example from Lees Ferry, Arizona. Geochemistry, Geophysics, Geosystems, 11, 18 p. ISSN: 1525-2027.

Hooghiemstra, H., Wijninga, V.M., Cleef, A.M., 2006. The paleobotanical record of Colombia: implications for biogeography and biodiversity. Annals of Missouri Botanical Garden, 93, 297–325.

Hoorn, C., Guerrero, J., Sarmiento, G.A., Lorente, M.A., 1995. Andean tectonics as a cause for changing drainage patterns in Miocene northern South America. Geology, 23, 237–240, doi: 10.1130/0091-7613(1995)023<0237:ATAACF>2.3.CO;2.

Horton, B.K., Saylor, J.E., Nie, J., Mora, A., Parra, M., Reyes-Harker, A., Stockli, D.F., 2010. Linking sedimentation in the northern Andes to basement configuration, Mesozoic extension, and Cenozoic shortening: Evidence from detrital zircon U-Pb ages, Eastern Cordillera, Colombia. Bulletin of the Geological Society of America, 122, 1423–1442, doi: 10.1130/B30118.1.

Hoyos, N., Monsalve, O., berger, G.W., Antinao, J.L., Giraldo, H., Silva, C., Ojeda, G., Bayona, G., Escobar, J., Montes, C., 2015. A climatic trigger for catastrophic Pleistocene-Holocene debris flows in the Eastern Andean Cordillera of Colombia. Journal of Quaternay Science, 30, 258-270, doi: 10.1002/jqs.2779.

Howard, A.D., 1965. Geomorphological systems – equilibrium and dynamics. American Journal of Science, 263, 302-312, doi: 10.2475/ajs.263.4.302.

Howard, A.D., Kerby, G., 1983. Channel changes in badlands. Geological Society of America Bulletin, 94, 739-752, doi: 10.1130/0016-7606(1983)94<739:CCIB>2.0.CO;2.

Humphrey, N.F., Konrad, S.K., 2000. River incision or diversion in response to bedrock uplift. Geology, 28, 43–46, doi:10.1130/0091-7613(2000)028<0043:RIODIR>2.3.CO;2.

Hurvich, C., Tsai, C., 1989. Regression and time series model selection in small samples. Biometrika 76, 297–307, doi:10.1093/biomet/76.2.297.

Ingeominas, 2001. Zonificación Sismo Geotécnica Indicativa del Área Metropolitana de Bucaramanga, Fase II. Convenio realizado entre la CDMB e Ingeominas, Bucaramanga.

Irving, E., 1975. Structural evolution of the northernmost Andes, Colombia. Geological Survey Professional Paper 846, 45pp.

Jarvis, A., Reuter, H.I., Nelson, A., Guevara, E., 2008. Hole-filled SRTM for the globe. Version 4. http://srtm.csi.cgiar.org.

Jimenez, L., Mora, A., Casallas, W., Silva, A., Teson, E., Tamara, J., Namson, J., Higuera-Diaz, I.C., Lasso, A., Stockli, D., 2013. Segmentation and growth of foothill thrust-belts adjacent to inverted grabens: the case of the Colombian Llanos foothills. Geological Society, London, Special Publications, 377, 189–220, doi: 10.1144/SP377.11.

Jimenez Diaz, G., Speranza, F., Faccena, C., Bayona, G., Mora, A., 2014. Magnetic stratigraphy of the Bucaramanga alluvial Fan: Evidence for a < 3 mm/yr slip rate for the Bucaramanga-Santa Marta Fault, Colombia. South American Earth Sciences, doi: 10.1016/j.jsames.2014.11.001.

Julivert, M., 1963. La morfoestructura de la zona de Mesas al SW de Bucaramanga. UIS. Bol. De Geología, 1, 7-43.

Julivert, M., 1963. Los rasgos tectónicos de la región de la Sabana de Bogotá y los mecanismos de la formación de las estructuras. Boletín de Geología Universidad Industrial Santander, 13-14, 5–102.

Julivert, M., 1970. Cover and Basement Tectonics in the Cordillera Oriental of Colombia, South America, and a Comparison with Some Other Folded Chains. Geological Society of America Bulletin, 81, 3623–3646.

Kammer, A., Mora, A., 1999. Structural styles of the folded Bogotá Segment, Eastern Cordillera, Colombia: Zentralblatt für Geologie und Paleontologie, v. Teil 1, 823-837.

Kammer, A., Sánchez, J., 2006, Early Jurassic rift structures associated with the Soapaga and Boyacá faults of the Eastern Cordillera, Colombia: Sedimentological inferences and regional implications: Journal of South American Earth Sciences, 21, 412-422, doi:10.1016/j.jsames.2006.07.006.

Kellogg, J.N., Vega, V., 1995. Tectonic development of Panama, Costa Rica, and the Colombian Andes: Constraints from global positioning system geodetic studies and gravity. Geological Society of America Special Paper 295, 75-90, doi: 10.1130/SPE295-p75.

Kirby, E., Whipple, K.X., 2012. Expression of active tectonics in erosional landscapes. Journal of Structural Geology, 44, 54–75, doi: 10.1016/j.jsg.2012.07.009.

Kirby, E., 2003. Distribution of active rock uplift along the eastern margin of the Tibetan Plateau: Inferences from bedrock channel longitudinal profiles. Journal of Geophysical Research, 108, 2217, doi: 10.1029/2001JB000861

Kirby, E., Whipple, K., 2001. Quantifying differential rock-uplift rates via stream profile analysis. Geology, 6, 415–418, doi: 10.1130/0091-7613(2001)029<0415:QDRURV>2.0.CO;2.

Knighton, A.D., 1999. Downstream variation in stream power. Geomorphology, 29, 293-306, doi:10.1016/S0169-555X(99)00015-X.

Kohl, C.P., Nishiizumi, K., 1992. Chemical isolation of quartz for measurement of in-situ-produced cosmogenic nuclides. Geochimica et Cosmochimica Acta, 56, 3583–3587, doi: 10.1016/0016-7037(92)90401-4

Kooi, H., Beaumont, C., 1996. Large-scale geomorphology: Classical concepts reconciled and integrated with contemporary ideas via a surface processes model. Journal of Geophysical Research, 101, 3361-3386, doi: 10.1029/95JB01861.

Koons, P.O., 1994. Three-dimensional critical wedges: Tectonics and topography in oblique collisional orogens. Journal of Geophysical Research, 99, 12301–12315, doi: 10.1029/94JB00611.

Koons, P.O., 1995. Modeling the topographic evolution of collisional belts. Annual Review of Earth and Planetary Sciences, 23, 375–408, doi: 10.1146/annurev.ea.23.050195.002111.

Lal D, Arnold JR. 1985. Tracing quartz through the environment. Proceedings of the Indian Academy of Sciences - Earth and Planetary Sciences, 94, 1–5, doi:10.1007/BF02863403.

Lal D., 1991. Cosmic ray labeling of erosion surfaces: in situ nuclide production rates and erosion models. Earth and Planetary Science Letters, 104, 424–439, doi: 10.1016/0012-821X(91)90220-C.

Laverde, F.E., Segall, M.P., Allen, R.B., Ressetar, R., 1989. Recognition of an ancient fluvial system in the Upper Magdalena Valley, Colombia. In Programme and Abstracts of the IV International Conference on Fluvial Sedimentology (Barcelona), p.165.

Mark, B.G., Helmens, K.F., 2005. Reconstruction of glacier equilibrium-line altitudes for the Last Glacial Maximum on the High Plain of Bogota, Eastern Cordillera, Colombia: Climatic and topographic implications. Journal of Quaternary Science, 20, 789–800, doi:10.1002/jqs.974.

Mather, A. E., 2000. Adjustment of a drainage network to capture induced base-level change: an example from the Sorbas Basin, SE Spain. Geomorphology, 34, 271–289, doi: 10.1016/S0169-555X(00)00013-1.

Mercader, J., Gosse, J.C., Bennett, T., Hidy, A.J., Rood, D.H., 2012. Quaternary Science Reviews, 47, 116-130, doi: 10.1016/j.quascirev.2012.05.018.

Molnar, P., England, P., 1990. Late Cenozoic uplift of mountain ranges and global climatic change: chicken or egg?. Nature, 346, 29–34, doi:10.1038/346029a0.

Montes, C., 2001. Three dimensional structure and kinematics of the Piedras-Girardot fold-belt in the northern Andes of Colombia. Ph.D Thesis, The University of Knoxville, Tennessee, 217pp.

Montes, C., Robert, D., Hatcher, R.D., Restrepo-Pace, P.A., 2005. Tectonic reconstruction of the Northern Andean blocks: oblique convergence and rotations derived from the kinematics of the Piedras–Girardot area, Colombia. Tectonophysics, 399, 221–250, doi:10.1016/j.tecto.2004.12.024.

Mora, A., Horton, B.K., Mesa, A., Rubiano, J., Ketcham, R.A., Parra, M., Blanco, V., Garcia, D., Stockli, D.F., 2010. Migration of cenozoic deformation in the Eastern Cordillera of colombia interpreted from fission track results and structural relationships: Implications for petroleum systems. AAPG Bulletin, 94, 1543–1580, doi:10.1306/01051009111.

Mora, A., Parra, M., Strecker, M.R., Kammer, A., Dimaté, C., Rodríguez, F., 2006. Cenozoic contractional reactivation of Mesozoic extensional structures in the Eastern Cordillera of Colombia. Tectonics, 25, 1–19, doi: 10.1029/2005TC001854.

Mora, A., Parra, M., Strecker, M.R., Sobel, E.R., Hooghiemstra, H., Torres, V., Jaramillo, J. V., 2008. Climatic forcing of asymmetric orogenic evolution in the Eastern Cordillera of Colombia. Bulletin of the Geological Society of America, 120, 930–949, doi: 10.1130/B26186.1.

Mora, A., Reyes-Harker, A., Rodriguez, G., Teson, E., Ramirez-Arias, J.C., Parra, M., Caballero, V., Mora, J.P., Quintero, I., Valencia, V., Ibanez, M., Horton, B.K, Stockli, D. F., 2013. Inversion tectonics under increasing rates of shortening and sedimentation: Cenozoic example from the Eastern Cordillera of Colombia. Geological Society, London, Special Publications, 377, 411–442, doi: 10.1144/SP377.6.

Moreno, N., Silva, A., Mora, A., Tesón, E., Quintero, I., Rojas, L.E., Lopez, C., Blanco, V., Castellanos, J., Sanchez, J., Osorio, L., Namson, J., Stockli, D., Casallas, W., 2013. Interaction between thin-and-thick-skinned tectonics in the foothill areas of an inverted graben. The Middle Magdalena Foothill belt. Geol. Soc. London, Spec. Publ. 377, 221-255, doi:10.1144/SP377.18.

Mudd, S.M., Attal, M., Milodowski, D.T., Grieve, S.W.D., Valters, D.A., 2014. A statistical framework to quantify spatial variation in channel gradients using the integral method of channel profile analysis. Journal of Geophysical Research: Earth Surface, 119, 138–152, doi:10.1002/2013JF002981.

Nie, J., Horton, B.K., Mora, A., Saylor, J.E., Housh, T.B., Rubiano, J., Naranjo, J., 2010. Tracking exhumation of Andean ranges bounding the Middle Magdalena Valley Basin, Colombia. Geology, 38, 451–454, doi: 10.1130/G30775.1.

Nie, J., Horton, B.K., Saylor, J.E., Mora, A., Mange, M., Garzione, C.N., Basu, A., Moreno, C.J., Caballero, V., Parra, M., 2012. Integrated provenance analysis of a convergent retroarc foreland system: U-Pb ages, heavy minerals, Nd isotopes, and sandstone compositions of the Middle Magdalena Valley basin, northern Andes, Colombia. Earth-Science Reviews, 110, 111–126, doi: 10.1016/j.earscirev.2011.11.002.

Niemi, N.A., Oskin, M., Burbank, D.W., Heimsath, A.M., Gabet, E.J., 2005. Effects of bedrock landslides on cosmogenically determined erosion rates. Earth and Planetary Science Letters, 237, 480–498, doi: 10.1016/j.epsl.2005.07.009.

Nishiizumi, K., Imamura, M., Caffee, M.W., Southon, J.R., Finkel, R.C., McAninch, J., 2007. Absolute calibration of 10Be AMS standards. Nuclear Instruments and Methods in Physics Research, Section B: Beam Interactions with Materials and Atoms, 258, 403–413, doi: 10.1016/j.nimb.2007.01.297.

O'Callaghan, J.F., Mark, D.M., 1984. The extraction of drainage networks from digital elevation data. Computer Vision, Graphics, and Image Processing, 28, 323–344, doi:10.1016/S0734-189X(84)80011-0.

Parra, M., Mora, A., Jaramillo, C., Strecker, M.R., Sobel, E.R., Quiroz, L., Rueda, M., Torres, V., 2009a. Orogenic wedge advance in the northern Andes: Evidence from the Oligocene-Miocene sedimentary record of the Medina Basin, Eastern Cordillera, Colombia. Bulletin of the Geological Society of America, 121, 780–800, doi: 10.1130/B26257.1.

Parra, M., Mora, A., Jaramillo, C., Torres, V., Zeilinger, G., Strecker, M.R., 2010. Tectonic controls on Cenozoic foreland basin development in the north-eastern Andes, Colombia. Basin Research, 22, 874–903, doi: 10.1111/j.1365-2117.2009.00459.x.

Parra, M., Mora, A., Sobel, E.R., Strecker, M.R., González, R., 2009b. Episodic orogenic front migration in the northern Andes: Constraints from low-temperature thermochronology in the Eastern Cordillera, Colombia. Tectonics, 28, TC4004, doi: 10.1029/2008TC002423.

Pelletier, J.D., 2004. Persistent drainage migration in a numerical landscape evolution model. Geophysical Research Letters, 31, L20501, doi: 10.1029/2004GL020802.

Perron, J.T., Royden, L., 2013. An integral approach to bedrock river profile analysis. Earth Surface Processes and Landforms, 38, 570–576, doi: 10.1002/esp.3302.

Perron, J.T., Richardson, P.W., Ferrier, K.L., Lapôtre, M., 2012. The root of branching river networks. Nature, 492, 100–103, doi: 10.1038/nature11672.

Perron, J.T., Royden, L., 2013. An integral approach to bedrock river profile analysis. Earth Surf. Process. Landforms, 38, 570–576, doi:10.1002/esp.3302.

Prince, P.S., Spotila, J.A., Henika, W.S., 2011. Stream capture as driver of transient landscape evolution in a tectonically quiescent setting. Geology, 39, 823–826, doi: 10.1130/G32008.1.

Pupim, N., Bierman, P.R., Luis, M., Rood, D.H., Silva, A., Renato, E., 2015. Geomorphology Erosion rates and landscape evolution of the lowlands of the Upper Paraguay river basin (Brazil) from cosmogenic 10 Be. Geomorphology, 234, 151–160, doi: 10.1016/j.geomorph.2015.01.016.

Resprepo-Pace, P.A., 1995. Late Precambrian to Early Mesozoic Tectonic Evolution of the Colombian Andes, Based on New Geochronological, Geochemical and Isotopic Data. Ph.D Thesis, The University of Arizona, Tucson, 194pp.

Restrepo-Pace, P.A., Colmenares, F., Higuera, C., Mayorga, M., 2004. A Fold-and-thrust belt along the western flank of the Eastern Cordillera of Colombia—Style, kinematics, and timing constraints derived from seismic data and detailed surface mapping. In Thrust Tectonics and Hydrocarbon Systems: AAPG Memoir 82, 598–613.

Roeder, D., Chamberlain, R.L., 1995. Eastern Cordillera of Colombia: Jurassic–Neogene crustal evolution. In A. J. Tankard, S. R. Suarez, and H. J. Welsink, Eds., Petroleum Basins of South America: AAPG Memoir 62, 633–645.

Rolon, L.F., 2004. Structural Geometry of the Jura-Cretaceous Rift of the Middle Magdalena Valley Basin – Colombia. MSc thesis. West Virginia University.

Royden, L., Perron, J.T., 2013. Solutions of the stream power equation and application to the evolution of river longitudinal profiles. Journal of Geophysical Research: Earth Surface, 118, 497–518, doi: 10.1002/jgrf.20031.

Safran, E.B., Bierman, P.R., Aalto, R., Dunne, T., Whipple, K.X., Caffee, M., 2005. Erosion rates driven by channel network incision in the Bolivian Andes. Earth Surface Processes and Landforms, 30, 1007–1024, doi: 10.1002/esp.1259.

Sánchez, J., Horton, B.K., Tesón, E., Mora, A., Ketcham, R.A., Stockli, D.F., 2012, Kinematic evolution of Andean fold-thrust structures along the boundary between the Eastern Cordillera and Middle Magdalena Valley basin, Colombia. Tectonics, 31, TC3008, doi: 10.1029/2011TC003089.

Salgado, A.A.R., Braucher, R.V., Colin, F., Varajão, A.F.D.C., Nalini, H.A.Jr., 2008. Relief evolution of the Quadrilátero Ferrífero (Minas Gerais, Brazil) by means of (10Be) cosmogenic nuclei. Zeitschrift für Geomorphologie, 52, 317–323, doi:10.1127/0372-8854/2008/0052-0317.

Sarmiento-Rojas, L.F., 2001. Mesozoic Rifting and Cenozoic Basin Inversion History of the Eastern Cordillera, Colombian Andes: Inferences from tectonic models: PhD thesis, Vrije Universiteit, Amsterdam, 295 p.

Saylor, J.E., Horton, B.K., Nie, J., Corredor, J., Mora, A., 2011. Evaluating foreland basin partitioning in the northern Andes using Cenozoic fill of the Floresta basin, Eastern Cordillera, Colombia. Basin Research, 23, 377–402, doi: 10.1111/j.1365-2117.2010.00493.x.

Schumm, S.A., 1979. Geomorphic Thresholds: the concept and its application. Transaction of the Institute of British Geographers, 4, 485–515.

Segovia, A., 1965. Mapa Geológico de la plancha L-12 (Medina), de la República de Colombia, Bogotá.

Silva, A., Mora, A., Caballero, V., Rodriguez, G., Ruiz, C., Moreno, N., Parra, M., Ramirez-Arias, J.C., Ibanez, M., Quintero, I., 2013. Basin compartmentalization and drainage evolution during rift

inversion: evidence from the Eastern Cordillera of Colombia. Geological Society, London, Special Publications, 377, 369–409, doi:10.1144/SP377.15.

Small, R.J., 1978. The study of landforms (2nd edn). Cambridge: Cambridge University Press. 512pp.

Snyder, N.P., Whipple, K.X., Tucker, G.E., Merritts, D.J., 2003. Channel response to tectonic forcing: field analysis of stream morphology and hydrology in the Mendocino triple junction region, northern California. Geomorphology, 53, 97–127, doi:10.1016/S0169-555X(02)00349-5.

Sobel, E.R., Hilley, G.E., Strecker, M.R., 2003. Formation of internally drained contractional basins by aridity-limited bedrock incision. Journal of Geophysical Research: Solid Earth, 108, 2344, doi: 10.1029/2002JB001883.

Stokes, M., Mather, A.E., Harvey, A.M., 2002. Quantification of river-capture-induced base-level changes and landscape development, Sorbas Basin, SE Spain. Geological Society, London, Special Publications, 191, 23–35, doi:10.1144/GSL.SP.2002.191.01.03.

Stone, J.O., 2000. Air pressure and cosmogenic isotope production. Journal of Geophysical Research, 105, 23753, doi: 10.1029/2000JB900181.

Struth, L., Babault, J., Teixell, A., 2015. Drainage reorganization during mountain building in the river system of the Eastern Cordillera of the Colombian Andes. Geomorphology, 250, 370–383, doi: 10.1016/j.geomorph.2015.09.012.

Taboada, A., Rivera, L.A., Fuenzalida, A., Cisternas, A., Philip, H., Bijwaard, H., Olaya, J., Rivera, C., 2000. Geodynamics of the northern Andes: Subductions and intracontinental deformation (Colombia). Tectonics, 19, 787–813, doi: 10.1029/2000TC900004.

Tarboton, D. G., 1997. A new method of determination of flow directions and upslope areas in grid digital elevation models. Water Resources Research, 33, 309–319.

Teixell, A., Tesón, E., Ruiz, J.C., Mora, A., 2015. The structure of an inverted back-arc rift: insights from a transect across the Eastern Cordillera of Colombia near Bogotá. In C. Bartolini, and P. Mann, eds. Petroleum Geology and Hydrocarbon Potential of Colombia Caribbean Margin: AAPG Memoir 108, 499-515.

Tesón, E., Mora, A., Silva, A., Namson, J., Teixell, A., Castellanos, J., Casallas, W., Julivert, M., Taylor, M., Ibanez-Mejia, M., Valencia, V.A., 2013. Relationship of Mesozoic graben development, stress, shortening magnitude, and structural style in the Eastern Cordillera of the Colombian Andes. Geological Society, London, Special Publications, 377, 257–283, doi: 10.1144/SP377.10.

Tomkin, J.H., Braun, J., 1999. Simple models of drainage reorganisation on a tectonically active ridge system. New Zealand Journal of Geology & Geophysics, 42, 1–10, doi: 10.1080/00288306.1999.9514827.

Toro, J., Roure, Bordas-Le Floch, N., Le Cornec-Lance, S., Sassi, W., 2004. Thermal and Kinematic Evolution of the Eastern Cordillera Fold and Thrust Belt, Colombia. Am. Assoc. Pet. Geol. 1, 79-115, doi: 10.1306/1025687H13114.

Torres, V., Vandenberghe, J., Hooghiemstra, H., 2005. An environmental reconstruction of the sediment infill of the Bogotá basin (Colombia) during the last 3 million years from abiotic and biotic proxies. Palaeogeography, Palaeoclimatology, Palaeoecology, 226, 127–148, doi: 10.1016/j.palaeo.2005.05.005.

Ulloa, C., Rodríguez, E., 1979. Geología del Cuadrángulo K12, Guateque. Bol. Geol. Ingeominas, 22, 3–55.

Ulloa, C., Rodriguez, G.I., 1982. Intrusiones ácidas ordovícicas y post-devónicas en Floresta (Boyacá). Resum IV Congr. Colombiano Geol. Cali

Van der Beek, P., Champel, B., Mugnier, J.L., 2002. Control of detachment dip on drainage development in regions of active fault-propagation folding. Geology, 30, 471–474, doi: 10.1130/0091-7613(2002)030<0471:CODDOD>2.0.CO;2.

Van der Hammen, T., Werner, J.H., van Dommelen, H., 1973. Palynological record of the upheaval of the Northern Andes: A study of the pliocene and lower quaternary of the Colombian Eastern Cordillera and the early evolution of its high-Andean biota. Review of Palaeobotany and Palynology, 16, 1–122, doi: 10.1016/0034-6667(73)90031-6.

Veloza, G., Taylor, M., Mora, A., Gosse, J., 2015. Active mountain building along the eastern Colombian Subandes: A folding history from deformed terraces across the Tame anticline, Llanos Basin. Geological Society of America Bulletin, 127, 1155, doi: 10.1130/B31168.1.

Von Blanckenburg F., 2005. The control mechanisms of erosion and weathering at basin scale from cosmogenic nuclides in river sediment. Earth and Planetary Science Letters, 237, 462–479, doi: 10.1016/j.epsl.2005.06.030.

Whipple, K.X., 2004. Bedrock rivers and the geomorphology and geodynamics of a passive continental margin: the Konka and Kanaran lowlands of western peninsular India. In: Thiry, M., Simon-Coincon, R. (Eds.), Palaeoweathering, Palaeosurfaces, and Related Continental Deposits, 27: International Association of Sedimentologistst Special Publication, 28, 245-274.

Whitfield, E., Harvey, A.M., 2012. Interaction between the controls on fluvial system development: Tectonics, climate, base level and river capture - Rio Alias, Southeast Spain. Earth Surface Processes and Landforms, 37, 1387–1397, doi:10.1002/esp.3247.

Willett, S.D., 1999. Orogeny and orography: The effects of erosion on the structure of mountain belts. Journal of Geophysical Research, 104, 28957, doi: 10.1029/1999JB900248.

Willett, S.D., McCoy, S.W., Perron, J.T., Goren, L., Chen, C.-Y., 2014. Dynamic reorganization of river basins. Science (New York, N.Y.), 343, 1248765, doi: 10.1126/science.1248765.

Willett, S.D., Slingerland, R., Hovius, N., 2001. Uplift, shortening, and steady state topography in active mountain belts. Am. J. Sci, 301, 455–485, doi: 10.2475/ajs.301.45.455.

Wobus, C., Whipple, K.X., Snyder, N., Johnson, J., Sheehan, D., 2006. Tectonics from topography : Procedures, promise, and pitfalls, 2398, 55–74, doi: 10.1130/2006.2398(04)

Yang, R., Willett, S.D., Goren, L., 2015. In situ low-relief landscape formation as a result of river network disruption. Nature, 520, 526–529, doi: 10.1038/nature14354.

Yanites, B.J. Tucker, G.E., Anderson, R.S., 2009. Numerical and analytical models of cosmogenic radionuclide dynamics in landslide-dominated drainage basins. J. Geophysical Research, 114, F01007, doi: 10.1029/2008JF001088.

Appendix

Supplementary Data – Chapter 2 and 3

Longitudinal profiles of the main rivers in the flanks and in the Sabana de Bogotá plateau

We extracted the elevation values of major rivers in the flanks of the Eastern Cordillera and of the Bogotá river with headwaters in the Sabana de Bogotá (see location in Fig.1.2), with the aim of illustrating their contrasting pattern. The Bogotá river flows with very gentle slope at an elevation of c.a. 2500 m in the Sabana plateau and experiences a sudden slope increase in the outlet of the plateau into the western flank of the Cordillera (SD.1A). The associated knickpoint has a difference in elevation of ca. 2300 m. Rivers with the headwaters in the flanks (SD.1B-I) show a general concave pattern, which may be disrupted by localized knickpoints with smaller difference in elevation. These lower knickpoints are related with the main tectonic structures in the flanks. In the eastern flank, the Guatiquía, Machetá and Turmequé rivers (SD.1B-F) increase in channel slope when they cross the Santa Maria anticline (see location in Fig.2.4). The Turmequé river, related to a wide reentrant and low elevated segment in the mean divide (and thus with a large area of capture), shows a series of knickpoints. The uppermost is located just in the elbow of capture (see Fig.2.1B and D), and hence the profile segment upstream of the knickpoint is related with a relict segment of the old longitudinal drainage. In the western flank, the rivers San Miguel, Batán and Sabaneque (SD.1G-I) do not show major knickpoints along their profiles, although occasional knickpoints located in the upper river reaches are associated with reentrants and depressions in the divide, arguing for capture processes and divide migration in this flank as well.

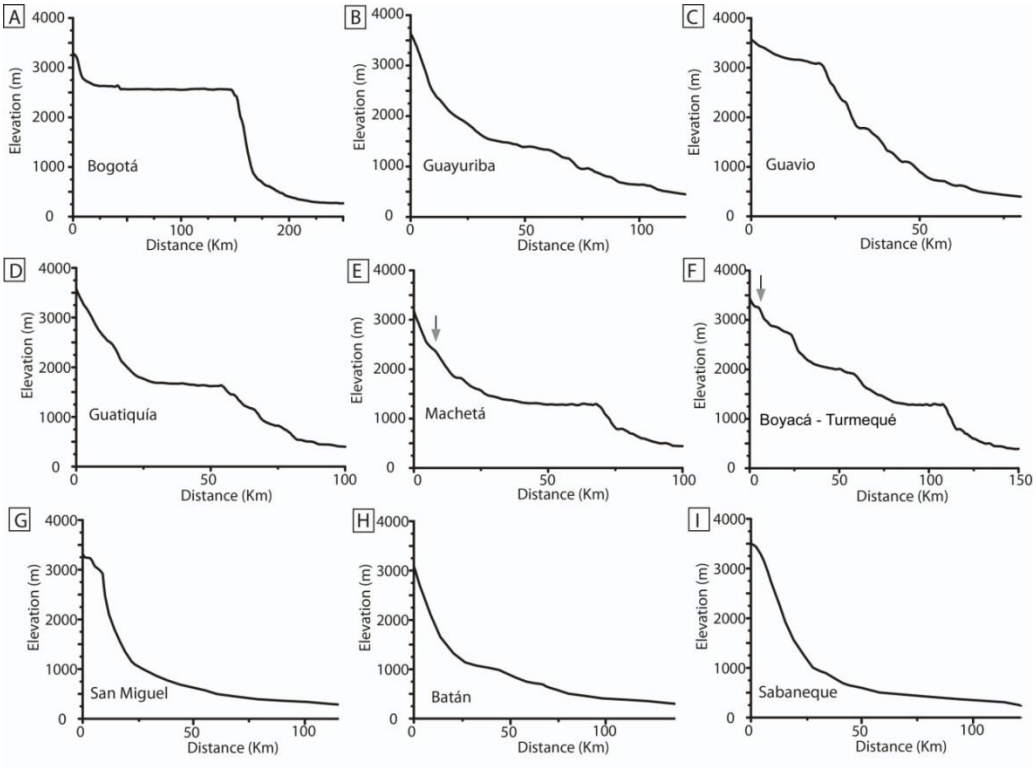

SD.1. *Longitudinal elevation profile of the Bogotá river and of the main rivers in the flanks of the Eastern Cordillera of Colombia. The grey arrows indicate the location of the knickpoints shown in Fig.2.6.*

Results of χ analysis

The calculation of the Mx parameter (the slope in chi-elevation space) is dependent on the best fit m/n ratio (concavity) based on AICc-collinearity test and chi-plots, following the method developed by Mudd et al., (2014). The statistical method to select a model that balances goodness of the fit against model complexity is the corrected Akaike Information Criterion (AICc) (Akaike, 1974; Hurvich and Tsai, 1989, Burnham and Anderson, 2002). We extract the AICc –collinearity test and the chi-plots for each basin in order to define the best fit concavity.

The AICc plots (SD.2) show the best fitting concavity value for each fluvial basin based on an iteration through a range of m/n (concavity) values for the main channel and tributaries. The concavity with the minimum AICc value will be the best fitting one. The mean concavity for all the basins is 0.45. Based in this mean value of concavity, we calculated the chi-plots.

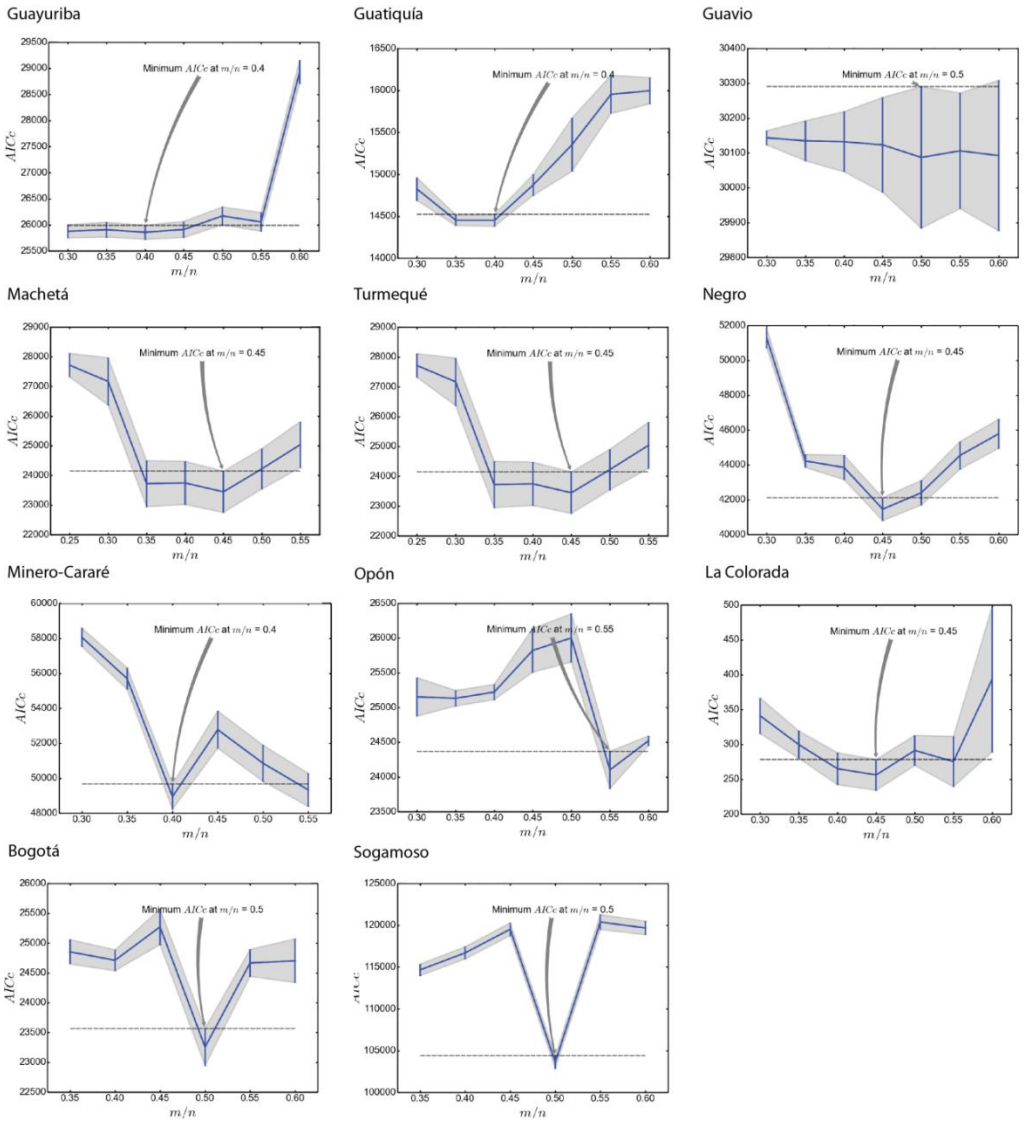

***SD.2**. The collinearity tests show the location of the minimum AICc values, arguing for the best concavity for each basin. The mean value resulted in 0.45.*

The chi-plots (SD.3) are plots of channel elevation against the transformed length variable “chi”, and show the steepness of river reaches without having to calculate channel slopes (Perron and Royden, 2013; Mudd et al, 2014). Additionally, we show the mean Mx value for each basin. It is worth noting the contrast between the high Mx values of the cordillera flanks and the low values of the Sabana de Bogotá plateau.

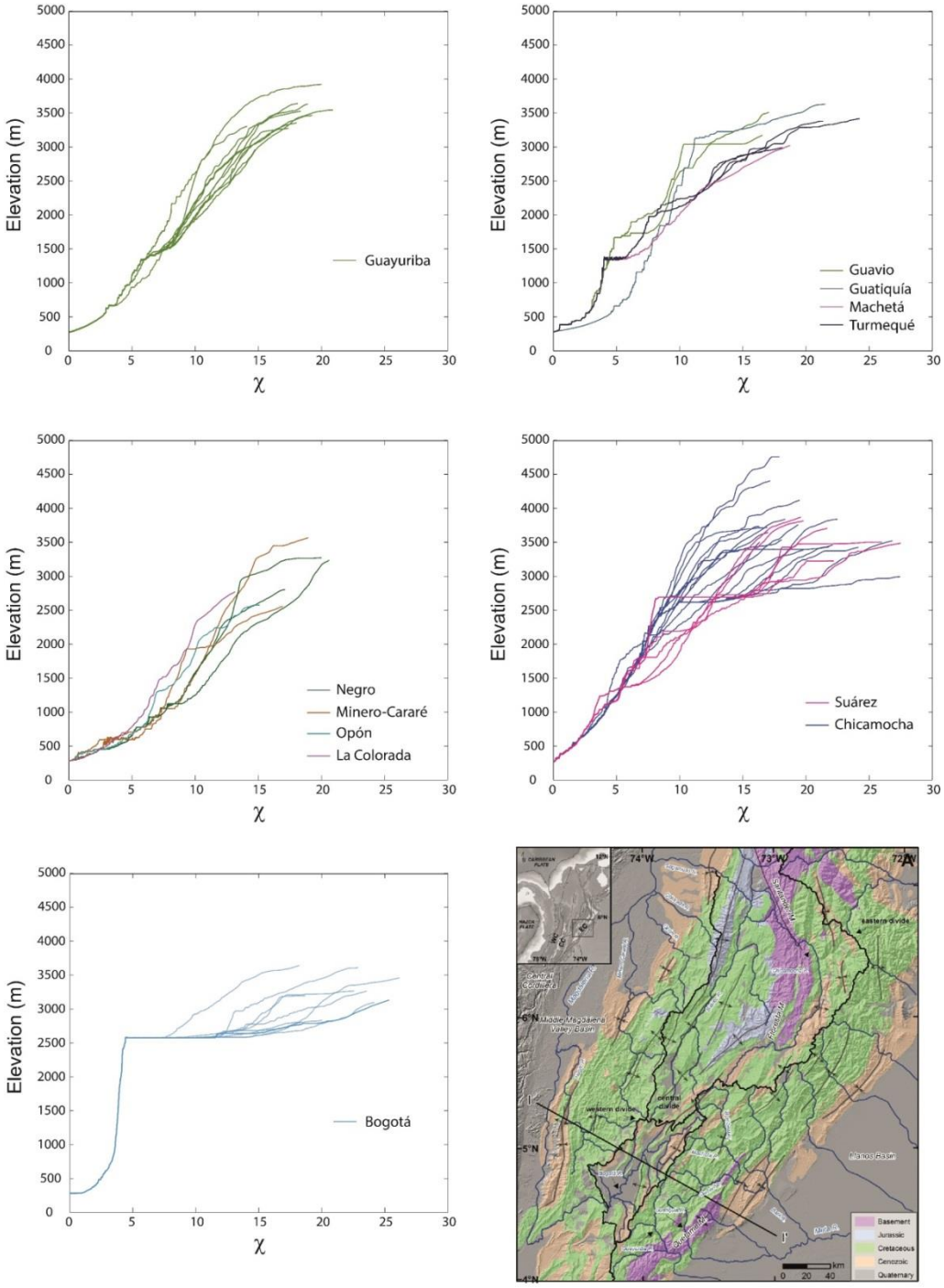

SD.3. *Plots of channel slope profiles in chi-elevation space for a concavity of 0.45. Dashed lines represent the best fit segments, and solid lines represent the transformed data. The mean Mx for each basin is also shown. Chi plots for m/n ratio of 0.45 and the Figure 1 of the main text for location reference*

Supplementary Data – Chapter 4

Statistic	Age (ka)	^{10}Be inheritance (10^4 atoms g^{-1})	Erosion rate (cm ka^{-1})
mean	432.1	10.68	0.06
median	426.4	10.69	0.06
mode	407.2	12.09	0.08
χ^2 optimum	377.8	12.11	0.00
χ^2 maximum	680.7	19.44	0.12
χ^2 minimum	285.2	2.10	0.00
Bayesian optimum	404.5	11.76	0.08
Bayesian 2σ upper	596.4	20.96	0.12
Bayesian 2σ lower	269.9	1.56	0.00

***SD4**. Depth profile results for the Bucaramanga terrace.*

Acknowledgments

Una vez llegados a este punto se me hace imposible no mirar atrás y ver el camino que he recorrido, las personas que he conocido y los conocimientos que he adquirido. Al fin y al cabo, una tesis no es el trabajo de una sola persona y por esta razón, me gustaría agradecer a todos aquellos que han colaborado y hecho posible de una manera u otra la culminación de este trabajo. Personas cuyo apoyo, comprensión y dedicación han sido claves para hacer, de este camino, un viaje lleno de conocimiento y pasión por la Geología.

En primer lugar quiero agradecer al director de esta tesis, Antonio Teixell, por la confianza depositada en mí para la realización de esta tesis doctoral. Tu gran dedicación en el crecimiento de este trabajo, así como el apoyo científico que he recibido durante estos años no se puede describir, así como el soporte material, logístico y económico. Es un placer trabajar con una persona de tal calibre, la cual no solo es un gran apoyo científico, sino también personal.

I am very thankful to Lewis Owen for invite me to use the Cosmogenic lab in the University of Cincinnati and for your advice in the sampling, analyzing and interpretation of the data. Your scientific dedication and humanity were very important for the culmination of this thesis. I want to acknowledge Craig Dietsch and his family for their hospitality, Sarah Hammer (Lab Manager) for her constant advice and curiosity on my research (thanks for the energetic bagels in the "crushing-days"!!), and Kat Rivers for made the quartz processing easier. I would like to acknowledge in the same way all the department members, specially to the Prof. Yurena Yanes. Finally, thanks to the "wine-tasting club" for the laughs and special moments along the stay.

I want to thank Danny Stockli for bring me the opportunity to use the Thermochronoly lab in the Jackson School of Geosciences in the University of Texas at Austin. Thank you for invite me to your research team and contribute with your point of view on my research project. The apatites did not appear, however I learnt and enjoyed a lot in the stay. Thanks also to all the department members!

I deeply thank Sean Willett for invite me to the ETH-Zürich and for provide me an important scientific knowledge and a different point of view about my work. You gave me the motivation to culminate my thesis. My most sincere acknowledgement to Emanuele Giachetta for the scientific discussion, help and guidance provided. Thanks also for all the ETH research members, special to Sean Gallen, Giuditta Fellin, Vincenzo Picotti, Gaia Siravo (buona fortuna con la tesi!) and to Sean Gallen for his advice with Matlab.

I am also very grateful to Alan Hidy who helped me with the cosmogenic depth profile modelling.

A Andrés Mora y Eliseo Tesón por su implicación en el proyecto, asistencia en campo y discusión científica, así como por la ayuda en la logística del campo en Colombia y su preocupación por el avance de la tesis.

A María Luisa Arboleya por su asistencia en campo y en recogida de muestras para Isótopos Cosmogénicos, así como el soporte brindado con los resultados y la preocupación por la tesis.
A David Gómez por su incondicional apoyo durante estos años, tanto en lo personal como científico.
A Albert Griera per tots aquests anys compartint despatx… el despatx de l'ordre dins el desordre, però sempre amb café!!! Moltes gràcies per ser allà quan ho necessitava.

Als membres del "menjador" (Toni, David, Albert, Mercè, Maria Luisa, Paco, Esteve, Pini, Geneta, Reche,..) per els moments de "coffee time" en els quals desconnectes una mica del treball i tornes amb força a escriure de nou. Sense oblidar les paelles, calçotades i dinars varis en els quals he rigut i disfrutat molt. Un agraïment especial a les secres, sou les millors!!

A los becarios precarios Salva, Camilo, Marta, Dídac, Laura y a los no ya tan becarios: Mireia, Marc, Isaac, Ana y Alvar. Me gustaría agradecer de manera especial a Mireia, Isaac y Salva por la infinidad de tiempo y vivencias que hemos compartido.

A Mireia Domènech per ser allà sempre i fer oficial la choco-terapia amb la qual resolem tot tipus de problema amb un somriure i sucre a les venes. Gràcies també per les geo conversacions, per ajudar-me amb el mostreig i pel camí que ens queda per endavant. Merci per tot, farolaaa!

A Isaac Corral por la amistad que tenemos desde hace ya muchos años y la cual se refuerza cada día más. Has sido y eres uno de los pilares fundamentales tanto profesional como personal. Gracias por los ánimos y consejos.

A Salvador Boya, por apoyarme siempre y aunque a veces me digas que deje de inventarme palabras, me escuchas e intentas digerir las historias fluviales que te explico (o eso creo). Gracias por los empujones necesarios cuando más los necesitaba y por esos esquemas nocturnos de la facies Utrillas en el frío asfalto.

A los compañeros de carrera y a mis amigos, en especial a Irene, Xavier, David, Vero, Kno, Cris y Bea por ayudarme a desconectar, animarme y motivarme en todo momento.

A toda mi familia, especialmente a mis padres y a mi hermano por el apoyo incondicional y su preocupación constante por el avance de la tesis y de mis ánimos, haciéndome ver y valorar el lado positivo de las cosas. Por confiar en mí y animarme a realizar todo aquello en lo que soñaba. Gracias por las risas durante los momentos más estresantes!! Pirri!
Moltíssimes gràcies també a la Tere, Cesc i Joel, pels vostres ànims constants i per creure en mi des d'un principi.

A Pau Garcia por aguantar lo inaguantable y aun así, hacerme ver que siempre hay un lado bueno de las cosas. Por animarme y creer en mí más que yo misma, convirtiéndote en el pilar fundamental de esta tesis y de mi desarrollo como doctora y como persona. A seguir viviendo aventuras y discusiones geológicas mientras caminamos por Chamonix. Gracias weroma!

This research work is funded by a predoctoral FPI grant (BES-2011-050262) from Ministerio de Educación, Ciencia y Deporte (España) and supported by Spanish MINECO projects CGL2010-15416 and CGL2014-54180-P.